Long-Distance Foam Propagation

Yu, G.

DOI
10.4233/uuid:20d9fea6-8b48-43a8-af60-9c4e1f7b94a8

Publication date
2021

Document Version
Final published version

Citation (APA)
Yu, G. (2021). *Long-Distance Foam Propagation*. [Dissertation (TU Delft), Delft University of Technology]. https://doi.org/10.4233/uuid:20d9fea6-8b48-43a8-af60-9c4e1f7b94a8

LONG-DISTANCE FOAM PROPAGATION IN HOMOGENEOUS POROUS MEDIA

Guanqun YU

Long-Distance Foam Propagation in Homogeneous Porous Media

Proefschrift

Ter verkrijging van de graad van doctor aan de Technische Universiteit Delft,
op gezag van de Rector Magnificus prof.dr.ir. T.H.J.J. van der Hagen
voorzitter van het College voor Promoties,
in het openbaar te verdedigen op
woensdag 13 october 2021 om 12:30 uur

door

Guanqun YU

Master of Science in Applied Earth Sciences, Technische Universiteit Delft, Nederland

geboren te Changchun, China

Dit proefschrift is goedgekeurd door de promotoren.

Samenstelling promotiecommissie bestaat uit:

Rector Magnificus,	voorzitter
Prof.dr. W.R. Rossen	Technische Universiteit Delft, promotor
Dr. D.V. Voskov	Technische Universiteit Delft, copromotor

Onafhankelijke leden:

Prof.dr.ir. R.A.W.M. Henkes	Technische Universiteit Delft
Prof.dr. P.L.J. Zitha	Technische Universiteit Delft
Prof.dr. H. Bertin	Université de Bordeaux
Dr. K.H.A.A. Wolf	Technische Universiteit Delft
Dr. M. Almajid	Saudi Aramco

The experiment and modeling work of this dissertation were carried out in Delft University of Technology, Department of Geoscience and Engineering, Delft, the Netherlands. This doctorial project is funded by the Joint-Industry-Project (JIP) on Foam for Enhanced Oil Recovery at Delft University of Technology.

Cover design by G.Y. (Guanqun) YU.

Best wishes to:

My dearest, and ever loving parents

Xueying Han

Zhongxiang Yu

And my dearest grandmother

Shuming Wong

A kind of magic

Aside from being an amazing substance of academic research, foam can also create a lot of fun in life. I remember vividly the first time I saw the colourful bubbles when I was a child, my mind was totally blown away by this sublime magic of nature. I have never seen anything that's so odd and beautiful at the same time. And even odder than that, 23 years later, I am studying bubbles in the lab! Speaking of fate…

Guanqun Yu

Table of Contents

Summary

Creating a gas-liquid foam means dispersing gas as individual bubbles in an aqueous solution, in which each gas bubble is separated by liquid films or lamella. The most common form of liquid foam (as opposed to solid foams, like polymer sponges) seen in day-to-day life is bulk foam. This refers to a foam that rests in a large container (or flows in a free open space) that has a volume considerably larger than the bubble size. Foam in a porous medium, however, resides and flows in a network of narrow pore spaces. The behaviour of foam is therefore complicated by many complex capillary phenomena.

Foam in a porous medium reduces the mobility of gas significantly. During gas-injection Enhanced Oil Recovery and environmental applications such as aquifer remediation, foam improves the sweep efficiency of gas by making the displacing fluid more viscous than the resident fluid(s) (such as crude oil, or other non-aqueous-phase liquids). In addition, foam also mitigates the impact of gravity when it comes to the vertical conformance of fluids with a large density contrast. Specifically, it reduces the rate of gas-water segregation under gravity. Therefore, foam is a highly efficient agent for displacing resident fluid(s) in subsurface formations.

In field applications, fluids are injected or produced from wells that connect surface facilities and subsurface formations. It's usually economically favourable to reduce the number of wells (or increase the inter-well spacing) as much as possible. In a petroleum reservoir, for instance, in-depth penetration of foam into subsurface formation is required due to the large inter-well distances. Previous experience in field application of foam indicates that foam is capable of propagating away from the wellbore and reaching deeper into formations. However, due to the limited field data and the uncertainties involved, the limiting distance/conditions for foam propagation remains unknown.

Theories and experiments suggest a minimum pressure gradient and a corresponding minimum velocity for the triggering of foam generation in porous media in steady flow of gas and water. A fractional-flow model of foam, when combined with a population-balance foam model and analysis of the traveling wave at the foam front, also predicts a minimum pressure gradient and superficial velocity for foam propagation. These studies imply that the creation of foam is almost always guaranteed in the near-wellbore region. The large pressure gradient and superficial velocity there insures the mobilization and reproduction of gas bubbles. As foam spreads out deeper into formations, however, pressure gradient and superficial velocity decrease, and the propagation and maintenance of foam becomes increasingly uncertain.

In this dissertation, the theoretical background for experiments on foam propagation is based on the dominant role of pressure gradient and the corresponding superficial velocity in foam generation in steady flow of gas and water. The assumption of an initial steady-state of gas and water flow before foam propagation is justifiable. In a petroleum reservoir, gas injection is usually applied prior to foam injection. A steady-state of gas and water flow is also expected at locations far from the well, where the effects of alternating injection of gas and liquid slugs are damped.

Chapter 1 provides a brief introduction to the fundamental concepts of foam generation and propagation in porous media, and the main motivations and goals of this research. The dominant mechanisms behind the creation and destruction of foam bubbles are explained and supported with graphical illustration. The theory of foam propagation (from previous studies), formulated based on the theory and modeling of foam generation, is briefly discussed. The main structure of the dissertation is provided at the end of chapter.

Chapter 2 focuses on the impact of surfactant concentration on the minimum or triggering superficial velocity for foam generation. The presence of surfactant molecules in an aqueous phase is key to the creation of foam. The surfactant molecules are adsorbed to and preferentially

stay on the gas/water interface, which helps stabilize foam bubbles where gas is trapped. For the surfactant formulation we chose (AOS-Bioterge C14-16), we examine the impact of surfactant concentration on the minimum or critical superficial velocity for foam generation at a constant fractional flow of gas. Surfactant concentration affects the stability and the coalescence rate of lamellae, and therefore impacts the superficial velocity at which the generation of strong foam is triggered. The superficial velocity for foam generation is also tested as a function of the injected gas fraction at a fixed surfactant concentration. In total, three surfactant concentrations are tested at various injected gas fractions. The results are consistent with a population-balance model for foam generation as a function of velocity and pressure gradient.

The results in this chapter also provide a benchmark to guide the design of experiments on foam propagation in chapter 3. Criteria are defined to standardize the conduct and interpretation of experiments on foam generation in the steady flow of gas and water. These criteria can be used to guide the design of future experiments.

Chapter 3 focuses on answering the most crucial question of the thesis: that is, the propagation and stability of foam at low superficial velocity and pressure gradient. The experiments on foam propagation are performed in a Bentheimer sandstone core of variable diameter. We define a series of criteria to standardize the procedures for dynamic experiments on foam propagation. The criteria aim to provide guidelines for experimenters to perform similar experiments in the future. Some of these criteria have to be strictly followed to avoid unwanted perturbations and uncertainties, while others can be applied flexibly.

Our experiments identify the critical superficial velocities for foam generation, propagation and collapse. These three critical velocities are plotted against injected gas fraction (foam quality), for two different surfactant concentrations. The experiments are carried out in a vertically mounted, homogeneous sandstone core, where gravity segregation of gas and water can be neglected. The critical velocity for foam generation (and the influence of surfactant concentration and foam quality) can be cross-referenced to the results in chapter 2. In addition, the corresponding pressure gradient at all the velocities (including the critical velocities) during foam propagation are plotted. Such a plot indicates the correlation between the three critical superficial velocities to the mobilities of foam in its various steady-states.

Application of our experimental results directly to field application of foam is complicated by various factors, including reservoir heterogeneity, gravity segregation, surfactant adsorption, etc.

Chapter 4 provides insights into a number of widely studied foam models, specifically in their ability to represent a minimum superficial velocity for foam generation. The chapter can be divided into two sections. The first section deals with the steady-state (local-equilibrium) solutions of the investigated foam models. We propose mathematical criteria that can be applied to any foam model. These criteria test the model's equations and their ability to produce a minimum velocity for foam generation. In total four foam models are investigated in this chapter. We compare the models' formulas and our criteria, and conclude on each model's ability to represent a triggering velocity (as well as reasons why they are or aren't able to do so).

In the second section, we perform a simulation study for one of the models examined. The CMG-STARS foam model can represent a trigger velocity for foam generation. We extend our analysis to numerical simulation of long-distance foam propagation with this model. This model can represent a minimum velocity for foam propagation as well as foam generation, but the velocity for foam propagation coincides with that for foam stability, in contrast our experimental results in Chapter 3. The simulation result is analysed and discussed in comparison to the theories and experimental results in Chapter 3. In particular, we point out a fundamental problem with simulation models for foam generation based on velocity and

pressure gradient, in that conventional simulations do not calculate the velocity to pressure gradient near an injection well.

Chapter 5 summarizes and discusses the results in of Chapters 2 to 4. In addition, we also discuss the various aspects of foam propagation that are worth further examination in the future. Our experiments are carried out based on simplifications and assumptions. In reality, a real petroleum reservoir or aquifer is likely to have more complicated physical, chemical, geological and geometrical conditions. There is a need to generalize and extend our experimental and simulation results to more-realistic conditions.

Samenvatting

Het creëren van een gas-vloeistof schuim gebeurt door het verspreiden van gas als individuele bellen in een waterige oplossing, waar elke gasbel van elkaar is gescheiden door vloeistof films genaamd lamellae. De meest voorkomende vorm van vloeibaar schuim (in tegenstelling tot vast schuim, zoals polymeersponzen) is zogeheten bulk schuim. Dit is een schuim dat zich in een grote container bevindt (of stroomt door een vrije open ruimte) en een volume heeft dat veel groter is dan de belgrootte. Schuim in een poreus medium bevindt zich echter in een netwerk van kleine poriën. Het gedrag van schuim wordt daardoor gecompliceerd door complexe capillaire verschijnselen.

Schuim in een poreus medium vermindert de mobiliteit van gas in significante mate. In toepassingen zoals verbeterde oliewinning en het opschonen van aquifers kan schuim het sweep rendement van het gas verbeteren door het verplaatsende fluïdum viskeuzer te maken dan het fluïdum dat zich in de poriën bevindt (zoals ruwe olie of andere niet-waterige fluïda). Verder kan schuim ook de impact van de zwaartekracht beperken voor fluïda met een groot contrast in dichtheid. Zo wordt bijvoorbeeld de mate waarin gas en water zich van elkaar scheiden door toedoen van de zwaartekracht beperkt. Dus is schuim effectief in het verplaatsen van fluïda in de ondergrond.

In het veld worden fluïda geïnjecteerd in of geproduceerd uit bronnen die de faciliteiten aan het oppervlak verbinden met het ondergrondse gesteente. Het is meestal economisch gezien wenselijk om het aantal bronnen zoveel mogelijk te beperken (of de afstand tussen bronnen te vergroten). In een petroleumreservoir is het bijvoorbeeld nodig dat het schuim ver in het gesteente penetreert vanwege de grote afstand tussen de bronnen. Ervaring vanuit het veld leert dat schuim in staat is om ver van de bron en dieper het gesteente in te propageren. Vanwege de beperkte beschikbaarheid van data uit het veld en de mate van onzekerheid zijn de beperkingen in de mate waarin het schuim kan propageren nog niet bekend.

Theorie en experimenten suggereren dat er een minimale drukgradiënt met bijbehorende minimumsnelheid is voor het triggeren van schuim-generatie in poreuze media bij stabiele stroming van gas en water. Een fractioneel stromingsmodel van schuim dat gecombineerd wordt met een populatie-balans model en analyse van de reizende golf bij het schuimfront voorspelt ook een minimum drukgradiënt en stromingssnelheid voor het propageren van schuim. Deze onderzoeken impliceren dat bijna altijd gegarandeerd kan worden dat schuim wordt gevormd nabij de bron. De grote drukgradiënt en stromingssnelheid ter plaatse zorgen ervoor dat er gasbellen worden gevormd. Als het schuim zich verder verspreidt door het gesteente worden de drukgradiënt en stromingssnelheid echter steeds lager waardoor het propageren en in stand houden van het schuim onzekerder wordt.

In dit proefschrift is de theoretische achtergrond voor schuimpropagatie-experimenten gebaseerd op de dominante rol van de drukgradiënt en de bijbehorende stromingssnelheid bij de generatie van schuim bij stabiele stroming van gas en water. De aanname dat er een initiële stabiele toestand is van stroming van gas en water voordat het schuim propageert is hierbij verantwoord. In een petroleum reservoir wordt gasinjectie meestal toegepast voor schuiminjectie. Een stabiele toestand van gas en waterstroming wordt ook verwacht op locaties verder van de bron af waar effecten van de alternerende injectie van gas en vloeistof beperkt zijn.

Hoofstuk 1 geeft een korte introductie van de fundamentele concepten van schuimgeneratie en propagatie in poreuze media en de hoofdmotivaties en doelstellingen van dit onderzoek. De dominante mechanismes achter het aanmaken en vernietigen van schuimbellen worden uitgelegd en ondersteund door grafische illustraties. De theorie van schuimpropagatie (uit vorige onderzoeken) die gebaseerd is op de theorie en het modelleren van schuimgeneratie

wordt hier ook kort beschreven. De overkoepelende structuur van dit proefschrift wordt gegeven aan het eind van dit hoofdstuk.

Hoofdstuk 2 is gericht op de impact van surfactant concentratie op de minimum stromingssnelheid waarbij schuim wordt gegenereerd. De aanwezigheid van surfactant moleculen in de waterige fase is benodigd om schuim aan te maken. De surfactant moleculen worden geadsorbeerd aan een gas/water interface en blijven daar ook waardoor schuimbellen worden gestabiliseerd waarin het gas in zit gevangen. We hebben gekozen voor de surfactant AOS-Bioterge C14-16. We bestuderen de impact van surfactant concentratie op de minimum of kritische stromingssnelheid waarbij schuim wordt aangemaakt bij een constante fractionele stroming van gas. De surfactant concentratie heeft invloed op de stabiliteit en de snelheid van coalescentie van lamellae, waardoor het dus ook impact heeft op de stromingssnelheid waarbij een sterk schuim wordt gecreëerd. De stromingssnelheid voor schuimgeneratie is ook getest als een functie van de geïnjecteerde gasfractie bij een vaste surfactant concentratie. In totaal zijn er drie surfactant concentraties getest bij verschillende geïnjecteerde gasfracties. De resultaten zijn consistent met een populatie-balans model voor schuimgeneratie als een functie van snelheid en drukgradiënt.

De resultaten in dit hoofdstuk worden ook als benchmark gebruikt voor het ontwerp van experimenten over schuimpropagatie (zie hoofdstuk 3). Hierbij zijn verschillende criteria gedefinieerd om de aanpak en interpretatie te standaardiseren van experimenten over schuimgeneratie bij stabiele stroming van gas en water. Deze criteria kunnen worden gebruikt bij het opzetten van toekomstige experimenten.

Hoofdstuk 3 is gericht op het beantwoorden van de meest cruciale vraag van dit proefschrift: de propagatie en stabiliteit van schuim bij lage stromingssnelheid en drukgradiënt. De schuimpropagatie-experimenten zijn uitgevoerd in een Bentheimer zandsteenkern met een variabele diameter. We definiëren een serie van criteria om de procedures omtrent dynamische experimenten over schuimpropagatie te standaardiseren. De criteria hebben als doel om richtlijnen op te stellen voor toekomstige soortgelijke experimenten. Enkele van deze criteria moeten strict worden opgevolgd om ongewenste onzekerheden te vermijden, terwijl andere flexibeler kunnen worden toegepast.

Onze experimenten identificeren de kritische stromingssnelheden voor schuimgeneratie, propagatie en ineenstorting. Deze drie kritische snelheden zijn geplot tegen geïnjecteerde gasfractie (schuimkwaliteit) voor twee verschillende surfactant concentraties. De experimenten zijn uitgevoerd in een verticale, homogene zandsteenkern, waardoor zwaartekrachtsscheiding van gas en water kan worden verwaarloosd. De kritische snelheid voor schuimgeneratie (en de invloed van surfactant concentratie en schuimkwaliteit) kan worden vergeleken met de resultaten uit hoofdstuk 2. Verder worden de bijbehorende drukgradiënten bij alle snelheden (inclusief de kritische snelheden) tijdens schuimpropagatie geplot. Zo'n plot geeft de correlatie aan tussen de drie kritische stromingssnelheden en de mobiliteit van het schuim in verschillende stabiele toestanden.

Directe toepassing van onze experimentele resultaten in het veld wordt gecompliceerd door verschillende factoren, zoals reservoir heterogeniteit, zwaartekrachtsscheiding, surfactant adsorptie, etc.

Hoofdstuk 4 geeft inzicht in een aantal breed onderzochte schuimmodellen, vooral in hun vermogen om een minimale stromingssnelheid voor schuimgeneratie te modelleren. Het hoofdstuk kan worden verdeeld in twee secties. Het eerste deel beschrijft stabiele toestand (lokaal evenwicht) oplossingen van de bestudeerde schuimmodellen. We stellen wiskundige criteria voor die kunnen worden toegepast op elk schuimmodel. Deze criteria testen de vergelijkingen van het model en hun vermogen om een minimum snelheid voor schuimgeneratie te berekenen. In totaal worden er vier schuimmodellen bekeken in dit

hoofdstuk. We vergelijken de vergelijkingen van de modellen en onze criteria. Hieruit concluderen we of een model in staat is om een trigger-snelheid voor schuimgeneratie te berekenen en geven we redenen waarom het model daar wel of niet toe in staat is.

In het tweede deel doen we simulaties voor een van de onderzochte modellen. Het CMG-STARS schuimmodel voorziet in een trigger-snelheid voor schuimgeneratie. We breiden onze analyse uit naar numerieke simulatie van lange afstand schuimpropagatie met dit model. Dit model omvat een minimum snelheid voor zowel schuimpropagatie als generatie. De snelheid voor schuimpropagatie is hier echter hetzelfde als de snelheid voor schuimstabiliteit, dit in tegenstelling tot onze experimentele resultaten uit Hoofdstuk 3. Het resultaat van deze simulatie is geanalyseerd en vergeleken met de theorieën en experimentele resultaten uit Hoofdstuk 3. Hierbij kijken we vooral naar een fundamenteel probleem binnen simulatiemodellen voor schuimgeneratie die gebaseerd zijn op snelheid en drukgradiënt. Conventionele simulaties zijn niet in staat om de snelheid en drukgradiënt vlakbij een injectieput te berekenen.

Hoofdstuk 5 geeft een samenvatting en discussie van de resultaten in Hoofdstukken 2 t/m 4. Verder beschrijven we ook de verschillende aspecten van schuimpropagatie die de moeite waard zijn om verder te onderzoeken. Onze experimenten zijn gebaseerd op vereenvoudigingen en aannames. Een echt petroleum reservoir of aquifer zal waarschijnlijk gecompliceerdere fysische, chemische, geologische en geometrische eigenschappen hebben. Daarom is het nodig om onze experimentele en simulatieresultaten uit te breiden naar meer realistische condities.

Chapter 1

Introduction

1.1 Energy transition and EOR

The world must make a transition from fossil-based fuels to renewable energy in the coming decades to avoid a climate-change disaster. Sophisticated power-generating technologies such as solar and wind power will lead the first step of energy transition, from conventional fossil fuel based power generation to a renewable, sustainable, greener and cleaner forms of power generation. However, a such transition will take a considerable period of time, and may not be a pragmatic strategy for developing and undeveloped countries in their near future. It remains important now (and in coming decades) that oil and gas shall be produced while keeping an eye on carbon emissions.

The production life of a conventional oil reservoir comprises three major stages (Alagorni et al., 2015). In the primary production stage of an oil field, oil is produced using natural power: depletion of reservoir pressure, rock expansion, gravity drainage, solution gas drive, aquifer influx etc. (Willhite, 1986). The initially high reservoir pressure (sometimes assisted by a strong aquifer and/or gravity) pushes oil to wells and then to the surface. Eventually the reservoir pressure becomes too low to propel the flow of oil (especially if the reservoir pressure/temperature falls below the bubble point). Therefore secondary recovery is applied, when water (or produced natural gas) is injected to maintain reservoir pressure. The efficiency of water flooding in reducing residual oil where water sweeps can be quantified by the capillary number (Bethel and Calhoun, 1953; Foster, 1973; Green and Willhite, 1998; Tang et al., 2020). Displacement efficiency refers to the efficiency of mobilizing oil at the pore scale. The fraction of the field swept by injected fluid is called sweep efficiency. It is affected by factors such as geological heterogeneity/permeability variation (Dykstra and Parsons, 1950; Lake, 1989; Qi and Feng, 1998; Green and Willhite, 1998), gravity segregation (Stone, 1982; Jenkins, 1984; Shi and Rossen, 1998; Rossen and van Duijn, 2004; Rossen et al., 2010) of the injected fluid and the stability of the displacement front (Dake, 1978). In the first two stages of production, oil production can reach an average of 30% of original oil in place (OOIP) (Alagorni et al., 2015). In the third (tertiary) stage of oil recovery, the main goal is to enhance oil recovery by injecting solutions that lead to improved displacement and sweep efficiencies. These methods are called enhanced oil recovery (EOR) methods. These EOR methods usually involve injection of chemical solutions (surfactant or polymer EOR), gases with favourable phase-behaviour properties with oil (miscible or immiscible EOR), or high-temperature fluids such as hot water and steam (thermal EOR). Applying EOR methods may increase oil recovery up to 40-60% of OOIP.

In this dissertation, we explore the potential of deep penetration of foam in porous media. A major application of foam (see definition in Section 1.3) has been to enhanced oil recovery in the oil and gas industry. However, in this research, we wish to provide generalized understanding of foam's attributes in porous media, instead of promoting its value in oil production only. Foam is a good method for enhanced oil recovery but not limited to that application. It helps sweep efficiency by improving the mobility ratio of the displacement (see 1.2) relative to conventional gas injection techniques. Such advantages of foam can be great in the application of petroleum production, but also enables foam to be applied to other practical purposes such as chemical washing of polluted soils. More details on valuable prospects of foam application are proposed and discussed in Chapter 5.

1.1.1 Gas injection EOR

Injection of miscible and immiscible gas is a widely used EOR method (Lake, 1989). The efficiency of gas injection is determined by both displacement efficiency and volumetric sweep efficiency. In the case of miscible gas injection, oil and gas may flow as one phase without an interface. As a result, the capillary force that traps the oil phase is eliminated and residual oil can be displaced by gas. In the case of immiscible gas injection, injected gas (i.e., N_2) dissolves in the oil phase and makes it swell, which leads to the mobilization of trapped oil. Injection of immiscible gas also helps maintain reservoir pressure above bubble point.

There are three main factors that contribute to poor sweep efficiency: unstable viscous flow at the displacement front, gravitational force, and geological heterogeneity. Unstable viscous flow is a result of a large mobility ratio of gas to oil, which encourages the formation of gas fingers at the displacement front. Severe fingering of gas at the displacement front is commonly seen in field application of gas EOR. These gas fingers, once developed, create thief zones/channels that are favourable to gas flow. As a result, a large fraction of oil remains untouched and left behind, forming a considerable volume of residual oil. Poor vertical sweep efficiency of gas injection is caused by the large density contrasts between gas and both oil and water. Injected gas tends to segregate towards the top of reservoir, forming a thief zone of high gas mobility. The fraction of oil that stays below the gas zone hence remains untouched by gas. Gravity segregation between gas and water is seen in water-alternating-gas injection (Stone, 1982; Jenkins, 1984), where a mixed zone of gas and water flow ends at the point of complete segregation between gas override and water underride. Foam can help address the issue of poor sweep efficiency of gas. It greatly reduces the relative mobility of gas injected, as explained below, which mitigates the formation of gas fingers at the leading edge of foam bank. In the vertical dimension, the reduction of gas relative mobility slows down the segregation between gas and water significantly (Shi and Rossen, 1998; Rossen et al., 2010), and maximizes the height and length of the zone swept by gas.

1.1.2 Foam injection EOR

Foam can significantly reduce the relative mobility of the gas phase and leads to a more-favourable mobility ratio in the displacement. In EOR application, it creates a more-uniform sweep of gas on both horizontal and vertical dimensions, which lead to greatly improved production of liquid hydrocarbon. Applying foam as an EOR method requires in-depth penetration of foam into the oil-bearing layers. The penetration depth required depends on the distance between the injection well and production well(s). A field trial of steam foam (Friedmann et al., 1994) suggests that foam can propagate to a considerable distance away from injection well (see Chapter 3), which creates a uniform foam bank around the injection well and results in enhanced oil recovery. Foam generated in the near-well region can also be used to overcome the heterogeneity of non-communicating layers. It blocks the entrance to layer(s) of higher-permeability (thief zones), and directs fluids to layers of relatively lower permeability (Al Ayesh et al., 2016).

In addition to its merits as an EOR technique, foam can also be used as an acid diverter in near-well treatments. In well stimulation, foam helps direct treating fluid (acid solution) to the impaired region of low permeability (Smith et al., 1969; Zerhboub et al., 1994). Foam also plays an important role in remediation of soil and aquifers (Lawson and Reisberg, 1980; Hirisaki et al., 1997, 2000) that are contaminated by a variety of oils and chlorinated solvents. Creating foam in soil helps achieve a uniform sweep of chemical solutions that help remove the pollutants. Another environment-related application of foam is CO_2 sequestration, which helps reduce carbon footprint. CO_2 foam injection enhances oil recovery while also sequestering CO_2 within underground formations previously occupied by oil. In CO_2 injection into an aquifer,

foam expands the region swept by CO_2 before gravity brings CO_2 up to an override zone directly below the overburden.

In sum, foam in porous media is an effective method that achieves a uniform sweep of gas and liquid over a large region. It functions as a fluid diverter (for both gas and liquid) in porous media, which addresses the issue of poor sweep efficiency caused by heterogeneity, gravity, and unfavourable mobility ratio. Though foam was initially proposed as an EOR method, it has the potential for all applications that involve gas and water flow in porous media.

1.2 Foam in porous media

1.2.1 Definition of foam

Foam in porous media is the dispersion of gas bubbles in the water phase, with each bubble separated by thin liquid films and surrounded by solid surface (i.e., the pore wall) coated with water (Bikerman, 1973; Falls et al., 1988; Rossen, 1996; Exerowa and Kruglyakov; 1998; Weaire and Hutzler, 1999; Farajzadeh et al., 2014). A thin liquid film between two bubbles, stabilized by surfactant molecules, is also called a *lamella* (plural *lamellae*). Mobilization of gas bubbles requires mobilization of lamellae, a process that strongly depends on local pressure gradient (see Section 1.2.4 below) (Rossen, 1990a, b, c; Rossen and Gauglitz, 1990; Rossen et al., 1994). The generation, collapse and propagation of foam in porous media is a result of a competition between lamella creation and destruction (Falls et al., 1988; Friedman et al., 1991; Kovscek and Radke, 1994; Rossen, 1996; Kam and Rossen, 2003). Upon achieving a local-equilibrium (or local steady-state) of foam, the rate of lamella creation reaches a balance with that of lamella destruction. For dynamic propagation of foam in homogeneous porous media, the competition of lamella creation and destruction near the leading edge of foam bank determines the ability and efficiency of foam propagation to a large distance from an injection well (Ashoori et al., 2012). There are four mechanisms (Rossen, 1996; Chen et al., 2005) by which a lamella can be created in porous media (as summarized below). For an existing lamella stabilized by surfactant molecules, its stability is a function of local capillary pressure (see 1.2.5).

The steady-state of strong foam can be divided into two regimes based on foam quality f_g (injected gas fraction) (Osterloh and Jante, 1992; Alvarez et al., 2001). For foam that flows in the high-quality regime, foam texture and foam stability is dominated by capillary pressure. High-quality foam flows with a pressure gradient proportional to water superficial velocity. Low-quality foam features shear-thinning rheology, where total relative mobility increases with increasing gas flow rate (Cheng et al., 2000).

1.2.2 Foam and gas mobility reduction

Foam reduces the mobility of gas significantly by reducing gas relative permeability (trapping much of the gas in place) and increasing its apparent gas viscosity (because of the capillary forces and drag on moving lamellae). For a water-wet porous medium whose porespace is filled with only gas and water (i.e. aqueous surfactant solution), water is the strongly wetting phase and gas is the non-wetting phase. Due to capillary action (Young, 1805; Leverett, 1941; Haines, 1927), water preferentially accumulates in relatively smaller pores, and gas preferentially stays in the relatively larger pores.

For immiscible two-phase flow of gas and water without foam, gas and water each form their own separate flow paths, with gas preferentially flowing in intermediate- and large-sized pores, and water in smaller pores and in the corners and crevices of larger pores. In the absence of foam, the relative mobility of the gas phase can be modelled as a function of water (or gas) saturation. Gas mobility is high due to its small viscosity (50× smaller than that of water at room temperature). When foam is generated in porous media, the relative mobility of gas can

be greatly reduced. Foam generation is defined here as a transition from a state of no-foam (with high gas relative mobility) to a state of strong foam (with much lower gas relative mobility). The magnitude of flow resistance to gas in the presence of foam depends on the average size of gas bubbles. Foam texture is defined as the number of foam bubbles or lamellae per unit volume n_f, which is the inverse of bubble size. The relative mobility of gas decreases with increasing foam texture (Rossen and Gauglitz, 1990; Friedmann et al., 1991; Kovscek and Radke, 1995; Kam and Rossen, 2003) due to greater resistance to flow.

The mechanisms by which foam reduces gas mobility are associated with the dynamics of lamella trapping and mobilization at the pore scale. A standing lamella can block a pore throat which was previously open to gas flow. Gas is then diverted to other paths. Alternatively, gas can flow across the pore throat by either mobilizing (at sufficient pressure difference) or rupturing (at high capillary pressure) the lamella. If at least one continuous flow path of gas, with no lamellae, exists, a "continuous-gas foam" is flowing inside the pore network (Falls et al., 1988). The existing lamellae in other pores reduce the available area for gas flow and increases the tortuosity/length of gas flow path(s). When a "discontinuous-gas foam" is generated, the gas phase is divided into separate bubbles and the only way to mobilize gas is through lamella mobilization. In a discontinuous-gas foam, the relative mobility of gas can be reduced by a factor of 1000 or more (Rossen, 1996), due to effects related to both gas relative permeability (gas trapping) and effective viscosity of the foam. For a non-Newtonian fluid with a yield stress, like foam, however, there is no rigorous distinction between gas relative permeability and effective viscosity (Rossen, 1992).

1.2.3 Lamella-creation mechanisms

The most common (and perhaps easiest) way of making foam in day-to-day life is by dispersing gas in liquid under strong externally applied turbulence. This is how foam is created when we wash hands or dishes, or shake a bottle of beer. Inside a petroleum reservoir, however, such strong turbulence is not present (especially at a location distant from wells). Instead, capillary forces (related to wettability of the medium, structure of the pore network, gas/water interfacial tension, etc.) play a dominant role in the distribution of gas and water and creation of lamellae. The creation of foam bubbles in porous media (in the laboratory and field) relies on a number of different physical mechanisms. Below we list the mechanisms for lamella creation that are commonly seen and verified in porous media.

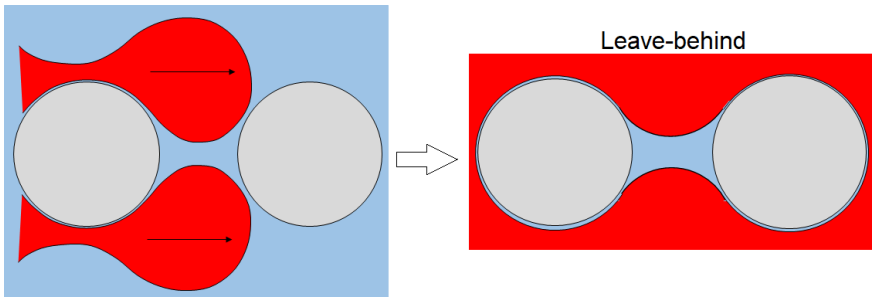

Figure 1.1. Creation of a leave-behind lamella during primary drainage of aqueous surfactant solution. A lens of liquid is "left behind" in the narrow pore throat as gas invades the relatively larger pore bodies on either side.

1) Leave-behind. Leave-behind lamellae are formed during primary drainage, when gas is injected into a porous medium fully saturated with surfactant solution (Ransohoff and Radke, 1988; Rossen, 1996). A leave-behind lens/lamella is formed when liquid is 'left behind' in a pore throat as gas drains the liquid in the pore bodies on either side (Rossen, 1996) (Fig. 1.1). Leave-behind lamellae created during drainage help create a continuous foam of relatively low gas mobility (Rossen, 1996). The ramified structure of the gas-invaded pores

of this continuous foam creates an ideal condition to trigger the generation of discontinuous foam by lamella division (Rossen, 1996).

2) Lamella division. Mobilization of existing lamella and subsequent division contributes to refinement of foam texture (Rossen and Gauglitz, 1990; Rossen, 1996; Kam and Rossen, 2003). In a 2-D configuration, as a lamella flows into a fork in a flow path (Falls et al., 1988) (Fig. 1.2), the lamella can be divided into two separate lamellae. And if the two lamellae remain stable, the division is successful and results in a larger quantity of lamellae. In a different scenario, if a stationary lamella is present in one of the branches, the moving lamella flows through the other branch without dividing (Falls et al., 1988). A successful lamella division would require a sufficient pressure gradient to keep the lamellae mobilized. Upon repetition of successful lamella division, bubble density increases and leads to a finer foam texture. Bubble creation by lamella division is also observed in experiments on foam flow in fractures (AlQuaimi and Rossen, 2018).

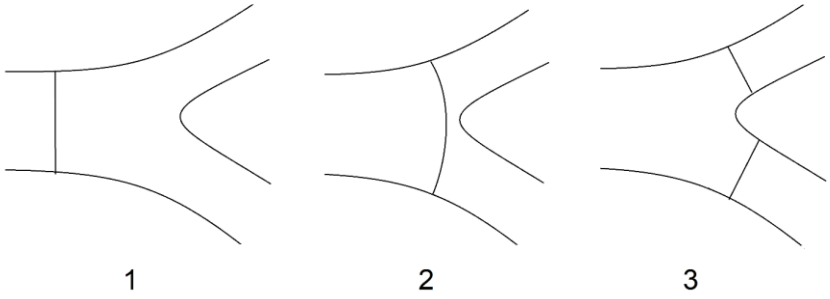

Figure 1.2. Lamella division at a fork in the flow path (1-3). In 1 and 2, a lamella flows into a pore body driven by a sufficient pressure gas across the lamella. In 3, the original lamella is divided in two, representing successful lamella generation by division.

3) Liberation of dissolved gas (Bernard and Holm, 1967; Richardson et al., 1980; Rossen, 1996). Dissolved gas may come out of the liquid phase with falling pressure; then individual gas bubbles form from the liquid phase (Rossen, 1996). Such a bubble-generation mechanism requires the presence of dissolved gas in the liquid as well as a considerable amount of pressure reduction. In field application of foam, the generation of foam leads to a significant increase of pressure inside the reservoir. Therefore liberating dissolved gas is not expected to play an important role in foam in petroleum reservoirs.
4) Snap-off (Roof, 1970; Falls et al., 1988; Rossen, 1996). Snap-off was first identified and explained as an oil-trapping mechanism (Roof, 1970) during imbibition of water. There are many ways in which snap-off of liquid takes place in porous media (Rossen, 2003). One common mechanism of snap-off takes place during primary drainage (Fig. 1.3), when gas flows across a narrow capillary constriction and makes its entry into a large pore body occupied by water (Falls et al., 1988; Rossen 1996, Rossen 2003, Kovscek et al., 1995; Kovscek and Radke, 1996). Snap-off may also take place as gas and water flow across a sharp capillary transition (Shah et al., 2019). As gas and water flow across this boundary, water tends to accumulate at the transition and blocks the flow of gas (non-wetting phase). Bubble creation by snap-off is also observed in experiments in model fractures (AlQuaimi and Rossen, 2018).

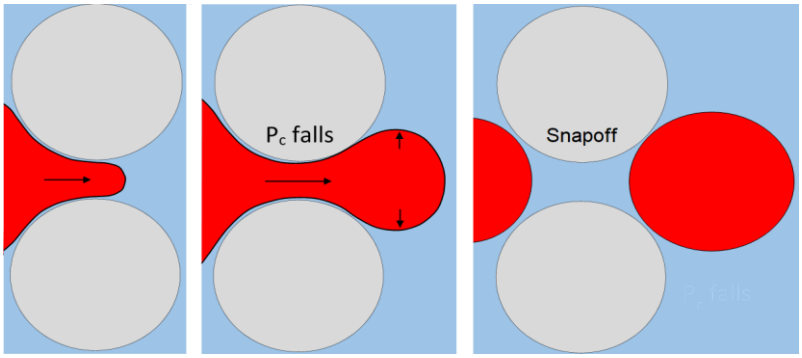

Figure 1.3. Creation of a liquid lens by Roof snap-off. As gas invades and expands into a pore body across a relatively narrow pore throat, a temporary drop in capillary pressure P_c (Rossen, 1996; Rossen, 2003; Chen et al., 2005) can lead to the bridging of liquid across the pore throat.

1.2.4 Lamella mobilization and subsequent division

The Young-Laplace equation (Eq. 1.1) describes the equilibrium condition for a stationary liquid film.

$$\Delta P = 2\left(\frac{\sigma}{r_1} + \frac{\sigma}{r_2}\right) \qquad \text{Eq. 1.1}$$

where ΔP in Eq-1.1 is the pressure difference across the lamella, σ is surface tension between gas and water, and r_1 and r_2 are the principle radii of curvature at any point on the lamella. For a thin liquid film of spherical shape, $r_1 = r_2 \equiv R$:

$$\Delta P = \frac{4\sigma}{R}. \qquad \text{Eq. 1.2}$$

When the imposed pressure difference across a liquid film is zero, the film tends to locate in the narrow pore throat (or the constricted section of a capillary tube), where it achieves a surface with minimum surface area and zero mean curvature, as shown in Fig. 1.2.1. To displace a lamella from a narrow pore throat to a wider pore body, the lamella is curved and stretched and creates a pressure difference across its two interfaces. The pressure difference across a curved lamella is inversely proportional to the radius of curvature. The maximum pressure difference a lamella experiences before it starts moving out of a pore throat is the minimum pressure difference required for lamella mobilization. The existence of a minimum pressure difference makes foam behaves as if it were a non-Newtonian fluid with yield stress such as Bingham plastic (Balan et al., 2011).

In steady flow of gas and liquid (or in regions swept by gas), mobilization of leave-behind lamellae and subsequent division is considered the primary mechanism of foam texture refinement (Prieditis, 1989; Rossen and Gauglitz, 1990). Lamella division was observed as a primary foam-generation mechanism in etched-glass micromodels by Prieditis (1989). The theory of foam generation by lamella mobilization and division (Rossen and Gauglitz, 1990) matches results seen in the laboratory (Gauglitz et al., 2002) (see 1.3.1).

1.2.5 Lamella stability and limiting capillary pressure

Foam stability at the macroscopic scale relies on the stability of individual lamellae at the microscopic scale (Bergeron and Radke, 1992; Bergeron and Radke, 1995; Bergeron, 1997). Upon creation of a lamella, it must be stabilized by surfactant molecules, which occupy the gas-liquid interface. The double-layer repulsion between the charged heads of ionic surfactant molecules saturating the opposite surfaces of a lamella provides a "disjoining pressure". This disjoining pressure includes electrostatic repulsion, van der Waals attraction, and close-range steric/hydration forces (Aronson et al., 1994; Bergeron, 1997). Disjoining pressure, as a function of film thickness, resists the capillary pressure (as function of pore size, interfacial

curvature at the plateau border, interfacial tension) applied by the porous medium and maintains the metastable thin film (Bergeron, 1997). For a static common black film (CBF), a primary maximum of disjoining pressure (related to film thickness) exists, which defines the critical capillary pressure above which the film jumps to an even thinner Newton black film (NBF) (Aronson et al., 1994; Bergeron and Radke, 1992). An NBF could break upon a further increase of capillary pressure (Aronson et al., 1994).

Disjoining pressure governs the capillary pressure at which a static film breaks. However, it is not the only factor that affects the stability of liquid films flowing through porous media (Aronson et al., 1994). As a lamella flows into a wider pore body where it is stretched and thinned-down rapidly, wetting liquid may have difficulty flowing to the lamella rapidly enough to maintain its stability (Jimenez and Radke 1989; Chen et al., 2010). Falls et al. (1988) also pointed out other factors behind lamella coalescence, such as the kinetics lamella movement (including touching a new pore wall, as between Figs. 1.2.1 and 1.2.2).

It is found experimentally that foam flowing through a porous medium also coarsens abruptly around a particular value of capillary pressure, the "limiting capillary pressure" – P_c^* (Khatib et al., 1988). The limiting capillary pressure is a function of rock type (Rossen, 1992), permeability (Rossen and Zhou, 1995), wettability, surfactant type and concentration and other factors (Apaydin and Kovscek, 2001; Kahrobaei and Farajzadeh, 2019). In a given porous medium, capillary pressure is directly related to aqueous-phase saturation.

Since capillary pressure is a function of liquid saturation, the limiting capillary pressure plays a dominant role in the properties of strong foam in the high-quality foam regime, where water saturation approaches and the limiting capillary pressure. However, for a wetter foam with relatively low foam quality and higher water saturation, the role of limiting capillary pressure on foam stability is less important.

1.3 Foam generation and propagation in porous media

1.3.1 Foam generation in homogeneous porous media

Foam can be created in porous media in several different ways: injection of pre-generated foam, creating foam in-situ by injecting gas into a porous medium fully saturated with surfactant solution (i.e., in drainage), and creating foam in-situ in steady flow of gas and surfactant solution. In field applications of foam, gas and surfactant solution are often injected alternatively to create foam near the injection well. Some distance from an injection well, however, the reservoir experiences a nearly steady flow of gas and water. In this study, therefore, we focus on generating foam in-situ at an initial condition of steady flow of gas and water.

Rossen and Gauglitz (1990) show that there is a minimum pressure gradient that triggers the generation of foam in steady flow, which is often reported as a minimum superficial velocity. In their study (Rossen and Gauglitz, 1990), a bond percolation model is employed which accounts for the interconnectivity of the porous medium and the effect of leave-behind lamellae on gas flow. The model relates the mechanism of mobilizing an individual lamella at the microscopic scale to the initialization of foam generation at macroscopic scale in homogeneous porous media. Gauglitz et al. (2002) further explore the minimum superficial velocity and pressure gradient for foam generation. Chapter 2 examines the impact of surfactant concentration on the minimum superficial velocity that triggers foam generation in Bentheimer sandstone.

Once strong foam is created upon reaching sufficiently large total velocity (Fig. 1.4a) or pressure gradient (Fig. 1.b), it can be maintained, and propagate, at lower superficial velocity (but larger pressure gradient) than that required to create it (Gauglitz et al., 2002). Fig. 1.4b shows that there are three steady-states of foam at fixed superficial velocity: weak foam (low

pressure gradient), intermediate foam (intermediate pressure gradient) and strong foam (large pressure gradient). The presence of both strong foam and weak foam at velocities lower than the triggering velocity is essential for mobilizing foam and keeping foam stable in reservoir (Gauglitz et al., 2002; Kam and Rossen; Ashoori et al., 2012; Yu et al., 2020).

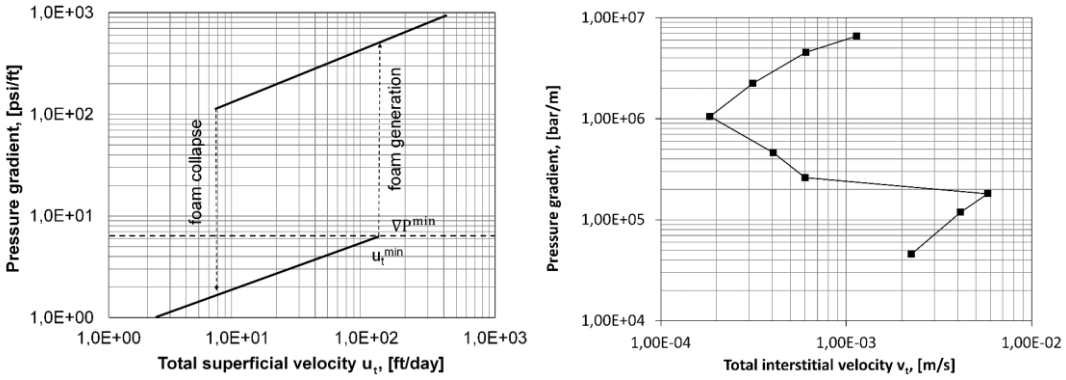

(a) **(b)**

Figure 1.4. Foam generation at (a) fixed total superficial velocity and foam quality and (b) fixed pressure difference and foam quality (Gauglitz et al., 2002).

1.3.2 Foam propagation in homogeneous porous media

Successful application of foam for enhanced oil recovery usually requires foam propagation to a large radial distance from the injection well. In such applications, foam is usually created in the vicinity of the injection well by injecting alternating slugs of gas and surfactant solution (Kibodeaux and Rossen, 1997; Farajzadeh et al., 2009); foam then propagates radially away into the reservoir.

Friedmann et al. (1991) studied foam propagation in a core of different diameters. N_2 foam was created in-situ in (or pre-generated and injected into) the narrow entrance section of the core and then propagated to wider sections of lower superficial velocity. The rate of foam propagation decreased with increasing core diameter, by more than the increase in cross-section area, and foam was weaker at lower superficial velocity.

Based on the foam model of Kam (2008), Ashoori et al. (2012) proposed an analytical model for foam propagation at low superficial velocity. They analyse the advance of the foam front in terms of the convection, destruction and creation of lamellae at the front. Their model predicts a slowdown and eventual failure of foam propagation upon decreasing total superficial velocity. As total superficial velocity decreases to a threshold value, the characteristic velocity of foam front approaches zero. In other words, reduction of total superficial velocity in radial flow toward this threshold velocity leads to slower propagation and eventually the failure of propagation of foam.

1.3.3 Foam generation and propagation in heterogeneous porous media

Previous work suggested an alternative way of creating foam, as gas and surfactant solution flows across a sharp permeability boundary. Such a boundary is commonly seen in layered geological beddings. Shah et al. (2019) demonstrated successful foam generation at the sharp transition of permeability in a synthetic porous media made from sintered glass. Bubble creation at sharp geological boundaries reflects the sharp reduction of capillary pressure across the boundary (from low permeability to high permeability), an effect analogous to the capillary end effect. The intermittent trapping and flowing of gas across the boundary results in repeated creation of lamella by snap-off and subsequent lamella mobilization. Such a phenomenon provides a possible alternative to foam propagation at locations of low pressure gradient and superficial velocity far from an injection well.

1.4 Foam simulation models

There are two types of foam models to describe and predict the macroscopic behaviour of foam in porous media: Implicit-Texture models (Ma et al., 2015; Lotfollahi et al., 2016a, 2016b), and Population-Balance models (Falls et al., 1988; Friedmann et al., 1991; Kovscek and Radke, 1994; Kam and Rossen, 2003; Kam, 2008; Lotfollahi et al. 2016a, 2016b). The Implicit-Texture models assume local equilibrium between processes of lamella creation, destruction and trapping. With additional assumptions, either type of model can be analysed using Fractional-Flow theory, also known as the Method of Characteristics (MOC).

1.4.1 Implicit-Texture foam models

Implicit-Texture (IT) foam models don't explicitly represent foam texture or account for the dynamics of lamella generation, destruction and convection. These models assume instantaneous achievement of local steady-state of these processes as well as thermodynamic properties (pressure, temperature, phase volume fractions). The effects of foam texture on gas mobility are represented implicitly as a function of phase saturations, velocities, concentration/fraction of surfactant, etc. Therefore, this type of model cannot represent the entrance region (Ashoori et al., 2011) seen in coreflooding experiments of foam, nor the dynamics of bubble transport at the displacement front of foam (Ashoori et al., 2012). One widely used IT foam model is that in the STARS simulator of The Computer Modeling Group (CMG) (Cheng et al., 2000; Lotfollahi et al. 2016a). In this model, the presence of foam and its effect on flow is represented by a factor specifying the magnitude of gas relative-permeability reduction, which in turn depends on a local properties such as phase saturations, surfactant concentration, surface tension, pressure gradient, etc.

IT models have the advantage of modeling foam processes on the field scale without the need to calculate (and iterate) for the convection, creation and destruction of foam bubbles locally. In a field application of foam, the time scale of the kinetics of lamellae creation and destruction are many orders of magnitude shorter than the period of field application to be modelled (Kam et al., 2007; Ashoori et al., 2012). IT models have shown that they can represent foam behaviour accurately in various applications (Lotfollahi et al., 2016b).

1.4.2 Population-Balance foam models

A Population-Balance (PB) foam model explicitly represents foam texture. In these models, in addition to the mass-conservation equations, there is an equation for the change in local foam texture, based on convection of lamellae in and out, and creation and destruction of lamellae. The rates of lamella creation and destruction may reflect local properties such as pressure gradient, water saturation, phase velocities, flowing bubble density, trapping of gas, surfactant concentration, capillary pressure, etc. The representation of the dynamics of lamella creation and destruction varies between different versions of PB models (Falls et al., 1988; Friedmann et al., 1991; Kovscek and Radke, 1994; Kam and Rossen, 2003; Chen et al., 2010). In the PB model of Kovscek and Radke (1995) and Chen et al. (2010), and its variants, repeated Roof snap-off is assumed to be the dominating mechanism for lamella creation. Kam and Rossen (2003) proposed a PB model where lamella creation depends on local pressure gradient. This model predicts the minimum pressure gradient (and velocity) for foam generation as seen in experiments (Gauglitz et al., 2002). Kam (2008) later revised the formula of lamella creation; for simplicity we refer to this family of models here as "Kam's model."

One advantage of Population-Balance models is that they account explicitly for the convection of foam bubbles. Kam's PB model (Kam and Rossen, 2003; Kam and Rossen, 2007; Kam, 2008) can represent a minimum superficial velocity or pressure gradient for foam generation as seen in experiments (Fig. 1.4) (Gauglitz et al., 2002; Kam, 2008). In this model and its variants, pressure gradient controls the rate at which lamella is created. The model's

components and functionality is explained in detail (with examples) in Chapter 4. Ashoori et al. (2012) combined Kam's PB with fractional-flow and traveling-wave analysis to long-distance foam propagation: specifically, the ability of foam to propagate at decreasing superficial velocity and pressure gradient in radial flow from an injection well. They concluded that there is a critical superficial velocity at which the propagation velocity of foam approaches zero. This prediction is explored with dynamic experiments and discussed in Chapter 3.

1.5 Objectives and components of this dissertation

This dissertation investigates the conditions for foam generation and propagation in homogeneous porous media (specifically, Bentheimer sandstone). Specifically, we examine the dependence of foam generation on surface tension and the concentration of surfactant in the aqueous phase. Next, we examine previous experimental results (Friedmann et al., 1991 and 1994) and theoretical prediction (Ashoori et al., 2012) of a minimum total superficial velocity for foam propagation. In addition, we review some of the prominent foam models for their ability to represent the critical conditions for foam generation and foam propagation.

This dissertation comprises five chapters.

Chapter 1 introduces the background related to this dissertation.

Chapter 2 examines the effect of surfactant concentration on the minimum velocity that triggers foam generation at a moderate pressure of 41 bar (4.1×10^6 Pa) and a temperature range of 20-23°C. Surfactant concentration is not the key to lamella creation, but it is key to maintain the stability of an existing lamella. Since foam generation is the result of lamella creation and destruction, and surfactant concentration affects lamella stability through the limiting capillary pressure P_c^* (see 1.2.5), we expect conditions for foam generation to depend on surfactant concentration.

Our experimental results in cores of Bentheimer sandstone confirm the impact of surfactant concentration. The critical velocity for foam generation decreases with increasing injected liquid fraction and increasing surfactant concentration.

The experimental results in this chapter also serves as useful input for the experiments on dynamic foam propagation described in Chapter 3. A test of dynamic foam propagation requires a successful generation of foam generation at the core inlet. We therefore need knowledge of the critical superficial velocity for foam generation at various injected water fractions and surfactant concentrations.

Chapter 3 describes a coreflooding study of the minimum superficial velocities for foam generation, propagation and stability. The Bentheimer sandstone core used in this experiment is crafted into a shape of increasing diameter from the inlet to outlet, where gas and water can flow at different superficial velocities at one volumetric injection rate. This design of core shape was first proposed by Friedmann et al. (1991). Three minimum/critical superficial velocities are predicted by Ashoori et al. (2012). The minimum velocity for foam propagation is greater than the minimum velocity for maintaining the stability of foam. Data also fit trends predicted by theory for the effect of injected liquid fraction and surfactant concentration.

Chapter 4 evaluates some of the widely used foam-simulation models for their ability to represent the critical superficial velocities that are illustrated in Chapter 3.

Our investigation focus on four different foam models (and their variants).

1. Kam's Population-Balance model (Kam and Rossen, 2003) and its variants (Kam, 2008)
2. CMG-STARS foam model (Martinsen and Vassenden, 1999; Cheng et al., 2000; Computer Modeling Group, 2017)
3. Modification of STARS foam model proposed by Lotfollahi et al. (2016) to represent hysteresis in foam properties as a function of superficial velocity.
4. The Population-Balance model of Chen et al. (2010)

We evaluate each model for its ability to predict a minimum velocity for foam generation, propagation and foam stability. We examine the nonlinear behaviour represented in some of these models that allows them to represent multiple foam states as illustrated in Fig. 1c. In the case of the STARS foam model we offer the first examination of its model for foam generation and propagation in a simulation of radial flow. The model of Chen et al. (2010) and the variants (Kovscek and Radke, 1994; 1995) was not designed to include a critical velocity for foam generation (Kovscek and Radke, 1993). Because of the complexity of that model, we are unable to state conclusively whether it could represent a minimum velocity for foam generation or multiple foam steady states. Instead, we define conditions that the choice of model parameters/coefficients would have to satisfy in order to represent a critical superficial velocity for foam generation.

We also identify for the first time a critical issue in models where foam generation depends on pressure gradient: the failure of conventional simulators to represent explicitly the pressure gradient at an injection well within a grid block.

Chapter 5 summarizes the conclusions and implications drawn from the experimental and modelling results of this study. We also propose extensions of this work (experiment and modeling) that deserve further research.

References

Alagorni, A., Yaacob, Z., and Nour, A. (2015). An Overview of Oil Production Stages: Enhanced Oil Recovery Techniques and Nitrogen Injection. *International Journal of Environmental Science and Development*. 6(09): 693-701. https://doi.org/doi:10.7763/IJESD.2015.V6.682

Al Ayesh, A. H., Salazar, R., Farajzadeh, R., Vincent-Bonnieu, S., and Rossen. W. R. (2017). Foam Diversion in Heterogeneous Reservoirs: Effect of Permeability and Injection Method. *SPE J.* 22(05): 1402–1415. Apr, 2017, https://doi.org/10.2118/179650-PA

Apaydin, O. G., and Kovscek, A. R. (2001). Surfactant Concentration and End Effects on Foam Flow in Porous Media. *Transport in Porous Media*. 43, 511–536. https://doi.org/10.1023/A:1010740811277

Aronson, A. S., Bergeron, V., Fagan, M.E., and Radke, C. J. (1994). The influence of disjoining pressure on foam stability and flow in porous media. *Colloids and Surfaces A: Physicochemical and Engineering Aspects*. 83(02), 109-120. https://doi.org/10.1016/0927-7757(94)80094-4

Ashoori, E.; Marchesin, D.; and Rossen, W.R. (2012). Multiple Foam States and Long-Distance Foam Propagation in Porous Media. *SPE J.* 17(04): 1231-1245, Dec 2012, SPE-154024-PA, https://doi.org/10.2118/154024-PA

Ashoori, E., Marchesin, D., & Rossen, W. R. (2011). Dynamic foam behaviour in the entrance region of a porous medium. *Colloids and Surfaces A: Physicochemical and Engineering Aspects*, 377(1-3): 217-227, https://doi.org/doi:10.1016/j.colsurfa.2010.12.043

Bergeron, V., & Radke, C. J. (1992). Equilibrium Measurements of Oscillatory Disjoining Pressures in Aqueous Foam Films. *Langmuir* 8 (12): 3020-3026. https://doi.org/doi:10.1021/la00048a028

Bergeron, V., & Radke, C. J. (1995). Disjoining Pressure and Stratification in Asymmetric Thin-liquid Films. *Colloid Polym Sci*, 273**:** 165–174. https://doi.org/10.1007/BF00654014

Bergeron, V. (1997). Disjoining Pressure and Film Stability of Alkyltrimethylammonium Bromide Foam Films. *Langmuir* 13(13), 3474-3482. https://doi.org/10.1021/la970004q

Bethel, F. T., & Calhoun, J. C. (1953). Capillary Desaturation in Unconsolidated Beads. *J Pet Technol*, 5(08): 197-202. https://doi.org/10.2118/953197-G

Bikerman, J. J. (1973). Foams. Springer: New York.

Chen, Q., Gerritsen, M. G., & Kovscek, A. R. (2010). Modeling Foam Displacement with the Local-Equilibrium Approximation: Theory and Experimental Verification. *SPE J.* 15 (01): 171–183, https://doi.org/10.2118/116735-PA.

Cheng, L., Reme, A. B., Shan, D., Coombe, D. A., and Rossen, W. R. (2000). Simulating Foam Processes at High and Low Foam Qualities. Paper presented at the SPE/DOE Improved Oil Recovery Symposium, Tulsa, Oklahoma, April 2000. https://doi.org/10.2118/59287-MS

Dykstra, H. and Parsons, R. L. (1950). The Prediction of Oil Recovery by Waterflooding in Secondary Recovery of Oil in the United States. 2nd Edition, API: Washington DC.

Falls, A. H., Hirasaki, G. J., Patzek, T. W., Gauglitz, P. A., Miller, D. D., & Ratulowski, J. (1988). Development of a mechanistic foam simulator: The population balance and generation by snap-off. *SPERE* 3(03): 884–892. https://doi.org/10.2118/14961-PA

Farajzadeh, R., Andrianov, A., and Zitha, P. L. J. (2009). Investigation of immiscible and miscible foam for enhancing oil recovery. *Ind Eng Chem Res* 49(4):1910–9. https://doi.org/10.1021/ie901109d.

Foster, W. R. (1973). A Low-tension Waterflooding Process, *Journal of Petroleum Technology* 25: 205-210. https://doi.org/10.2118/3803-PA.

Friedmann, F., Chen, W.H., Gauglitz, P.A. (1991). Experimental and simulation study of high-temperature foam displacement in porous media. *SPERE* 6(01): 37–45. https://doi.org/10.2118/17357-PA

Friedmann, F., Smith, M.E., Guice, W.R., Gump, J.M., Nelson, D.G. (1994). Steam-foam mechanistic field trial in the midway-sunset field. *SPERE* 9(04): 297–304. https://doi.org/10.2118/21780-PA

Gauglitz, P. A., Friedmann, F., Kam, S. I., and Rossen, W. R. (2002). Foam Generation in Porous Media. *Chem. Eng. Sci.* 57: 4037–4052. https://doi.org/10.1016/S0009-2509(02)00340-8

Green, D. W., & Willhite, G. P. (2018). Enhanced Oil Recovery, Second Edition. Society of Petroleum Engineers, Richardson, TX, USA.

Haines, W. (1927). Studies in the physical properties of soils: IV. A further contribution to the theory of capillary phenomena in soil. The Journal of Agricultural Science, 17(2), 264-290. https://doi.org/10.1017/S0021859600018499

Hirasaki, G. J., Jackson, R.E., Jin, M., Lawson, J.W., Londergan, J., Meinardus, H., Miller, C.A., Pope, G.A., Szafranski, R., and Tanzil, D. (2000). Field Demonstration of the Surfactant/Foam Process for Remediation of a Heterogeneous Aquifer Contaminated With DNAPL, *NAPL Removal: Surfactants, Foams, and Microemulsions.* Fiorenza, S., Miller, C.A., Oubre, C.L., and Ward, C.H. Editors. Lewis Publishers, Boca Raton, (2000), 1-166.

Hirasaki, G.; Miller, C.; Szafranski, R.; Tanzil, D.; Lawson, J.B.; Meinardus, H.; Jin, M.; Londergan, J.T.; Jackson, R.; Pope, G.A.; Wade, W.H. (1997). Field Demonstration of the Surfactant/Foam Process for Aquifer Remediation. Paper 39292 presented at the SPE Annual Technical Conference and Exhibition, San Antonio, TX, October 1997. https://doi.org/10.2523/39292-MS .

Jenkins, M. K. (1984). An Analytical Model for Water/Gas Miscible Displacements. SPE-12632-MS, presented at the 1984 SPE/DOE Symposium on Enhanced Oil Recovery, Tulsa, OK, 15-18 April.

Jiménez, A. I., & Radke, C. J. (1989). Dynamic Stability of Foam Lamellae Flowing Through a Periodically Constricted Pore, *Oil-Field Chemistry.* July 10, 1989, 460-479. https://doi.org/10.1021/bk-1989-0396.ch025 .

Kahrobaei, S., and Farajzadeh, R. (2019). Insights into Effects of Surfactant Concentration on Foam Behavior in Porous Media. *Energy & Fuels* **33** (2), 822-829 https://doi.org/10.1021/acs.energyfuels.8b03576

Kam, S.I. and Rossen, W.R. (2003). A Model for Foam Generation in Homogeneous Media, *SPE J.* 8(04): 417-42, Dec 2003. https://doi.org/10.2118/87334-PA.

Kam, S.I.; Nguyen, Q.P.; Li, Q. and Rossen, W.R. (2007). Dynamic Simulations With an Improved Model for Foam Generation, *SPE J.* 12(01): 35-28. https://doi.org/10.2118/90938-PA.

Kam, S.I. (2008). Improved Mechanistic Foam Simulation with Foam Catastrophe Theory, *J Coll & Surf A* 318(1-3): 62-77, https://doi.org/10.1016/j.colsurfa.2007.12.0417.

Khatib, Z.I., Hirasaki, G.J., and Falls, A.H. (1988). Effects of Capillary Pressure on Coalescence and Phase Mobilities in Foams Flowing Through Porous Media. *SPERE.* 3(3): 919926. https://doi.org/10.2118/15442-PA .

Kibodeaux, K.R. and Rossen, W.R. (1997). Coreflood Study of Surfactant-Alternating-Gas Foam Processes: Implications for Field Design. Paper SPE 38318 presented at the SPE Western Regional Meeting, Long Beach, California, 25–27 June. https://doi.org/10.2118/38318-MS .

Kovscek, A. R., & Radke, C. J. (1994). Fundamentals of foam transport in porous media. In: L. L. Schramm (Ed.), Foams: Fundamentals and applications in the petroleum industry. Washington DC: ACS Advances in Chemistry Series No. 242 (Am. Chem. Soc.).

Kovscek, A. R., Patzek, T. W., and Radke, C. J. (1995). A Mechanistic Population Balance Model for Transient and Steady-State Foam Flow in Boise Sandstone. *Chem. Eng. Sci*. 50: 3783–3799. https://doi.org/10.1016/0009-2509(95)00199-F

Lake, L. W. 1989. Enhanced Oil Recovery. Prentice-Hall, Englewood Cliffs, NJ.

Lawson, J. B., & Reisberg, J. (1980). Alternate Slugs of Gas and Dilute Surfactant for Mobility Control during Chemical Flooding. Paper presented at the SPE/DOE Enhanced Oil Recovery Symposium, 20-23 April, 1980, Tulsa, OK. https://doi.org/10.2118/8839-MS

Leverett, M. C. (1941). Capillary Behavior in Porous Solids. *Trans. AIME.* 142(01): 152-169. https://doi.org/10.2118/941152-G

Lotfollahi, M., Kim, I., Beygi, M. R., Worthen, A. J., Huh, C., Johnston, K. P., DiCarlo, D. A. (2016). Experimental Studies and Modeling of Foam Hysteresis in Porous Media. *SPE J.* https://doi.org/10.2118/179664-MS.

Lotfollahi, M., Farajzadeh, R., Delshad, M., Varavei, A., and Rossen, W. R. (2016). Comparison of implicit-texture and population-balance foam models. *J. Natural Gas Sci. Eng*. 31: 184-197.

Osterloh, W.T., Jante, M.J. (1992). Effect of Gas and Liquid Velocity on Steady-state Foam Flow at High Temperature. Paper presented at the SPE/DOE Enhanced Oil Recovery Symposium, Tulsa, Oklahoma, April 1992. https://doi.org/10.2118/24179-MS.

Prieditis J. (1989). A pore level investigation of foam flow behavior in porous media. PhD dissertation, University of Houston.

Qi, L. Q. & Feng, H. Q. (1998). Optimum Amount of Polymer Injection in Polymer Flooding. In Chemical Flooding Symposium-Research Results during the Eighth Five-Year Period (1991-1995), first edition. Ed. Q.-L. Gang, Vol. 1. Petroleum Industry Press, Beijing.

Roof, J.G. (1970) Snap-Off of Oil Droplets in Water-Wet Pores. Journal of Society of Petroleum Engineers. *SPE J*. 10(01): 85-90. Mar 1970. http://dx.doi.org/10.2118/2504-PA

Rossen, W. R. and Gauglitz, P. A. (1990). Percolation Theory of Creation and Mobilization of Foam in Porous Media. *AIChE J*. 36: 1176–1188. https://doi.org/10.1002/aic.690360807

Rossen, W. R. (1992). Rheology of foam in porous media at the limiting capillary pressure. *Revue de l'Institute France du Petrole* 47: 68-80. https://doi.org/10.3997/2214-4609.201411236

Rossen, W. R., Shi, J., Zeilinger, S. C. (1994). Percolation modeling of foam generation in Porous media. *AIChE J*. 40(06): 1082-1084, June 1994. https://doi.org/10.1002/aic.690400618

Rossen, W.R. (1996). Foams in Enhanced Oil Recovery, in: Prud'homme, R.K., Khan, S. Foams: Theory, Measurements, and Applications, Surfactant science series Vol. 57, Chap 11, Marcel Dekker, Inc. 270 Madison Avenue, New York 10016.

Rossen, W. R., and van Duijn, C. J., (2004). Gravity Segregation in SteadyState Horizontal Flow in Homogeneous Reservoirs. *J. Petr. Sci. Eng.* 43: 99-111. https://doi.org/10.1016/j.petrol.2004.01.004

Rossen, W. R., and Chun, S. (2007). Gravity Segregation in Gas-Injection IOR. Paper presented at the EUROPEC/EAGE Conference and Exhibition, London, U.K., June 2007. https://doi.org/10.2118/107262-MS.

Rossen, W. R., van Duijn, C. J., Nguyen, Q. P., and Vikingstad, A. K. (2010). Injection Strategies to Overcome Gravity Segregation in Simultaneous Gas and Liquid Injection Into Homogeneous Reservoirs. Paper SPE 99794 presented at the 2006 SPE/DOE Symposium on Improved Oil Recovery, Tulsa, OK, 22-26 April. https://doi.org/10.2118/99794-MS

Shah, S. Y., Wolf, K. H., Rashidah, M. P., and Rossen. W. R. (2019). Foam Generation by Capillary Snap-Off in Flow Across a Sharp Permeability Transition. *SPE J*. 24(01): 116–128. https://doi.org/10.2118/190210-PA.

Shi, J. X., & Rossen, W. R. (1998). Improved Surfactant-Alternating-Gas Foam Process To Control Gravity Override. Paper SPE 39653 prepared for presentation at the SPE/DOE Improved Oil Recovery Symposium, Tulsa, 19–22 April. https://doi.org/10.2118/39653-MS.

Smith, C. L., Anderson, J. L., and Roberts, P. G. (1969). New Diverting Techniques for Acidizing and Fracturing. Paper SPE 2751, presented at the 1969 SPE California Regional Meeting, San Francisco, 6–7 November.

Stone, H. L. (1982). Vertical Conformance in an Alternating Water-Miscible Gas Flood. Paper presented at the SPE Annual Tech. Conf. and Exhibition, New Orleans, LA, Sept 1982. https://doi.org/10.2118/11130-MS

Stone, H. L. (2004). A Simultaneous Water and Gas Flood Design with Extraordinary Vertical Gas Sweep. Paper presented at the SPE International Petroleum Conference in Mexico, Puebla Pue, Mexico, Nov 2004. https://doi.org/10.2118/91724-MS

Tang, J., Smit, M., Vincent-Bonnieu, S., and Rossen, W. R. (2019). New Capillary Number Definition for Micromodels: The Impact of Pore Microstructure. *Water Resources Research*. 55: 1167-1178. https://doi.org/10.1029/2018WR023429

Willhite, G. P. (1986). Waterflooding. Society of Petroleum Engineers: Richardson, TX.

Young, T. (1805) An Essay on the Cohesion of Fluids. *Philosophical Transactions of the Royal Society of London*. 95: 65-87. http://dx.doi.org/10.1098/rstl.1805.0005

Yu, G. Y., Rossen, W. R., and Sebastien, V.B. (2020). Foam Propagation at Low Superficial Velocity: Implications for Long-Distance Foam Propagation. *SPE J.* 25(06): 3457–3471. https://doi.org/10.2118/201251-PA.

Zerhboub, M., Ben-Naceur, K., Touboul, E. (1994). Matrix acidizing: A novel approach to foam diversion. *SPE Prod & Fac.* 9(02): 121–126. https://doi.org/10.2118/22854-PA.

Zhou, Z. H. and Rossen, W. R. (1995). Applying Fractional-Flow Theory to Foam Processes at the 'Limiting Capillary Pressure'. *SPE Advanced Technology Series.* 3(01): 154–162. https://doi.org/10.2118/24180-PA

Chapter 2

Effect of Surfactant Concentration on Foam Generation in Porous Media

Abstract

The propagation of foam in an oil reservoir depends on the creation and stability of the foam in the reservoir, specifically the creation and stability of foam films, or lamellae. As the foam propagates far from in injection well, superficial velocity and pressure gradient decrease with distance from the well. Experimental (Friedmann et al., 1994) and theoretical (Ashoori et al., 2011) studies relate concerns about foam propagation at low superficial velocity to the minimum velocity or pressure gradient for foam generation near the well (Rossen and Gauglitz, 1990; Gauglitz et al., 2002). The objective of this work is to measure the impact of surfactant concentration and gas fractional flow on foam generation. Theory (Rossen and Gauglitz., 1990; Kam and Rossen, 2003) relates foam generation to gas fractional flow and, indirectly, to the stability of foam films, or lamellae, which in turn depends on surfactant concentration (Apaydin and Kovscek, 2001). However, the link between foam generation and surfactant concentration has not been established experimentally.

In our experiments, nitrogen foam is generated in a core of Bentheimer sandstone. The foam-generation experiments consist of measuring the minimum velocity for foam generation as a function of gas fractional flow at three surfactant concentrations well above the critical micelle concentration (CMC). Experimental results show that the minimum velocity for foam generation decreases with increasing liquid fraction, as shown by previous foam-generation studies (Rossen and Gauglitz, 1990; Friedmann et al., 1994). Additionally, our results show that this velocity decreases with increasing surfactant concentration, far above the CMC. We also propose a workflow for screening out the experimental artefacts that can distort the trigger velocity.

2.1 Introduction

Gas-injection enhanced oil recovery (EOR) can efficiently displace oil (Mortis, 1990; Rossen, 1996; Lake et al., 2014). However, gas-injection EOR suffers from poor sweep efficiency and may achieve limited oil recoveries in field applications (Rossen, 1996; Lake et al., 2014), primarily due to low gas viscosity (leading to fingering and channelling), low gas density (leading to gravity override) and geological heterogeneity. Reducing the relative mobility of gas thus becomes a major challenge for gas-injection EOR. Foam can provide mobility control for gas flooding. Foam is a dispersion of gas bubbles in an aqueous phase, stabilized by surfactant molecules at the gas-liquid interfaces. When foam is generated in porous media, the flow paths of gas are blocked by liquid films, or lamellae, while the liquid phase remains continuous. The lamellae blocking the gas phase add additional capillary resistance to gas flow and thereby make the gas phase less mobile.

The conditions for foam generation depend in part on the method of injection. In our experiments, we consider steady gas and liquid injection at a fixed gas fraction, where gas has already been injected for a time before surfactant is added to the system (Rossen and Gauglitz, 1990). This initial state is relevant to the propagation of a foam front far from a well, where alternating slugs of gas and liquid have mixed and where gas has advanced ahead of the foam front. During these steady-state experiments, foam is created in the porous medium by co-injecting gas and surfactant solution at a fixed gas fraction; foam generation requires exceeding a minimum superficial velocity u_t^{min}, or pressure gradient ∇p^{min} (Rossen and Gauglitz, 1990). For consistency, we rename the critical velocity and pressure gradient for foam generation as u_t^{gen} and ∇p^{gen} in all the chapters of this dissertation. It is pressure gradient ∇p, not total superficial velocity u_t, that triggers foam generation, but results are often reported in terms of u_t^{min}, which is easier to control and measure in the laboratory. "Foam generation", in this context, refers to an abrupt jump from a state of high gas mobility to one of very low mobility. This abrupt change depends on the rate of lamella creation exceeding the rate of lamella destruction in the porespace (Kovscek et al., 1995; Falls et al., 1988), leading to a spontaneous run-away process and a jump in state (Kam and Rossen, 2003; Kam, 2008). In this paper, we refer to this minimum pressure gradient or superficial velocity as the 'trigger' for foam generation.

The triggers u_t^{gen} and ∇p^{gen} depend on the volume fraction of gas injected (also defined as foam quality f_g). Foam generation at a larger foam quality f_g requires a greater triggering velocity u_t^{gen} (Rossen and Gauglitz., 1990). In the vicinity of an injection well, in-situ foam generation and foam propagation are usually easy due to large superficial velocity and pressure gradient. Alternating injection of gas and surfactant solution also contributes to a success of foam generation near the injection well (Rossen, 1996). The real concern for generation and propagation, therefore, lies in locations far from the injection well, where both superficial velocity and pressure gradient are low (Friedmann et al., 1994; Ashoori et al., 2011). Hence, the minimum velocity for foam generation and propagation in porous media is of great importance to foam application.

Previous experimental studies (Gauglitz et al., 2002; Kam, 2008) haven't identified a strong connection between the minimum velocity for foam generation and surfactant concentration. The mechanisms of individual lamella generation (leave-behind, snap-off, and lamella mobilization) are not believed to depend on the presence of surfactant (Gauglitz and Radke., 1989; Ransohoff and Radke, 1988). For a given homogeneous porous medium, the trigger velocity and pressure gradient for foam generation depend on the capillary resistance of a lamella to be displaced from a pore throat and subsequent division (Rossen and Gauglitz, 1990). This resistance is proportional to the gas-liquid surface tension γ. Therefore, the minimum condition for foam generation depends on surface tension, but this dependence

affects foam generation only for surfactant concentrations below the critical micelle concentration (CMC).

The survival of lamellae once created, however, does depend on surfactant formulation and concentration (Rossen, 1996). Foam generation therefore requires not only production of lamellae in the porous medium, but also the survival of the newly created lamellae. The greater the lamella-destruction rate (either due to ineffective surfactant or insufficient surfactant concentration), the greater the lamella-creation rate needed to generate foam. The stability of foam in porous media, reflected in the limiting capillary pressure P_c^* or water saturation S_w^* for foam stability, increases with increasing surfactant concentration far above the CMC (Apaydin and Kovscek, 2001; Jones et al., 2016). Therefore, one would expect that increasing surfactant concentration reduces the minimum superficial velocity or pressure gradient for foam generation by reducing the rate of lamella breakage. However, this link has not been demonstrated experimentally. In this paper we present experimental verification of the connection between the minimum velocity for foam generation and surfactant concentration for one surfactant formulation. We also propose a workflow for identifying the triggering velocity and screening out the experimental artefacts. We relate the experimental results to a population-balance model for foam generation. The model agrees with the trends of the experimental results.

2.2 Experiments on foam generation

2.2.1 Experimental method and materials

In our experiments, foam is generated in-situ by co-injecting surfactant solution and nitrogen into a homogeneous Bentheimer sandstone core at a back-pressure of 40 bar and a temperature of 30°C. The main objective of our experiments is to map out the minimum total superficial velocity u_t^{min} required to trigger foam generation for different foam qualities (gas fractional flow) f_g and three surfactant concentrations C_s. Based on the measurement of the CMC by Jones *et al*. (2016), all three surfactant concentrations are far above the CMC, which is approximately 0.005 wt% for our surfactant with 3.0 wt% NaCl.

We use the same surfactant, Sodium C14-16 Alpha Olefin Sulfonate (AOS-1, Bioterge AS-40), for all experiments. Both brine and surfactant solutions contain 3 wt% NaCl. Fig. 2.1 shows the experimental apparatus. The Bentheimer core is 17 cm in length, with a diameter of 1 cm. The permeability of the core is 1.87×10^{-12} m^2. Four absolute-pressure transducers are located along the core. Two of them are located on the inlet and outlet lines, respectively, while the other two are in direct contact with the core. The core is thus divided into three sections, with inlet and outlet sections 5.25 cm long, and the middle section 6.5 cm long (Fig. 2.1). Three different surfactant concentrations are tested for impact on foam generation: 0.1 wt%, 0.3 wt% and 0.5 wt% (Table 2.A1 in Appendix 2.A).

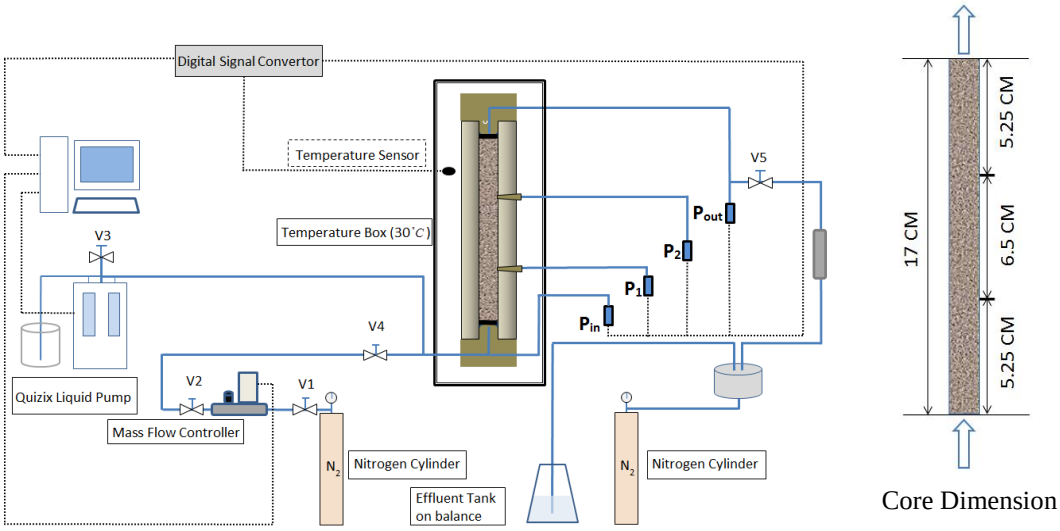

Figure 2.1. Experimental apparatus for foam-generation experiments. The core is mounted vertically in an oven at a temperature of 30℃. Four absolute-pressure meters are connected along the core, with pressure ranges of 120 bar. Gas and liquid are injected from the bottom and exit from the top. A small metal container is connected between the last pressure meter P_{out} and the back-pressure regulator to stabilize pressure in the outlet section of the core.

A small pressure cell of volume 150 ml lies between the core and the back-pressure regulator (BPR) to mitigate any fluctuations at the BPR. Since, as mentioned above, pressure gradient is thought to play an essential role in foam generation, any sudden increase or decrease in back-pressure would lead to an abrupt change in pressure gradient at the outlet of the core. In such cases, foam generation could be triggered near the outlet.

The core is initially fully saturated with brine. Then N_2 and brine are co-injected at constant gas fractional flow. After steady state is achieved, brine injection is replaced by injection of surfactant solution at the same injection rate and fractional flow of gas. After 1 pore volume of surfactant solution has been injected, we begin the process of raising superficial velocity in steps until foam generation is triggered. At each step, we wait for a time to see if foam generation has occurred; details are given below. The trigger for foam generation could lie between the measured velocity at which foam generation occurs and the velocity just before it. The resulting uncertainty range for each experiment is illustrated by the error bars in the results shown below.

2.2.2 Experimental artifacts and screening criteria

Our goal is to determine the velocity at which foam generation occurs in steady flow in a homogeneous porous medium. Identification of the foam trigger (with regard to either velocity or pressure gradient) can be problematic, and experimental results are typically scattered, as illustrated in Fig. 2.2. There are at least two experimental artefacts that contribute to the scatter: 1) the “incubation effect”, and 2) the capillary end effect. Both effects may lead to foam generation at superficial velocities lower than the minimum velocity u_t^{min}. These two effects are described below.

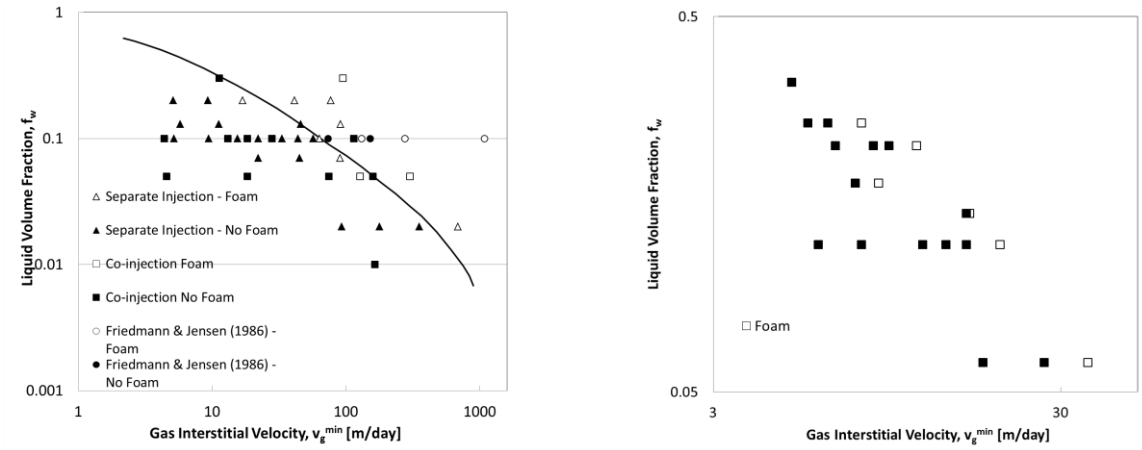

(a) **(b)**

Figure 2.2. (a) Minimum gas interstitial velocity required to trigger foam generation as a function of injected liquid volume fraction (or f_w, i.e., $(1-f_g)$). The plot is reproduced from data of Rossen and Gauglitz (1990). Trends superimposed on data are from a percolation-theory analysis for foam generation described in Rossen and Gauglitz. (b) A similar plot based on data from our experiments (C_s = 0.5 wt%). White dots represent the observed trigger velocity for the given injected liquid volume fraction, and black dots represent the velocities tested before the trigger of foam generation.

Baghdikian and Handy (1990), injecting liquid and gas into cores at steady, low velocities, observed a slow increase in ∇p until, many hours or even days later, there was an abrupt increase in ∇p over a period of minutes or hours: that is, "foam generation". They call this foam generation occurring after a delay the "incubation effect" (Chou, 1991; Huh and Handy, 1989; Rossen, 1996). The reason for this behavior is not clear, but it is likely the result of an accumulation of local perturbations in flow rates, foam quality, and capillary pressure, etc. over time, leading to creation of static lamellae and increasing pressure gradient (Rossen, 1996). We exclude these cases from our results, because we want to identify the point where velocity or pressure gradient triggers foam generation without the effects of extraneous fluctuations accumulated over time.

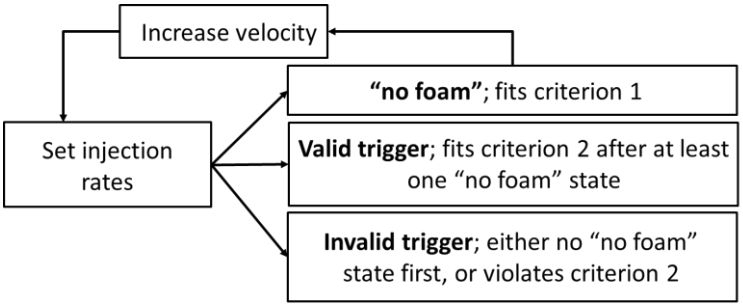

Figure 2.3. Experimental procedures for identification of a valid trigger velocity. Each experiment should begin at a superficial velocity lower than the trigger velocity. Three possible scenarios could play out at a particular velocity. (1) If no foam is created at this velocity (criterion 1), then a stepwise increase of superficial velocity is required, until a valid trigger, at which foam generation begins, is identified. (2) If foam generation takes place (meeting all conditions specified in criterion 2) after at least one "no foam" state, then a valid trigger velocity is identified. (3) If foam generation takes place at the very first injection rate, or any event(s) that violate criterion 2 take place during the process of velocity increase, the experiment is be aborted and repeated, until it meets both criteria and a valid trigger is identified.

The capillary end effect (Perkins, 1957; Douglas et al., 1958; Kyte and Rapoport, 1958) is another complicating artefact in foam-generation experiments. Apaydin and Kovscek (2001)

studied the role of surfactant concentration and end effects on foam flow in porous media. The classic capillary end effect is an accumulation of water near the outlet face of the porous medium caused by contact with fluid outside the porous medium at a capillary pressure of zero or near zero. The wet conditions near the core outlet are ideal for foam generation (Ransohoff and Radke, 1988; Rossen and Gauglitz, 1990). At larger surfactant concentrations, Apaydin and Kovscek (2001) reported, the end effect results in a larger pressure gradient building first near the outlet and propagating upstream, against the direction of flow, toward the inlet. Similar effects, where a large increase in pressure gradient first occurs near the outlet and then propagates upstream, are reported by Nguyen et al. (2003) and Simjoo et al**.** (2013). The mechanism of upstream propagation of a stronger foam state is unclear, but, in any case, the origin of the state is a result of the capillary end effect, and therefore it is not representative of a homogeneous porous medium. Hence, we exclude cases in which a large pressure gradient is created near the outlet and then propagates to or disturbs upstream core sections.

We define the trigger as the total superficial velocity at which foam is created quickly near the core inlet, without a long period of steady injection or propagation of foam first created near the outlet. Below we define the criteria to define a valid trigger velocity and to identify unacceptable cases. Fig. 2.3 illustrates how we identify a valid trigger according to two criteria:

1. The experiment should begin with at least one velocity lower than the trigger velocity for foam generation. In Fig. 2.3 we call this state "no foam" for simplicity. In reality, it could be a state with a modest reduction of gas mobility, or what Ransohoff and Radke (1988) refer to as a "leave-behind foam." At this velocity, there should be no significant pressure drop in any core section. There are two criteria to define the condition before the trigger:
   - 1a Pressure gradient along the entire core increases within the next 10-20 sec upon the increase of superficial velocity, and settles down to a new steady state quickly (usually within 20-30 sec). When the new steady state is achieved, the increase in pressure drop is of the same magnitude as the proportional increase in velocity from the previous step. Ideally this rule applies to all core sections. In many cases, however, the ΔP across the outlet section increases much more than proportionately with the velocity increase, and more than the pressure drop in other sections. We accept cases with a modest ΔP in the outlet section (no more than 1 bar, too little to affect gas volume or superficial velocity upstream) if the state of large ∇p doesn't migrate upstream to the second section. In other words, if there is foam generation near the outlet but this is not the cause of subsequent foam propagation to the inlet, we accept that case.
   - 1b Pressure gradient along the core should remain constant, without an upward trend, once a steady state is achieved. The period during which a steady pressure gradient is verified should be limited to avoid the "incubation effect" (see criterion 2a, below). We checked the steady-state of an injection rate for about 15 to 20 min, before raising injection rate to the next level. If the injection period lasts for more than 40-60 min, the incubation effect could compromise the validity of result.
2. The trigger should be characterized by a rapid increase in pressure drop in all sections while keeping injection rate and foam quality constant. Specifically
   - 2a The pressure drop across the first section rises steeply in the first section within 2 to 5 min of the increase in injection rate. The zone of large pressure gradient propagates from the first section downstream, but not from the last section upstream. A pressure rise occurring after, say, an hour of injection at a given rate could be a symptom of the incubation effect and unreliable.
   - 2b At the trigger, the magnitude of increase in ΔP is larger, and the period to reach the new steady state is longer (20-40 min), than in the steps before the trigger. The magnitude of gradient of the newly formed steady-state should be substantially greater (10 to 100 times) than the pressure gradient before the trigger.

If and only if both criteria are satisfied in our experiment, we identify the minimum velocity for generation for the given surfactant concentration and foam quality. We denote this total superficial velocity as u_t^{min} below. If any of the above criteria are violated, the result of this experiment is discarded. The experiment should be repeated until a valid trigger is identified. Fig. 2.4 shows examples of both valid (Fig. 2.4a) and invalid (Fig. 2.4b) experimental results.

2.3 Results

Our results (Figs. 2.5 and 2.6) show that: 1) the minimum superficial velocity u_t^{min} required to trigger foam generation increases with decreasing liquid fractional flow f_w, and 2) u_t^{min} decreases with increasing surfactant concentration in the aqueous phase. Foam generation is easier for wetter foam (greater f_w) and at higher surfactant concentration, even far above the CMC. The trend on this log-log plot (Fig. 2.5) is roughly linear for each surfactant concentration. There is some scatter in the data, as in Fig. 2.2, and some overlap between the data at some surfactant concentrations.

Fig. 2.6 shows the regression lines as well as the 95% confidence intervals for the trends (Wonnacott and Wonnacott, 1972) for the three surfactant concentrations used in our experiments. Although there is some overlap between the data for different surfactant concentrations, there is relatively little overlap between the confidence intervals for the trends at 0.1 and 0.3 wt% concentrations. There is no overlap between the top two trends and that at the bottom for 0.5 wt% concentration. In summary, surfactant concentration has an effect on foam generation that transcends the scatter in the individual data.

2.4 Modeling the foam trigger

The population-balance model of Kam and Rossen (2003) and its variants (Kam et al., 2007; Kam, 2008) is the only population-balance model that has been shown to explain the minimum velocity for foam generation seen in experiments (Gauglitz et al., 2002). Like other population-balance models, this model represents foam texture explicitly, with rates of lamella creation and lamella coalescence defined by two functions. In this model, the rate of lamella creation depends on pressure gradient. Similar to other population-balance models, the rate of lamella destruction is controlled by water saturation and the limiting water saturation S_w^*, a parameter related to the limiting capillary pressure for foam destruction, P_c^* via the capillary-pressure/saturation function $P_c(S_w)$ (Khatib et al., 1988; Zhou and Rossen, 1995; Apaydin and Kovscek, 2001; Ma et al., 2013). As noted above, the process of lamella creation is not believed to depend on surfactant concentration; this assumption is incorporated into various population-balance models (Friedmann et al., 1991; Kam and Rossen, 2003; Kovscek et al., 1995). S_w^* and P_c^* do depend on surfactant concentration far above the CMC (Apaydin and Kovscek, 2001; Jones et al., 2016).

Fig. 2.7 shows the relationship between pressure gradient and superficial velocity predicted by the model for one value of S_w^*. The trigger for foam generation is the maximum velocity on the lower (weak-foam) branch, where the function bends back toward lower values of superficial velocity. The values of f_w and u_t at this maximum represent the relation between foam quality and minimum velocity for foam generation for one value of S_w^*. Fig. 2.8 shows how the trend shifts with S_w^* and, by implication, with surfactant concentration.

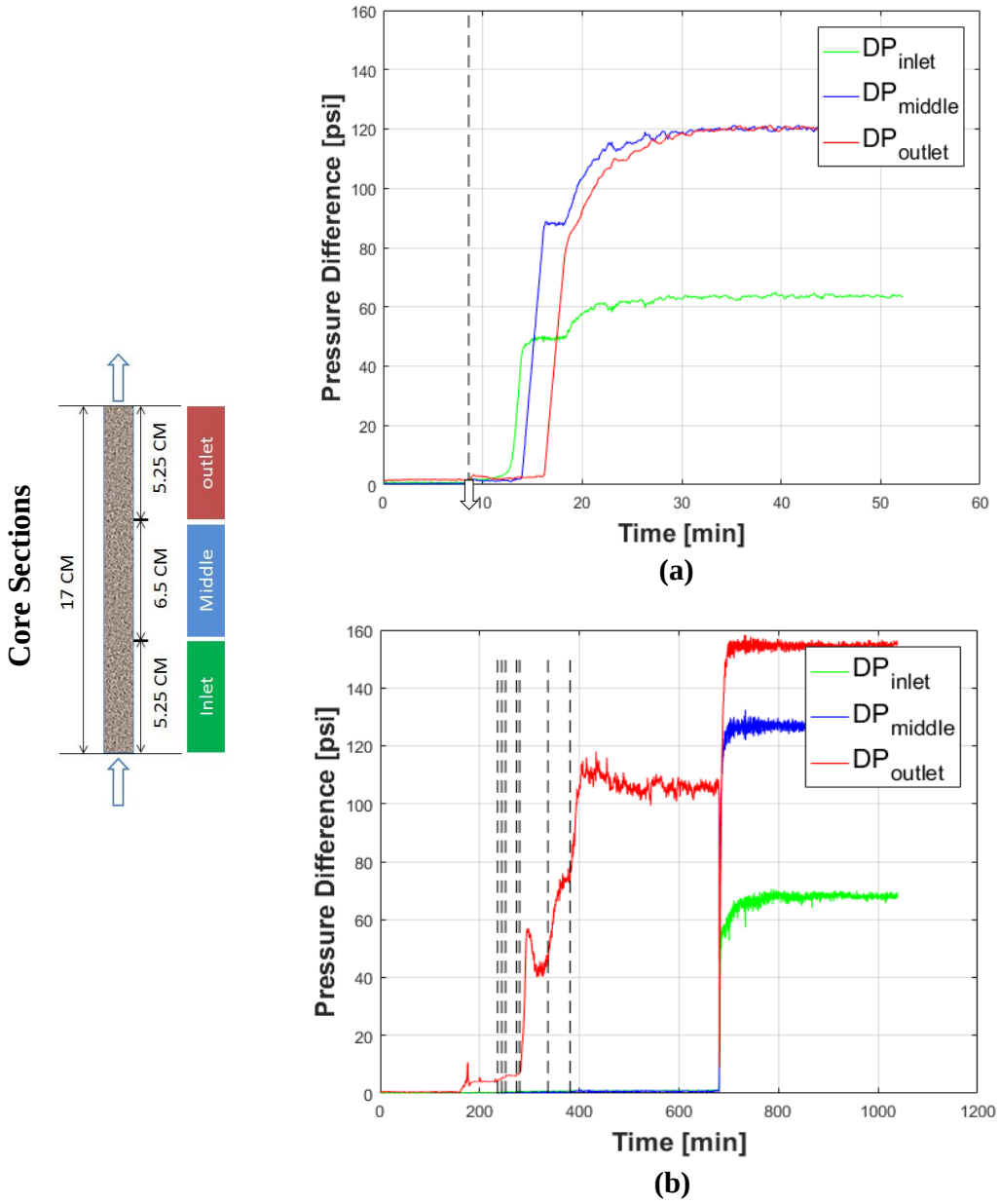

Figure 2.4. (a) A valid finding of a trigger velocity (C_s = 0.3 wt%, f_g = 85.04%). Upon the increase in injection rate at after about 8½ min. co-injection of surfactant solution and nitrogen (dashed vertical line), foam generation is triggered in the inlet section within 5 min. and propagates downstream. (b) An invalid result (C_s = 0.3 wt%, f_g = 87.98 %). Strong foam is created in the first section (at around 160 min.) but does not propagate. After several increases in injection rate (vertical dashed lines) foam propagates downstream. However, the delay before the start of propagation (around 300 min.) makes the result ambiguous: possibly a reflection of the "incubation effect." It is also odd that foam is created in the first section but fails to propagate downstream until injection rate is raised several times.

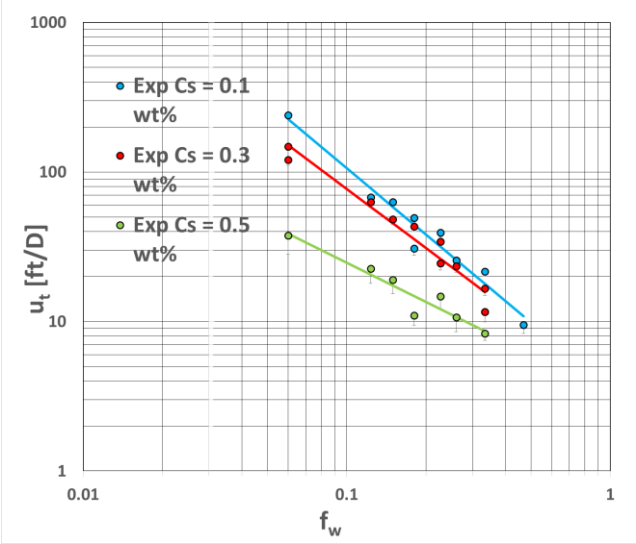

Figure 2.5. Experimental results for the trigger velocity for foam generation versus liquid fractional flow f_w for three different surfactant concentrations. Data plotted on log-log scale approximate a linear trend (solid lines) for each surfactant concentration; the least-squares fit to each trend is also shown. The error bars (below data points) represent the difference between the trigger velocity and the velocity tested immediately before it.

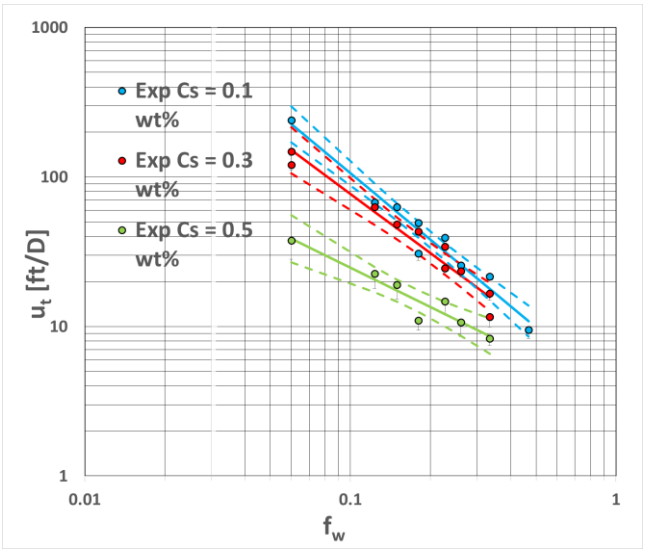

Figure 2.6. Estimated linear regression lines (solid lines) and 95% confidence intervals (dashed curves) for the underlying trends of the three surfactant concentrations. Markers represent the experimental results, as in Figure 2.5.

The trend in superficial velocity u_t against pressure gradient ∇p predicted by the model of Kam and Rossen (2003) (Fig. 2.8) is similar to our experimental results (Figs. 2.5 and 2.6). The model parameters (Eqs. A1, A2, Table 2.A2) were fit to data for a different foam formulation in a different porous medium. We present the model results with this set of parameters merely to indicate the trend predicted by the model. A quantitative fit would require fitting all the parameters, possibly adjusting the functional forms used to represent lamella creation as a function of ∇P and lamella destruction as a function of S_w in the model, and determining the relation between S_w^* and surfactant concentration for this surfactant formulation in our porous medium.

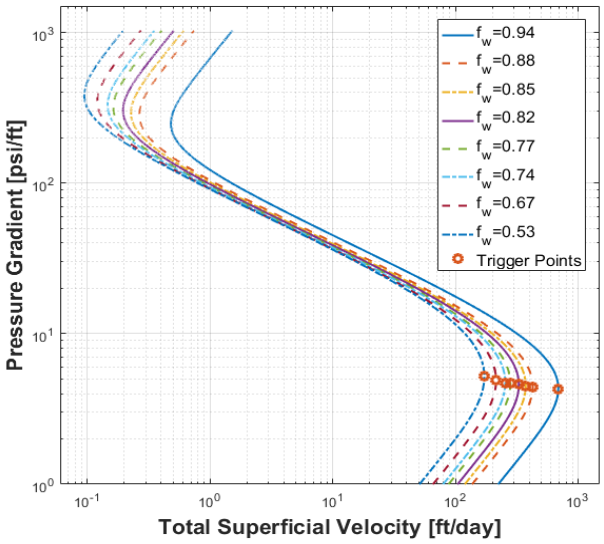

Figure 2.7. Steady-state total superficial velocity u_t as function of pressure gradient ∇p for given foam qualities f_g, from the population-balance model of Kam and Rossen (2003) with parameters from Appendix 2.A (specifically, $S_w^* = 0.201$, $S_{wc} = 0.2$). The lower branch represents the steady state of weak foam (or no foam); the upper branch represents the steady state of strong foam. The trigger for foam generation is the maximum of the lower branch (orange circles), where the $\nabla p(u_t)$ function bends back to lower superficial velocities. These maximum values produce the blue curve in Figure 2.8. In an experiment at fixed superficial velocity, there would be a jump from the weak/no-foam state to the strong-foam state at the maximum of the lower branch.

2.5 Conclusions

◊ Our data show that the minimum velocity for foam generation in steady flow decreases with increasing surfactant concentration and increasing injected liquid fractional flow (f_w).

◊ The impact of surfactant concentration on foam generation that we find in our results is in accord with the prediction of Kam and Rossen's population-balance model (2003), where the trigger velocity for foam generation increases with increasing foam quality f_g, and decreases with increasing surfactant concentration C_s (reflected as S_w^* in Kam and Rossen's model). This reflects an indirect link between lamella stability and foam generation, because creation of foam in porous media depends on the stability of lamellae.

◊ Foam generation is closely related to foam propagation. The stability and transport of bubbles at the leading edge of displacement front requires further investigation. However, our results suggest that foam propagation has a similar dependency on water fractional flow and surfactant concentration: wetter foam and greater surfactant concentration promote the transport of foam, even at surfactant concentrations far above the CMC.

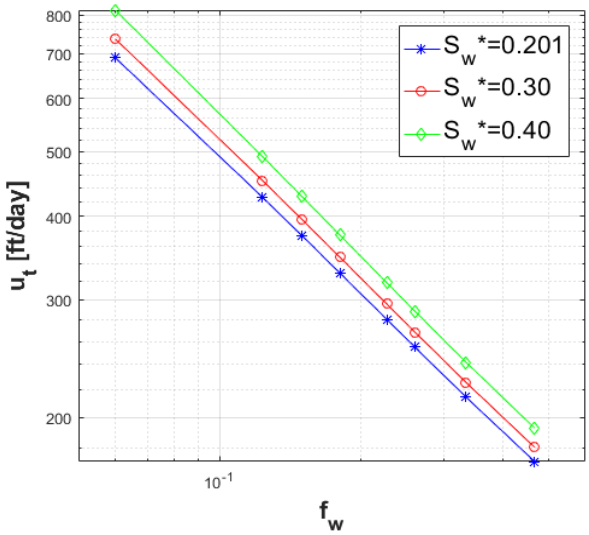

Figure 2.8. Prediction of model of Kam and Rossen (2003) of minimum superficial velocity for foam generation as function of liquid fractional flow f_w and limiting liquid saturation S_w^*.

Nomenclature

C_g	=	model parameter (Table 2.A2)
C_c	=	model parameter (Table 2.A2)
C_s	=	surfactant concentration, expressed as [wt%]
f_g	=	gas fractional flow
f_w	=	water fractional flow
k	=	permeability, [m^2]
k_{rg}	=	gas relative permeability in absence of foam
k_{rw}	=	water relative permeability
m	=	model parameter (Table 2.A2)
n	=	model parameter (Table 2.A2)
n_f	=	foam texture or density, inversely related to bubble size (Eq. 2.A2), [m^{-3}]
∇P	=	magnitude of pressure gradient
ΔP	=	pressure drop across core or section of core
∇P^{min}	=	minimum pressure gradient required to trigger foam generation
P_c	=	capillary pressure [Pa]
P_c^*	=	limiting capillary pressure [Pa]
S_w^*	=	limiting water saturation – water saturation at limiting capillary pressure
S_{gr}	=	trapped/residual gas saturation
S_w	=	water saturation
S_{wc}	=	connate water saturation (Eq. 2.A1)
u_g	=	gas superficial velocity (Darcy velocity), [m/s] in calculations, [ft/D] in figures and texts
u_w	=	water superficial velocity (Darcy velocity), [m/s] in calculations, [ft/D] in figures and texts
u_t	=	total superficial velocity (Darcy velocity), [m/s] in calculations, [ft/D] in figures and texts
$u_{t,c}$	=	minimum total superficial velocity (Darcy velocity) required for triggering of foam generation, [m/s] in calculations, [ft/D] in figures and texts
v_g^{min}	=	minimum gas interstitial velocity required for triggering of foam generation, defined in Fig. 2.2
μ_g^0	=	gas viscosity in absence of foam [Pa s]
μ_w	=	water viscosity [Pa s]
ϕ	=	porosity
σ	=	surface tension (Table 2.A2), shown here in unit of [N/m]

References

Ashoori, E.; Marchesin, D.; and Rossen, W.R. Roles of Transient and Local Equilibrium Foam Behaviour in Porous Media: Traveling Wave. 2011, *Colloids Surf. A.* 337(1-3): 228-242.

Apaydin, O.G. and Kovscek, A.R. Surfactant Concentration and End Effects on Foam Flow in Porous Media. 2001, *Transport in Porous Media*. 43: 511-536.

Baghdikian, S. and Handy, L.L. (1990). Flow of Foaming Solutions in Porous Media. *Modification of Chemical and Physical Factors in Steam-flood to Increase Heavy Oil Recovery*. Y. C. Yortsos, U. S. Dept. Energy Ann. Rep., DOE/BC/14126-14, Bartlesville, OK.

Chou, S.I. (1991). Conditions for Generating Foam in Porous Media, in: Paper *SPE22628* Presented at the SPE Annual Technical Conference and Exhibition, Dallas, TX.

Douglas, J.; Blair, P.M. and Wagner, R.J. (1958). Calculation of linear waterflood behaviour including the effect of capillary pressure. *Trans. AIME*. 214: 96-102.

Falls, A. H., Hirasaki, G. J., Patzek, T. W., Gauglitz, P. A., Miller, D. D., & Ratulowski, J. (1988). Development of a mechanistic foam simulator: The population balance and generation by snap-off. *SPERE* 3(03): 884–892. https://doi.org/10.2118/14961-PA

Friedmann, F., Chen, W.H., Gauglitz, P.A. (1991). Experimental and simulation study of high-temperature foam displacement in porous media. SPERE 6(01): 37–45. https://doi.org/10.2118/17357-PA

Friedmann, F., Smith, M.E., Guice, W.R., Gump, J.M., Nelson, D.G. (1994). Steam-foam mechanistic field trial in the midway-sunset field. SPERE 9(04): 297–304. https://doi.org/10.2118/21780-PA

Gauglitz, P.A. and Radke, C.J. (1989). The Dynamic of Liquid Film Breakup in Constricted Cylindrical Capillaries. *Colloid and Interface Science*. 134, No. 1.

Gauglitz, P.A.; Friedmann, F.; Kam, S.I. and Rossen, W.R. (2002). Foam Generation in Homogeneous Porous Media. *Chem. Eng. Sci.* 57: 4037-4052.

Huh, D.G. and Handy, L.L. (1989). Comparison of Steady- and Unsteady-State Flow of Gas and Foaming Solution in Porous Media. *Soc. Pet. Eng. Reservoir Eng.* 4: 77.

Jacquard, P. (1991). Improved Oil Recovery in the Global Energy Perspective. 6th European Symposium. Improved Oil Recovery (Stavanger, May 21-23), Plenary Conference.

Jones, S. A.; Laskaris, G.; Vincent-Bonnieu, S.; Farajzadeh, R. and Rossen, W. R. (2016). Effect of Surfactant Concentration on Foam: From Coreflood Experiments to Implicit-Texture Foam-Model Parameters. *J. Ind. & Eng. Chem*. 37: 268-276.

Kam, S.I. and Rossen, W.R. (2003). A Model for Foam Generation in Homogeneous Media. *SPE J*. 8(4): 417-42. SPE-87334-PA.

Kam, S.I.; Nguyen, Q.P.; Li, Q. and Rossen, W.R. (2007). Dynamic Simulations With an Improved Model for Foam Generation. *SPE J.* 12(1): 35-38. https://doi.org/10.2118/90938-PA.

Kam, S.I. (2008). Improved Mechanistic Foam Simulation with Foam Catastrophe Theory. *Colloids Surf., A.* 318(1-3): 62-77. https://doi.org/10.1016/j.colsurfa.2007.12.0417.

Kovscek, A.R.; Patzek, T.W. and Radke, C.J. (1995). A Mechanistic Population Balance Model for Transient and Steady-State Foam Flow in Boise Sandstone. *Chem. Eng. Sci.* 50(23): 3783-3799.

Khatib, Z.R.; Hirasaki, G.J. and Falls, A.H. (1988). Effects of Capillary Pressure on Coalescence and Phase Mobilities in Foams Flowing Through Porous Media. *SPERE*. 3(3): 919-926. SPE-15442-PA.

Kyte, J.R. Rapoport, L.A. (1958). Linear Waterflood Behaviour and End Effects in Water-Wet Porous Media. Petroleum *Trans. AIME*. 213: 47-50.

Lake, L.W.; Johns, R.T.; Rossen, W.R. and Pope, G.A. (2014). Fundamentals of Enhanced Oil Recovery. *SPE J. ISBN 978-1-61399-407-8*.

Ma, K.; Lopez-Salinas, J.L.; Puerto, M.C.; Miller, C.A.; Biswal, S.L. and Hirasaki, G.J. (2013). Estimation of Parameters for the Simulation of Foam Flow Through Porous Media. Part 1: The Dry-out Effect. *Energy & Fuels.* 27(5): 2363-2375.

Moritis, G. (1990). CO_2 and HC Injection Lead EOR Production Increase. *Oil & Gas J*. 49-81.

Nguyen, Q. P.; Currie, P. K. and Zitha, P. L. J. (2003). Determination of Foam Induced Fluid Partitioning in Porous Media Using X-Ray Computed Tomography. Paper *SPE80245* presented at the International Symposium on Oilfield Chemistry, USA, *5-8*.

Perkins F.M. (1957). An Investigation of the Role of Capillary Forces in Laboratory Water Floods. *Trans. AIME.* 207: 49-51.

Ransohoff, T.C. and Radke, C.J. (1988). Mechanics of Foam Generation in Glass Bead Packs. *SPERE.* 3 573.

Rossen, W.R. and Gauglitz, P.A. (1990). Percolation Theory of Creation and Mobilization of Foams in Porous Media. *AI Chem Eng. J.* 36(8).

Rossen, W.R. (1996). Foams in Enhanced Oil Recovery. In: Prud'homme, R.K., Khan, S. (Eds.), Foams: Theory Measurement and Applications. Marcel Dekker, New York City.

Simjoo, M. and Zitha, P. L. J. (2013). Effects of Oil on Foam Generation and Propagation in Porous Media. Paper *SPE 165271* presented at the SPE Enhanced Oil Recovery Conference, Kuala Lumpur, Malaysia, 2-4 July. https://doi.org/10.2118/165271-MS.

Wonnacott, T. H. and Wonnacott, R. J. (1972). Introductory Statistics for Business and Economics, John Wiley and Sons.

Zhou, Z. and Rossen, W.R. (1995). Applying Fractional-Flow Theory to Foam Processes at the "Limiting Capillary Pressure. *SPE J.* https://doi.org/10.2118/24180-PA.

Appendix 2.A

		Foam Quality f_g [%]							
Cs [wt%]	0.1	94.01	87.67	85.04	81.98	77.34	73.98	66.67	53.22
	0.3	94.01	87.67	85.04	81.98	77.34	73.98	66.67	-
	0.5	94.01	87.67	85.04	81.98	77.34	73.98	66.67	-

Table 2.A1. Foam qualities and surfactant concentrations selected for foam-generation experiments.

$$k_{rg} = \left(\frac{1-S_w-S_{gr}}{1-S_{wc}-S_{gr}}\right)^{2.2868} \quad \text{(Eq. 2.A1)}$$

$$k_{rw} = 0.7888\left(\frac{S_w-S_{wc}}{1-S_{wc}-S_{gr}}\right)^{1.9575} \quad \text{(Eq. 2.A2)}$$

Relative permeability functions used in model of Kam and Rossen (2003).

Parameter values used in Kam's model for prediction of triggering superficial velocities			
Foam Parameters		Other Parameters	
C_g/C_c	1×10^{-13}	k [m^2]	7.1×10^{-12}
m	4.4	ϕ	0.199
n	0.85	μ_w [Pa s]	0.001
C_f	1×10^{-14}	μ_g^0 [Pa s]	0.00002
S_w^*	[0.201, 0.30, and 0.40]	S_{wc}	0.2
		S_{gr}	0.1
		σ	0.03

Table 2.A2. Parameter values used with model of Kam and Rossen (2003) for prediction of trigger velocity for foam generation (Kam and Rossen, 2003).

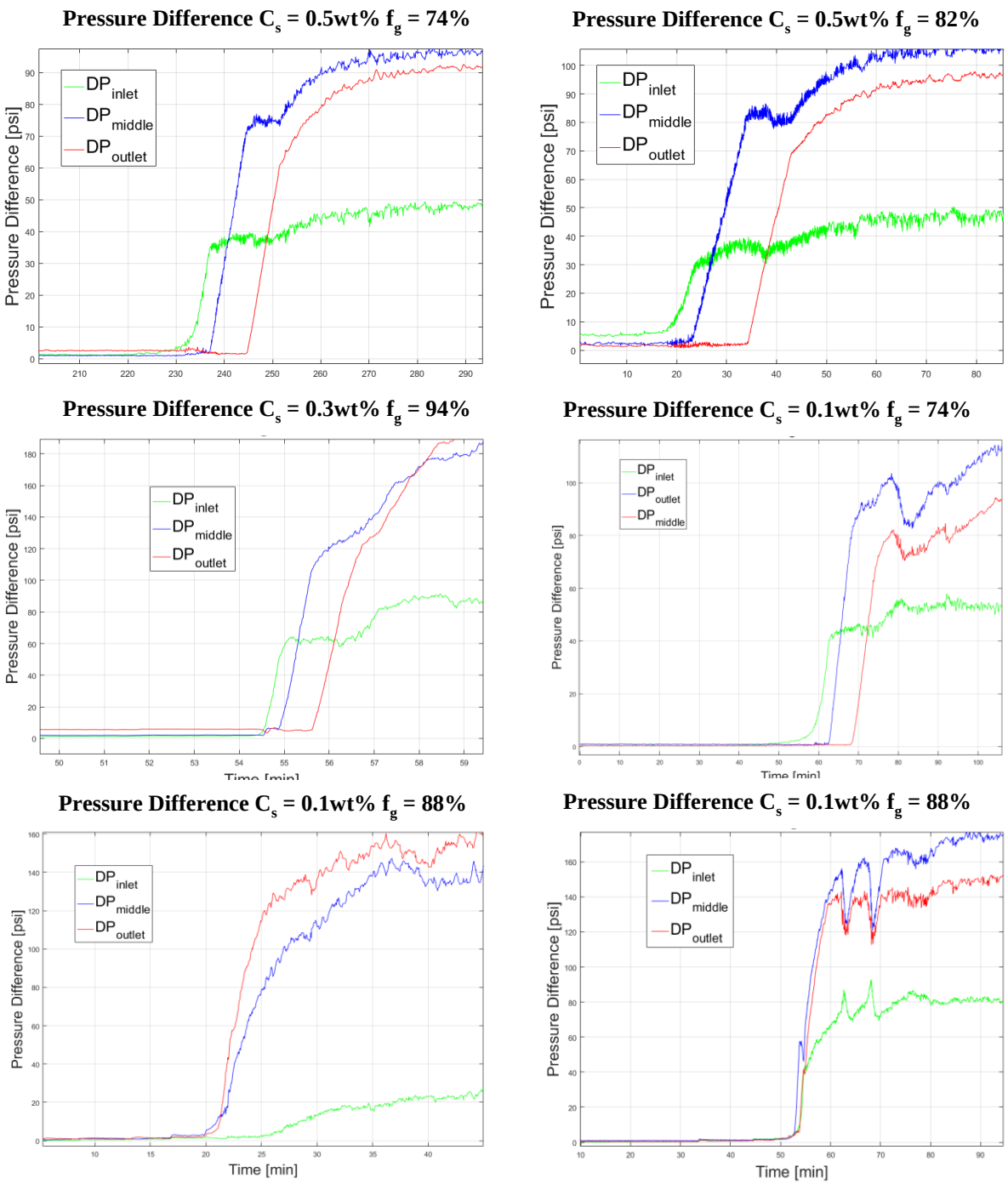

Figure 2.A1. Pressure-difference profiles for valid foam-generation experiments. The figures show the sequential responses of pressure drop in different core sections (inlet, middle and outlet), and the time scale of different events that take place during foam generation (see criteria). The top four figures indicate the fact that foam generation is oftentimes inseparable from foam propagation. The two figures at bottom illustrate the rare scenarios where foam generation takes place almost simultaneously/uniformly in different core sections, instead of propagating downstream in sequence.

Chapter 3

Foam Propagation at Low Superficial Velocity: Implications for Long-Distance Foam Propagation

Abstract

Since the 1980's, experimental and field studies have found anomalously slow propagation of foam (Friedmann et al., 1991, Friedmann et al., 1994; Patzek 1996), a phenomenon that cannot be fully explained by surfactant adsorption. Friedmann et al. (1994) conducted foam propagation experiments in a cone-shaped sandpack and concluded that foam, once formed in the narrow inlet, was unable to propagate at all at lower superficial velocities near the wider outlet. They hence concluded that long-distance foam propagation in radial flow from an injection well is in doubt.

Ashoori et al. (2012) provides a theoretical explanation for slower and non-propagation of foam front at decreasing superficial velocity. By linking foam propagation to the minimum superficial velocity u_t^{min} (or minimum pressure gradient ∇P^{min}) required for foam generation in homogeneous porous media (Rossen and Gauglitz, 1990, Gauglitz et al., 2002), the study reveals that the minimum velocity for maintaining the propagation of foam is far less than that for creating foam, but greater than the minimum velocity for maintaining foam in place. Lee et al. (2016) and Izadi and Kam (2019) find a minimum velocity for foam propagation from analysis of a similar population-balance model, but associate it with the minimum velocity for foam stability.

In this study, we extend the experimental approach of Friedmann et al. (1991) in the context of the theory of Ashoori et al. (2012). We observe dynamic propagation of foam in a cylindrical core with stepwise increasing diameter such that the superficial velocity decreases from inlet to outlet (in a ratio of 16:1). Previously (Yu et al., 2019), we mapped the conditions for foam generation (at large superficial velocities) in a Bentheimer sandstone core, in relation to surfactant concentration and injected gas fraction (foam quality). In this study, we enrich the map with the conditions for downstream propagation of foam (at significantly smaller superficial velocities). We also interpret our results for both foam generation and propagation in terms of local pressure gradient (following the implications of Ashoori et al., 2012), which plays a dominant role in the mobilization and creation of foam.

Our results suggest that the minimum superficial velocities for both foam generation and propagation increase with increasing foam quality and decreasing surfactant concentration, in agreement with theory (Rossen and Gauglitz, 1990). Additionally, the minimum velocity for propagation of foam is much less than that for foam generation, as has been predicted by Ashoori et al. (2012). Implications of our lab results for field application of foam are briefly discussed.

3.1 Introduction

Applications of foam in porous media range from enhanced oil recovery (EOR) (Schramm, 1994, Rossen, 1996) and acid diversion in well stimulation (Burman and Hall, 1987, Kennedy et al., 1992) to aquifer- and soil-remediation processes (Hirasaki et al., 1997). For petroleum reservoir engineers, foam EOR is of interest because foam significantly improves the volumetric sweep efficiency of injected gas. Foam in porous media comprises liquid films (called lamellae) restricting the flow of gas in the pore network. The presence of lamellae greatly reduces gas mobility, resulting in improved gas sweep. The number of lamellae per unit volume of gas (inversely related to bubble size) determines the mobility reduction (also called the "strength") of foam. The population of lamellae, and therefore properties of the foam, is the result of processes creating and destroying lamellae.

Propagation of foam over long distances far from the injection well is needed to divert gas flow deep into a reservoir. The conditions that dominate both creation and propagation of foam in porous media, therefore, have been a concern to foam researchers for decades. Various theories and experimental results cast light on the mechanisms of foam generation and propagation.

Theory suggests that a minimum pressure drop ΔP^{min} is required to mobilize a static lamella blocking a pore throat (Bikerman, 1973, Rossen and Gauglitz, 1990). Mobilized lamellae can multiply by lamella division (Rossen, 1996), triggering foam generation. A percolation theory for foam generation in steady gas-liquid flow (Rossen and Gauglitz, 1990) relates the minimum pressure gradient ∇P^{min} or minimum superficial velocity u_t^{gen} for foam generation to rock and fluid properties such as permeability k, surface tension and injected liquid volume fraction f_w. This theory fits experimental data (Friedmann et al., 1994; Rossen and Gauglitz, 1990, Yu et al., 2019) regarding the impact of injected liquid fraction f_w on the minimum velocity for foam generation. A greater injected liquid fraction f_w contributes to lamella creation (Rossen and Gauglitz, 1990) and also reduces the rate of lamella coalescence (Khatib et al., 1988). Foam generation hence becomes easier as f_w increases because of effects on both lamella creation and destruction. More-recent work (Yu et al., 2019) indicates an effect of surfactant concentration on the minimum velocity for foam generation, which reflects the link between lamella stability and foam generation. The surfactant concentrations used in that study (Yu et al., 2019; Chapter 2) are far above the critical micelle concentration (CMC) (Jones et al., 2016).

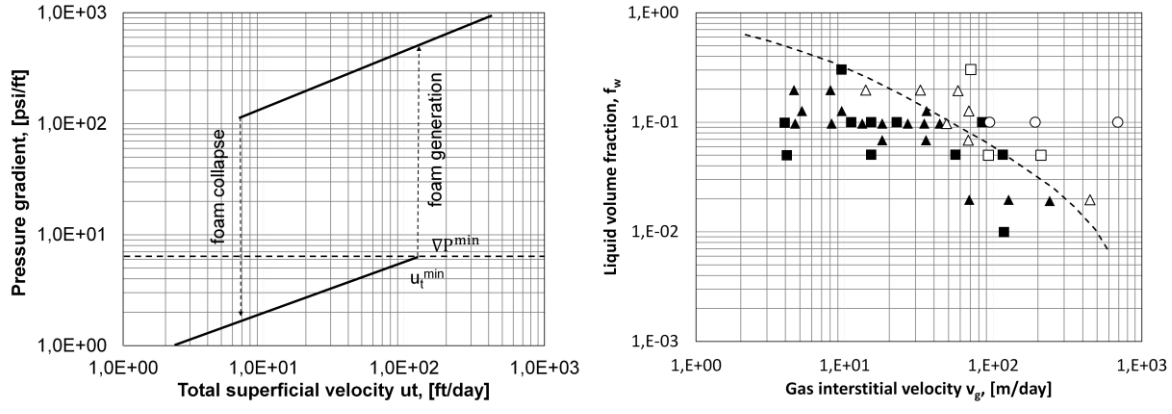

(a) **(b)**

Figure 3.1. (a) Schematic of fixed-rate experiment on foam generation (Gauglitz et al., 2002). Foam generation at steady flow requires exceeding a minimum pressure gradient ∇P^{min} or minimum superficial velocity u_t^{gen}. (b) The experimentally determined minimum gas interstitial velocity for foam generation v_g^{min} at different injected liquid volume fractions. Closed symbols represent conditions with no foam, and open circles conditions with strong foam. The trend superimposed on data is estimated from a percolation-theory-based model for foam generation in homogeneous porous media (Gauglitz et al., 2002).

Gauglitz et al. (2002) conducted three different types of foam-generation experiments. In fixed-injection-rate experiments (Fig. 3.1a), foam is generated by fixing total superficial velocity and foam quality (gas fractional flow, $f_g = (1-f_w)$). Superficial velocity is first set at a low initial value and is then increased in steps to larger values. Upon the triggering of foam generation at u_t^{gen}, pressure gradient along the core rises abruptly (Gauglitz et al., 2002, Yu et al., 2019) to a much-larger value reflecting strong foam. If superficial velocity is reduced after strong foam is created, strong foam can be maintained at superficial velocities at which it would not be created from a state of no-foam or coarse foam.

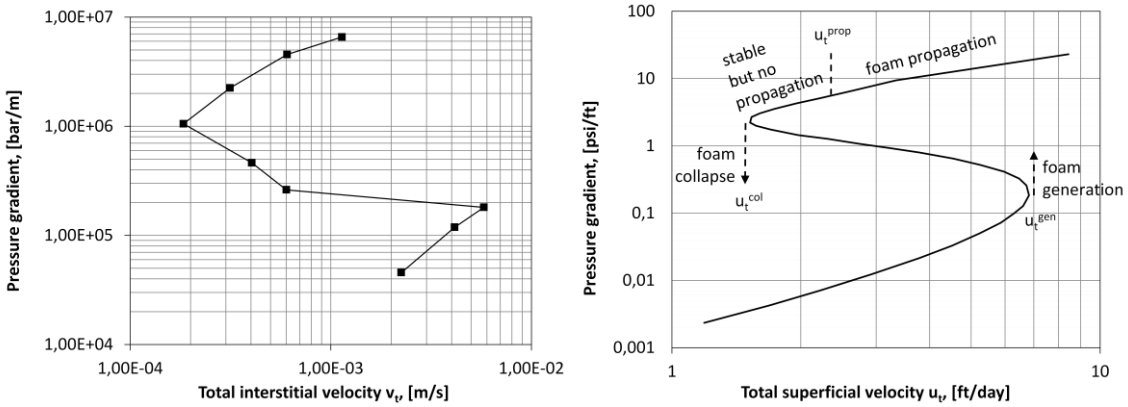

(a) **(b)**

Figure 3.2. (a) A reproduction data from a fixed-pressure-difference experiment on foam generation, based on data of Gauglitz *et al.* (2002). (b) Illustration of the population-balance model of Kam and Rossen (Kam, 2008) fitted to the data of previous foam generation experiments (Ashoori *et al.*, 2012). In the example shown here, the critical superficial velocity for foam propagation at $f_w = 0.1$ is $u_t^{prop} = 3.6$ ft/day (Ashoori *et al.*, 2012). Solid arrows illustrate the injection history of foam.

In fixed-pressure-difference experiments (Fig. 3.2a), foam is generated by maintaining the pressure drop across the core at a set value (Gauglitz et al., 2002). These experiments reveal a third, unstable steady state over a range of superficial velocities, with pressure gradient intermediate between the coarse-foam and strong-foam states. The values of ∇P^{min} and u_t^{gen} in an experiment at fixed injection rate correspond to the point where the plot of ∇P bends backwards toward smaller values of u_t with increasing ∇P.

Others have reported foam hysteresis in strong-foam behaviour, in the sense that, once strong foam is created, ∇P remains somewhat greater if superficial velocity u_t is reduced (Lotfollahi et al., 2016) than its value at the same superficial velocity when u_t was increasing. In contrast, the triggering of foam generation is an abrupt increase in ∇P by more than an order of magnitude, starting from a state of coarse foam or no foam, a distinct phenomenon from that sort of hysteresis in strong foam.

The population-balance model of Kam and Rossen (2003) and its variants (Kam et al., 2007, Kam, 2008; Lee et al., 2016) are designed to explain the experiments of Gauglitz et al. (2002). This model introduces a relation between pressure gradient, lamella creation and foam generation. It is the only foam model demonstrated to represent and explain the trigger and multiple steady-states seen in foam-generation experiments (Gauglitz et al., 2002). Its predicted behaviour is shown schematically in Fig. 3.2b.

Successful foam propagation in the field resembles a radial flow pattern with stable displacement of gas due to mobility control at the gas-displacement front. In the near-well region, the large velocities of gas and liquid, as well as large pressure gradient, favour the generation and propagation of foam (Rossen and Gauglitz, 1990). At large distances away from an injection well, however, both superficial velocity and pressure gradient are low, and the

issue of foam propagation further from the well comes into question. Some field applications of steam foam in the 1980's reported very slow foam propagation to limited distances from the injector, and hence raise concerns about long-distance foam propagation. Observation wells in a steam-foam pilot in the Mecca Lease, Kern River, reported foam propagation to a distance 43 m (140 ft) from the injector over 4.5 years (Patzek, 1996). This was slower than the rate that would be predicted from surfactant adsorption and the high foam quality in that test. In section 26 of the steam-foam pilot in the Midway-Sunset (MWSS) field, two observation wells 12 m (39 ft) from the injector reported a breakthrough of steam foam after 8 months of surfactant injection (Friedmann et al., 1994, Patzek, 1996). Based on the estimated foam propagation rate to 12 m, foam should have arrived at the observation well 21 m (69 ft) from the injector after about 24 months of surfactant injection (Friedmann et al., 1994, Patzek, 1996). Unfortunately, surfactant injection continued for a period of only 18 months before it was shut off, and hence left the hypothesis untested (Patzek, 1996).

Friedmann et al. (1994) conducted a foam-propagation experiment in a cone-shaped sandpack to seek explanations for what they interpreted as stalled propagation of steam foam in the MWSS pilot. Surfactant (Chevron Chaser SD1020, 0.3 wt%) and N_2 were co-injected at constant $f_g = 0.987$ from the narrow inlet of the cone-shaped sandpack with a 1.25:5.00 ratio of diameters between the injection and exit-faces. Foam generated near the inlet then propagated to increasingly wider downstream sections, with six pressure-difference measurements in total. According to the pressure response, strong foam stalled in the fifth section and didn't reach the end of the sand-pack, even after 300 pore volumes (PV) of foam injection.

Friedmann et al. (1991) combined core-flooding experiments and numerical simulation. They developed a population-balance simulation model and fit the model's coefficients to the results of six separate core-flooding experiments. Afterwards, they conducted a foam-displacement experiment in a Berea sandstone core with three different, increasing diameters (0.95 cm, 2.5 cm, and 5.0 cm) along the core length, and compared the data to the simulation results of their population-balance model. Surfactant solution and N_2 were co-injected (at f_g = 95%, and T = 100 ˚C) into the vertically mounted core at a velocity that creates strong foam only in the narrow section (d = 0.95 cm). Foam propagation in the widest portion (d = 5.0 cm) was then observed and documented based on the pressure-difference measurements across the three sections in the widest portion.

Their population-balance simulation model assumes a minimum velocity for lamella creation. Coalescence depends in the model on surfactant concentration but not on capillary pressure or water saturation. Their simulation and experimental results agree well with each other, and show that the breakthrough of strong foam at the core outlet was delayed by about 3.3 PV when compared to the breakthrough of surfactant. With a minimum velocity for lamella generation, the model should predict a minimum velocity for propagation and for maintaining foam, but this is not explored in the paper.

Ashoori et al. (2012) used the population-balance model of Kam and Rossen (2008) to explain and predict long-distance foam displacement in the context of multiple foam steady-states. They combined fractional-flow analysis (also called the method of characteristics) and numerical simulation to study long-distance foam propagation at various superficial velocities in a 1-D linear porous medium. At superficial velocities greater than the minimum velocity for generation u_t^{gen} (Rossen and Gauglitz, 1990; Gauglitz et al., 2002; Yu et al., 2019), strong foam can be created in-situ and propagate downstream (Fig. 3.2b). As superficial velocity drops to lower values, an intermediate state of weak foam propagates ahead of the strong-foam state, whose propagation rate slows. This may explain the delay in breakthrough of strong foam seen in Friedmann et al.'s (1991) experiment. With further reduction of superficial velocity to a minimum velocity for propagation, which we here call u_t^{prop}, the characteristic velocity of

strong foam drops to zero; foam stops moving forward. The model indicates that, however, strong foam remains stable in place at u_t^{prop}. At a yet-lower superficial velocity u_t^{col}, foam becomes unstable and collapses. Their analysis implies that the failure of foam propagation at u_t^{prop} is a result of insufficient lamella creation at the leading edge of foam front (from insufficient pressure gradient there), instead of complete destruction/collapse of foam. In other words, the flux of lamellae to the foam displacement front is quenched by the rate of lamella coalescence at the front.

Ashoori et al. (2012) solved for the traveling wave at the leading edge of the foam bank to conclude that the conditions for foam propagation are more stringent than for foam stability. Lee et al. (2016) and Izadi and Kam (2019) analyse a population-balance foam model incorporating trapped gas and a minimum ∇p for foam flow. They find that foam strong-foam mobility can vary with distance from the injection well, and report a minimum velocity for foam propagation. They associate minimum velocity for propagation with the minimum velocity for foam stability.

In this study, we focus on gathering experimental evidence on foam propagation in a core of variable diameter. The configuration of this core (Fig. 3.3), based on that originally designed by Friedmann et al. (1991), provides an opportunity for foam to flow at three different superficial velocities u_t in the three core sections of different diameter as it is injected at a constant volumetric flow rate Q_t. As described above, Ashoori et al.'s analysis (2012) suggests the existence of three transition points for foam behaviour in terms of superficial velocity, illustrated schematically in Fig. 3.2b: u_t^{gen}, the minimum velocity for foam generation; u_t^{prop}, the minimum velocity for foam propagation; and u_t^{col}, the velocity at which steady-state of strong foam becomes unstable and collapses. We therefore design our experimental procedures (described below) in a way that the model's implications (Ashoori et al., 2012) can be examined and verified. Furthermore, we also explore the impacts of surfactant concentration C_s and foam quality f_g (plotted in terms of injected liquid volume fraction f_w below) on foam propagation as a function of velocity. We plot the three key velocities (u_t^{gen}, u_t^{prop}, and u_t^{col}) against different foam qualities and surfactant concentrations. We then analyse the trend of data and discuss the implications.

3.2 Experimental apparatus and materials

Fig. 3.4 is a schematic of the apparatus. The core is mounted vertically with the narrow section at the bottom. Aqueous solutions and N_2 are co-injected from the bottom. In total 7 pressure transducers (0~150 bar) and 6 pressure-difference meters (0~10 bar) are placed along the core to monitor foam propagation. The safety range of the pressure-difference meters are between 0 and 20 bar, with the accuracy range calibrated between 0 ~ 10bar. If the measured pressure difference is between 10 and 20 bar (above the accuracy range but below the safety range of PD), the accuracy of measurement is slightly compromised without risking damage to the meter. The pressure gradient for strong foam (shown in results section) are calculated based on the difference of absolute pressure between two adjacent pressure gauges. The measurements from pressure-difference meters are used only if one or more of the absolute-pressure gauges is damaged and fails to provide accurate measurement. The pressure-difference meters are switched on when the flowing pressure difference is below 10 bar and are switched off when flowing pressure difference is likely to rise above 10 bar.

We use a cylindrical core of Bentheimer sandstone (k = 2.5 Darcy, ϕ = 0.25) with stepwise changing diameters (Fig. 3.3). All experiments are conducted at a lab temperature of approximately 22˚C. Surfactant solutions are made by weighing and mixing BIO-TERGE AS-40 (Sodium C14-16 Olefin Sulfonate) in brine (3.0 wt% NaCl). The vertically mounted core is divided into three sections (Fig. 3.3): 1) a narrow inlet Section 1 at the bottom, with 1 cm

diameter and 6.1 cm length (pore volume (PV) ≅ 1.2 ml); 2) a wider middle Section 2 with 2.67 cm diameter, and 6.9 cm length (PV ≅ 9.7 ml); and 3) the widest and longest Section 3, with 4 cm diameter and 27.0 cm length (PV ≅ 84.8 ml). The ratio of superficial velocities is 16.0:7.1:1.0 from Section 1 to Section 3. The core is drilled from one large piece of cylindrical core (40 cm long and 4 cm wide) to avoid capillary discontinuities. Fig. 3.3 illustrates the locations of the pressure gauges along the core.

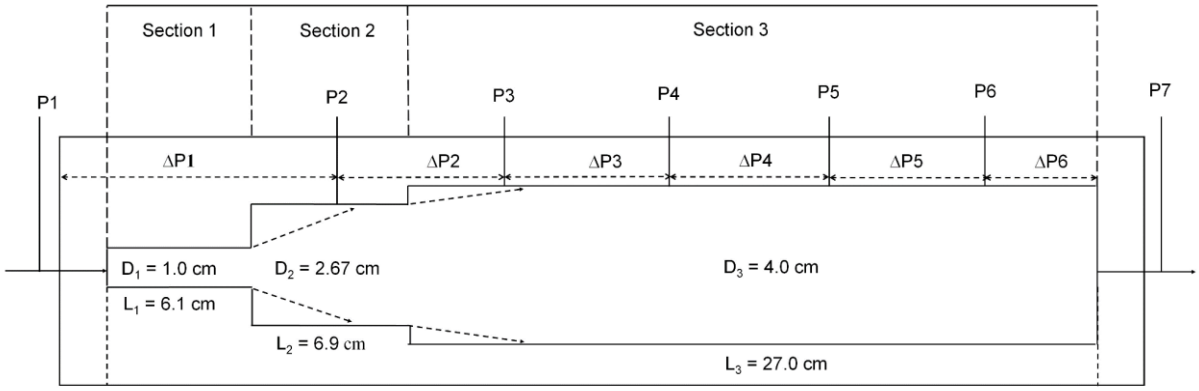

Figure 3.3. Schematic illustration of core geometry.

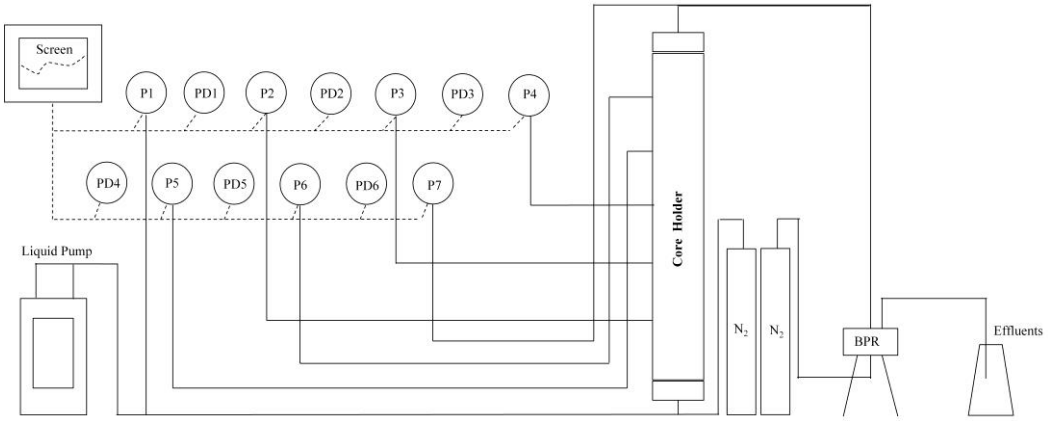

Figure 3.4. Apparatus design. The core is mounted vertically with the narrow section at the bottom. Aqueous solutions and N_2 are co-injected from the bottom. In total 7 pressure transducers (0~150bar) and 6 pressure-difference meters (0~10bar) are placed along the core to monitor foam propagation.

The pressure transducers used in our experiment are placed some distance from the section boundaries (Fig. 3.3): ΔP_1 measures the pressure drop of entire Section 1 and first half of (about 3.5 cm) of Section 2; ΔP_2 measures the second half of Section 2 and the beginning of (about 3.0 cm) of Section 3. Drilling holes directly at the section boundary would be difficult, and distortion in flow at the boundary is difficult to interpret. We can infer the presence of strong foam in the narrow section from a large pressure difference in between the first two taps ΔP_1; propagation through the second section from the pressure difference between the second and third taps ΔP_2; and propagation through the widest section from the next three pressure differences, ΔP_3, ΔP_4, and ΔP_5 (Fig. 3.3). The pressure difference near the outlet ΔP_6 could be distorted by the capillary end effect. The multiple pressure taps at the same diameter in Section 3 gives the most reliable indication of conditions for foam propagation and collapse. We describe how we infer ∇p in the first two sections below, and compare results inferred in Section 2 and measured in Section 3 in our results.

Back-pressure is held fixed in each experiment. In most experiments it was set to 10-15 bar, In some experiments we set back-pressure at 40 bar (C_s = 0.05 wt%, f_g = 88%) and 60 bar (C_s = 0.3 wt%, f_g = 88%) bar to allow attaining superficial velocities in the desired range. Gas compressibility is relatively unimportant in our results. In each case, whether foam is advancing or retreating, our focus is on behaviour at the leading edge of the foam bank. The pressure difference between this edge and the outlet of the core is insignificant.

3.3 Experimental method: defining criteria and procedure

Analogous to the criteria defined by Yu et al. (2019) (Chapter 2) for foam-generation experiments, we define here the criteria and procedures for foam-propagation experiments. The details of these criteria could change for studies in other porous media or with different foam compositions. The experiments proceed in three steps designed to determine the conditions for foam generation in Section 1, and then for propagation in Sections 2 and 3, and finally for foam collapse in Sections 3 and 2.

The first stage of our experiment is designed to measure u_t^{gen} in Section 1, and establish stable foam in that section before propagation into Sections 2 and 3. The criteria for determining u_t^{gen} are taken from Yu et al. (2019) (Chapter 2). A steady state of low ΔP_1 must first be established. Then superficial velocity is raised until, upon such an increase, ΔP_1 rises quickly to a much-larger value. The second stage of experiment focuses on the superficial velocity at which foam propagation begins, by increasing u_t in steps. After strong foam breaks through at the end of the core, we finalize our experiment by stepwise reducing u_t to obtain the superficial velocity at which foam collapses. The experimental procedures, along with associated experimental artifacts, are defined and explained below in 13 steps. For clarity, we also summarize the procedures in flowcharts (Figs. 3.A1 through 3.A3 in Appendix 3.A). The procedure to clean and initialize the core and apparatus are summarized in Step 13 below.

Step 1. To determine u_t^{gen} in the given experiment, start with an injection rate well below the expected value of u_t^{gen}. If u_t^{gen} for a particular surfactant concentration and liquid volume fraction is already known or can be estimated from available data (Yu et al., 2019), we can use that information to select and initial injection rate of surfactant and gas. If an estimate of u_t^{gen} is not available, start at a relatively low a value of superficial velocity in the first section.

Step 2. Initialize the core with steady flow of brine and N_2 at this superficial velocity.

Step 3. Start co-injection of surfactant solution and N_2 at this same superficial velocity and liquid volume fraction f_w. Since the pore volume of the first section is about 1.2 ml, keep the injection rate constant until at least 2.0 to 3.0 ml of surfactant is injected, to satisfy adsorption in in that section. If no foam generation is indicated (no substantial increase in ΔP_1), increase the injection rate in steps until foam generation is indicated by a sharp rise in ΔP_1 by at least a factor of 10, well beyond the magnitude of the increase in superficial velocity. As noted below, it is usually not possible to allow ΔP_1 to reach steady state before reducing injection rate to prepare for the next step. If foam is already indicated by a large value of ΔP_1 at the first injection rate, then u_t^{gen} cannot be determined from this experiment. The test for propagation can continue, however. The uncertainty in u_t^{gen} is the gap between the last superficial velocity before foam generation and the superficial velocity at which foam generation occurred.

The next series of steps are designed to determine u_t^{prop} from ΔP data from Sections 2 and 3 in turn, as follows:

Step 4. After foam generation has occurred in Section 1, allow ΔP_1 to rise up to between 4 to 5 bar. Before any significant increase is seen in ΔP_2, reduce injection rate to a much smaller value, one that is not expected to allow propagation through Section 2. If pressure continues to rise in Section 2, it is not possible to determine u_t^{prop} in that section in this experiment. (In that case, go to step 6 if desired to check propagation into Section 3, but first verify that propagation

does not proceed immediately into Section 3.) If propagation is not indicated in Section 2 at the first superficial velocity, continue with the low injection rate for a long period (~24 hr) before any further changes, to verify that propagation of strong foam has not occurred into Section 2. One must begin the test at a superficial velocity below u_t^{prop} in order to determine u_t^{prop}.

Step 5. If no strong foam is indicated in Section 2 after a long period of injection (~24 hrs), raise superficial velocity in a series of steps to greater values, and after each step keep the flow rate constant for a short period of time. Repeat this procedure until strong foam is indicated in Section 2 by a rise in ΔP_2. The first indication of propagation into Section 2 is a steady, large rise in ΔP_1, which should begin shortly after the increase in superficial velocity. (ΔP_1 comprises a significant part of Section 2). As ΔP_1 stabilizes, ΔP_2 should start to rise and come to a value of up to 100 times its earlier value. (One should avoid waiting too long (more than 24 hr) for a pressure response, to avoid the so-called "incubation effect", where slow accumulation of perturbations over long period co-injection of gas and surfactant solution can lead to foam generation under conditions in which it would not otherwise be seen (Baghdikian and Handy, 1991).)

Step 6. This superficial velocity is u_t^{prop} as measured in Section 2. From this superficial velocity estimate the injection rate at the inlet required for foam to propagate in Section 3.

Step 7. After a steady-state ΔP_2 is obtained, increase injection rate to a value somewhat lower than the injection rate for propagation in Section 3 estimated in the previous step. Verify that foam does not propagate at this velocity into Section 3 (i.e., ΔP_2 does not rise more than proportionately to the increase in injection rate, and ΔP_3 remains low).

Step 8. If no foam is indicated in Section 3 in 1 to 2 hr, raise superficial velocity in a sequence of steps (each lasting approximately 1~2 hours) until foam propagation is indicated by a rise in ΔP_3. As noted, the first indication of propagation into Section 3 is a steady, large rise in ΔP_2 from its previous steady value. Hold that injection rate constant until steady-state strong foam is established throughout Section 3 (i.e., in ΔP_4, ΔP_5, and ΔP_6). If foam does not propagate throughout the Section 3, raise velocity again in steps until strong foam is indicated throughout Section 3. This final value represents u_t^{prop} for Section 3. We exclude any cases where a large pressure gradient at the end of the core, which reflects at least in part the capillary end effect, propagates upstream into the rest of Section 3 (Ransohoff and Radke, 1988, Apaydin and Kovscek, 2001, Nguyen et al., 2003, Simjoo et al., 2013).

The uncertainty in u_t^{prop} for both Sections 2 and 3 is the gap between the largest velocity for which foam propagation is not indicated and the first velocity for which it is in each section.

Once foam is established throughout the core, collapse of foam in a given section is indicated when, upon a reduction in injection rate, there is a drop in pressure gradient in that section by an factor of 5 to 10. This reduction of pressure gradient should be complete in a relatively short period (roughly 2~5 hours). It is likely that this represents a transition to continuous-gas foam (Falls et al., 1988, Rossen, 1996) rather than disappearance of all foam lamellae. We proceed as follows:

Step 9. After the core is filled with strong foam, reduce superficial velocity in Section 3 in steps. The magnitude of velocity reductions should not be smaller than the velocity steps used in steps 5 to 8.

Step 10. Hold the injection rate constant for at least 2 to 3 hr, to see whether or not the state of strong foam is maintained. Here we make our judgement based on the measurement of ΔP_4 and ΔP_5. ΔP_3 is affected (with unknown magnitude) by the strong foam that flows out of Section 2, and ΔP_6 is likely affected by end-effects.

Step 11. Collapse of strong foam is indicated by a reduction of pressure difference by a factor of 5 to 10 (or greater) in Section 3. If foam collapse is indicated in Section 3 (both ΔP_4

and ΔP_5 decrease by a factor of 5 to 10), record this velocity as the minimum velocity to maintain strong foam, u_t^{col}. If strong foam remains stable, keep reducing velocity in steps until foam collapse is indicated (or until further reductions are not feasible with the apparatus). The uncertainty u_t^{col} is the difference between this velocity and the previous velocity tested.

Step 12. Repeat steps 9 to 11 for Section 2 (if there is sufficient pressure in the N_2 cylinder). Document the value of u_t^{col} for Section 2 in the same way as for Section 3.

Step 13. At the end of each experiment, we clean the apparatus in preparation for a new experiment. After injection of surfactant solution and N_2 is stopped, we inject a solution of 50 vol.% 2-proponal for 1.5 to 2 PV. Back-pressure is then reduced to 1 bar. Afterwards, we inject fresh water (20-40 PV) to wash surfactant out of the core and apparatus. We then flush the apparatus with CO_2 and then vacuum the system for 1.5-2.0 hours. After vacuuming, we saturate the system with fresh water, followed by injecting 1-1.5 PV of brine solution of 3.0 wt% concentration of NaCl.

In case any of these procedures or criteria is unsatisfied, it may not be possible to record the desired velocity for the given section. We illustrate application of this experimental approach in the following section.

3.4 Application of the experimental method

In this section, we illustrate the application of our experimental method and the way we interpret some of the experimental artifacts. The vertical solid lines in Fig. 3.5, Fig. 3.6, and Fig. 3.7 below represent times when superficial velocity is increased or reduced. The labelled curves represent the measured pressure differences between individual pairs of pressure taps.

Figs. 3.5a and 3.5b show an experiment to measure u_t^{gen} in Section 1, specifically an experiment with f_g = 95%, and C_s = 0.3 wt%. We start the test with co-injection of brine and N_2 at u_t = 22.21 ft/day in Section 1 (not shown). After steady-state is reached, we switch to co-injection of surfactant solution and N_2 (at the same u_t) at time zero (Fig. 3.5a). Through a successive increases in superficial velocity (221 ft/day, 228 ft/day, and 251 ft/day), strong-foam generation is triggered at u_t^{gen} = 251 ft/day at t = 1.4 hr (Fig. 3.5a). Before foam reaches steady state in Section 1, we reduce superficial velocity to 13.32 ft/day and hold it constant for approximately 20.5 hours (Fig. 3.5b), to verify that propagation of strong foam into Section 2 has not occurred. Pressure difference across Section 1 continues to increase, despite the reduced superficial velocity, and gradually stabilizes. Clearly there had been some reduction in mobility in Section 1 (rise in ΔP_1) upon the increase in u_t to 221 ft/day at about 0.6 hr, but it stabilizes at a ΔP value too low to be considered strong foam. We conclude that u_t^{gen} is 251 ft/day in this experiment. At t = 16.1 hr, ΔP_2 starts to rise, but then stabilizes at a value we consider to be too small to represent strong foam. At about 22 hr an increase in velocity triggers foam propagation in Section 2. Our next example focuses on a different experiment to illustrate the determination of u_t^{prop}.

Figs. 3.6a and 3.6b show an experiment with f_g = 95% and C_s = 0.05 wt% to illustrate the procedures for determining foam propagation in Sections 2 and 3. After foam generation is triggered in Section 1 (not shown), we keep the superficial velocity steady at u_t = 11.4 ft/day for approximately 18 hours. There is no significant increase of ΔP_2, ΔP_3, and ΔP_4 during this period. We begin by raising superficial velocity in Section 2. For the first two superficial velocities tested (3.1 ft/day from 19.1 to 21.7 hr and 4.6 ft/day from 21.7 to 22.9 hr), no significant increase in either ΔP_1 or ΔP_2 is observed (Fig. 3.6a). At t = 22.9 hr, we increase the superficial velocity to 6.2 ft/day. ΔP_1 immediately starts to increase (Fig. 3.6a), indicating that strong foam begins to propagate into the first half of Section 2. After approximately 1.5 hr, ΔP_1 stabilizes, and at about the same time ΔP_2 starts a sharp and continuous increase to a value of about 400 times greater than it had been. The sharp increase of ΔP_1, followed by the increase

of ΔP_2 to a much greater value, indicates the propagation of strong foam in Section 2 at u_t = 6.2 ft/day.

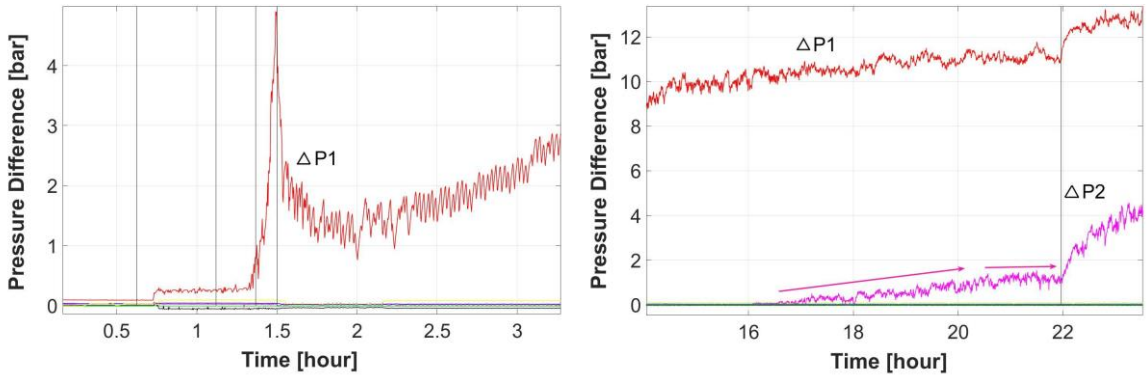

Figure 3.5. Illustration of the experimental procedure for determining foam generation in the inlet section (Section 1) for f_g = 95% and C_s = 0.3 wt%. (a) Foam generation is triggered at 251 ft/day. (b) Superficial velocity in Section 1 is reduced to 13.32 ft/day after foam generation (at about 1.5 hr) to prevent immediate propagation of strong foam into Section 2 and held constant for around 20.5 hours. The vertical solid lines mark the moment of velocity increase.

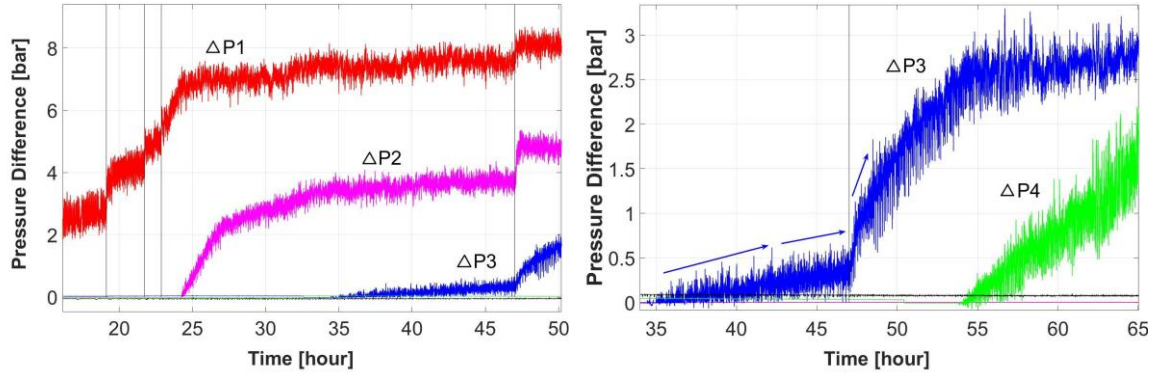

Figure 3.6. Illustration of the experimental procedure for determining foam propagation in wider sections (Section 2 and Section 3) for f_g = 95% and C_s = 0.05 wt%.

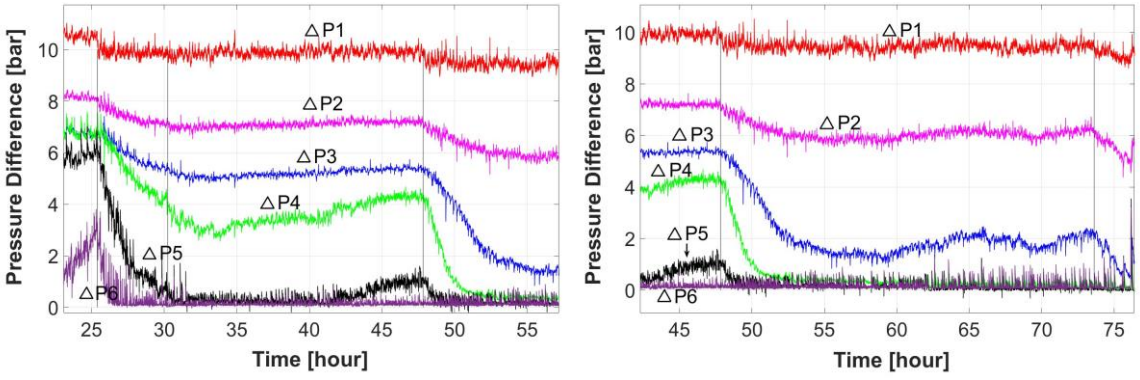

Figure 3.7. Illustration of experimental procedures for determining the velocity for foam collapse for f_g = 82% and C_s = 0.05 wt%.

We next repeat the same procedure for Section 3. As strong foam in Section 2 achieves steady state (at 34.5 hr), there is some increase of ΔP_3 (Fig. 3.6b). ΔP_3 fluctuates between 0.0 and 0.5 bar for 13 hours (Fig. 3.6b); eventually the trend stops increasing. This is similar to behaviour in Section 2 (ΔP_2) in the experiment in Fig. 5b. In both cases, we judge that this does not indicate successful propagation of strong foam. Upon an increase in superficial velocity to 2.86 ft/day at about 46 hr, there is an unmistakable rise in ΔP_3. Moreover, foam propagates at this superficial velocity to ΔP_4 and further downstream (not shown). We conclude that u_t^{prop} is 2.86 ft/day for Section 3 based on this result.

As noted, based on our criteria, a modest and stable increase in ΔP in a section is insufficient evidence for successful foam propagation. In addition, there is some scatter in results for Sections 2 and 3. For the experiment with f_g = 95% and C_s = 0.3 wt%, propagation of strong foam begins at 2.94 ft/day in Section 2 (Fig. 3.5b) and 1.94 ft/day in Section 3 (not shown). For the experiment with f_g = 95% and C_s = 0.05 wt%, propagation of strong foam begins at 6.2 ft/day in Section 2 (Fig. 3.6a) and 3.57 ft/day in Section 3 (Fig. 3.6b). These differences may reflect the flow distortions in Section 2 arising the change in diameter between sections (illustrated schematically in Fig. 3.3). We report both results in our results below. Compared to the overall trend, the differences are not great.

In Fig. 3.7a and 3.7b, we illustrate the procedures for determining u_t^{col} for an experiment with f_g = 82%, C_s = 0.05 wt%. Strong foam propagates to Section 3 at 1.15 ft/day. At t = 25.4 hr, superficial velocity in Section 3 is reduced to 0.72 ft/day (Fig. 3.7a). ΔP_5 and ΔP_6 start to drop, and fall below 1.0 bar in 5 hours (Fig. 3.7a). ΔP_3 and ΔP_4 also start to drop, but eventually stabilize, and ΔP_3 even rebounds at 42 hr (Fig. 3.7a). We further reduce superficial velocity to 0.58 ft/day at t = 47.8 hr (Fig. 3.7b). ΔP_4, ΔP_5, and ΔP_6 drop below 1 bar in about 4 hours, ΔP_3 lingers at about 1.5 bar for another 23 hours. At t = 73.6 hr, we reduce superficial velocity in Section 3 to 0.48 ft/day. ΔP_3 falls below 1.0 bar in 3 hours, indicating collapse of strong foam in Section 2. While there is some ambiguity in the exact value of u_t^{col}, we conclude that for Section 3, u_t^{col} is 0.48 ft/day.

3.5 Results

Figs. 3.8a and 3.8b plot the critical superficial velocities for foam generation, propagation and collapse against liquid fractional flow for the surfactant concentrations used. The corresponding foam qualities are labelled in the plots. A full summary of experimentally measured superficial velocities (in various core sections) and the uncertainty in data is presented in Tables. 3.B1 and 3.B2 in Appendix 3.B. Values corresponding to u_t^{gen}, u_t^{prop}, and u_t^{col} are labelled in the plot. The values of u_t^{prop} and u_t^{col} are considerably lower than u_t^{gen} for each surfactant concentration and foam quality. As in previous studies (Friedmann et al., 1994; Rossen and Gauglitz, 1990; Gauglitz et al., 2002; Yu et al., 2019) there is some scatter in our results. There is an additional uncertainty caused by the stepwise increase/decrease of superficial velocity. The magnitude of this uncertainty is indicated by the error bar for each datum in Fig. 3.8a and 3.8b, which represents the difference between the recorded superficial velocity (i.e., u_t^{prop}) and the superficial velocity tested at the previous step, at which foam doesn't propagate. The leftward error bars represent the size of the last velocity increase for u_t^{gen} u_t^{prop}. The rightward error bars represent the size of velocity reduction in determining u_t^{col}.

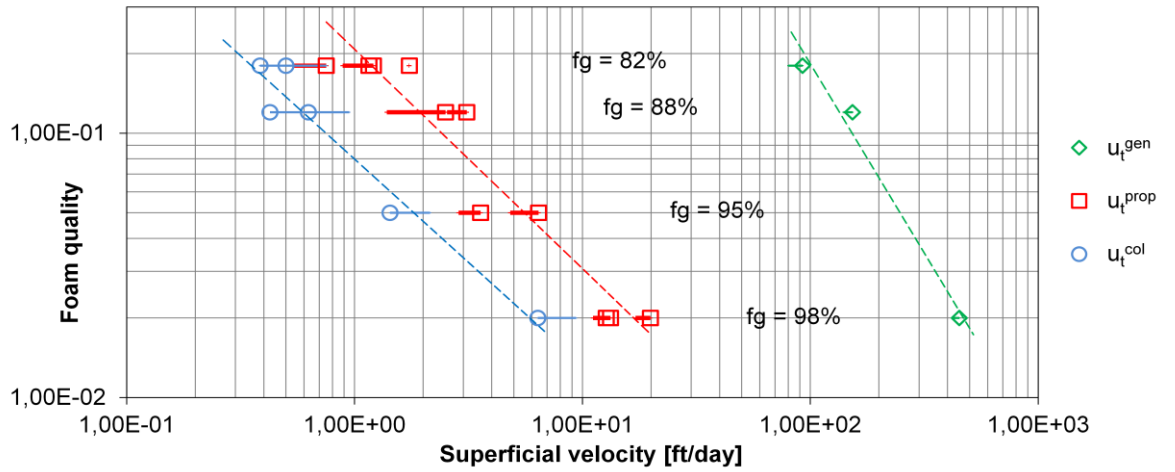

(a)

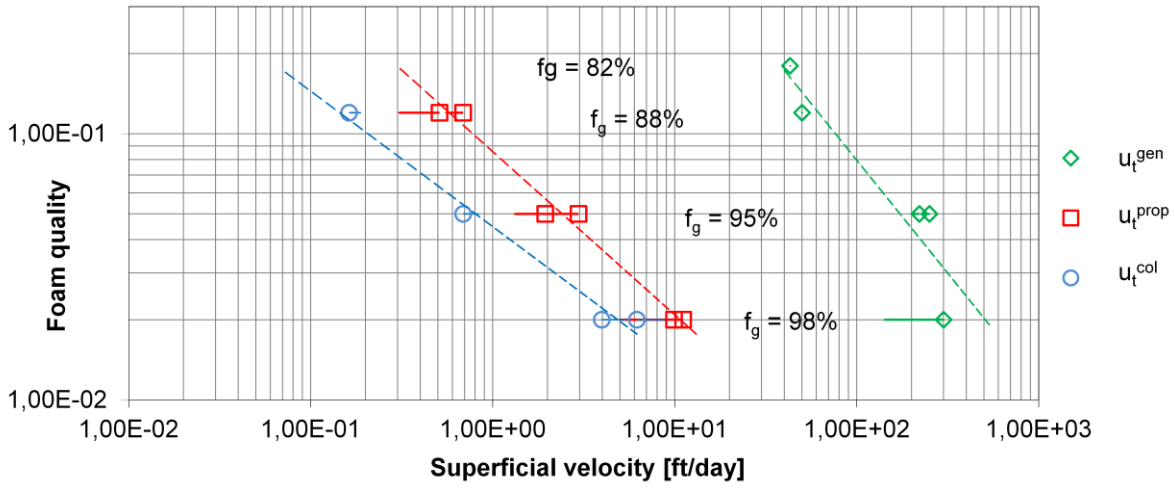

(b)

Figure 3.8. Critical superficial velocities for generation, propagation, and destruction of foam. (a) Experimental data for surfactant concentration of C_s = 0.05 wt%. (b) Experimental data for C_s = 0.3 wt%. At foam quality f_g = 88%, we reached the limitation of equipment (mass flow rate and back pressure). A summary of results is available in Tables 3.B1 and 3.B2.

The dashed lines interpolated from the critical superficial velocities divide the data into four sub-regions (Fig. 3.8a and 3.8b). The region to the right of the dashed line connecting values of u_t^{gen} indicates the flow conditions for foam generation. The region to the right side of the dash-line connecting values of u_t^{prop} defines conditions for propagation of strong foam into a region without foam. The region between the dashed lines connecting values of u_t^{col} and values of u_t^{prop} represents the conditions at which the stability of strong foam can be maintained. At flow conditions to the left side of the dashed-line connecting values of u_t^{col} strong foam can neither be generated nor maintained.

We observe successful propagation of strong foam at u_t = 0.385 ft/day for the experiment of f_g = 82%, and C_s = 0.3 wt% (Fig. 3.8b). We could not reduce the superficial velocity to smaller values during this experiment due to the limitation in the range of the gas mass-flow meter. Therefore, we could not identify a critical value of superficial velocity u_t^{prop} below which foam doesn't propagate at f_w = 0.18.

Although superficial velocity is fixed in our core-flood experiments, the theory of foam generation and propagation illustrated in Fig. 3.1 and 3.2 hold that pressure gradient ∇P plays the key role in both processes. Fig. 3.9a through 3.9d plot our experimental data in terms of superficial velocity and pressure gradient in the manner of Fig. 3.2. The vertical dashed lines

represent the range of superficial velocities for foam generation, propagation and collapse. The boundaries of the velocity interval are determined by the critical superficial velocities and their uncertainties plotted in Fig. 3.8. The dashed curves give a qualitative illustration of the multiple steady-state of foam in porous media. We plot our data such a manner (Fig. 3.9) to visualize the contrast of pressure gradient between different steady-states of foam. In addition, it helps relate our experimental results to implications from previous theories on foam generation (Gauglitz et al., 2002; Kam and Rossen, 2003; Kam, 2008; Lee et al.,2016) and propagation (Ashoori et al., 2012).

Interpreting ∇P at the critical transitions in our experiments is complicated by four issues:

First, as for determining transition superficial velocities, there is a gap between the last datum before the transition and that at which the transition is observed, represented by the error bars in Fig. 3.8 as discussed above.

Second, the transition itself is marked by a sudden, marked increase or decrease in ∇P away from the transition value, which cannot be observed directly. We estimate the pressure gradient at the onset of foam generation by linear extrapolation of data measured at superficial velocities just below u_t^{gen}. Similarly, we estimate the pressure gradient at foam collapse from strong-foam data at velocities just above u_t^{col}.

Third, we have no pressure tap entirely within the first and second sections of our core for measuring ∇P there (Fig. 3.4). We derive an approximate estimate using Darcy's law for incompressible rectilinear flow in two cores of different diameter. In that case, pressure difference scales roughly with the length of the section and the inverse square of the diameter. Based on this approximation, 12/13 of the pressure difference across the first tap (ΔP_1) arises from the first section, and (2.2/3.2) of ΔP_2 is from the second section. These are only approximations, of course, but allow us to obtain a rough estimate of ∇P in each section. For the Section 3, ΔP_3, ΔP_4 and ΔP_5, entirely within that section, directly reflect ∇P in that section.

Fourth, accurate measurement of pressure gradient of weak/course foam state are not always available. For instance, in the experiment of C_s = 0.3 wt% and f_g = 88% (Fig. 3.9a), the critical velocity for foam generation u_t^{gen} is taken from Yu et al. (2019).

3.6 Conclusions and Discussion

◊ Our experiments demonstrate the existence of three critical superficial velocities for the generation (u_t^{gen}), propagation (u_t^{prop}) and destruction (u_t^{col}) of foam in steady gas-liquid flow in homogeneous porous media. Consistent with previous theory (Ashoori *et al.*, 2012) and experiment (Friedmann *et al.*, 1991, 1994), mobilizing the displacement front of strong foam requires a minimum superficial velocity u_t^{prop}. At superficial velocities lower than u_t^{prop}, the steady-state of strong foam cannot move forward, but can be stable until a yet-lower superficial velocity u_t^{col} is reached.

◊ The critical superficial velocities needed to maintain the stability and the propagation of strong foam are considerably smaller than the superficial velocity required for triggering foam generation in steady flow (Fig. 3.8a and 3.8b).

◊ As previous experiments show (Rossen and Gauglitz, 1990; Gauglitz *et al.*, 2002; Yu *et al.*, 2019), foam generation becomes easier with increasing surfactant concentration (even far above the CMC) and liquid volume fraction injected. The same trend applies for foam propagation and maintenance (Figs. 3.8a and 3.8b). The impact of liquid volume fraction and surfactant concentration on foam propagation is less significant when compared to their impact on foam generation. However, the increase of propagation velocity u_t^{prop} as foam gets dryer is still substantial. The difficulty of generating and maintaining foam in porous media reflects the reduction of lamella stability.

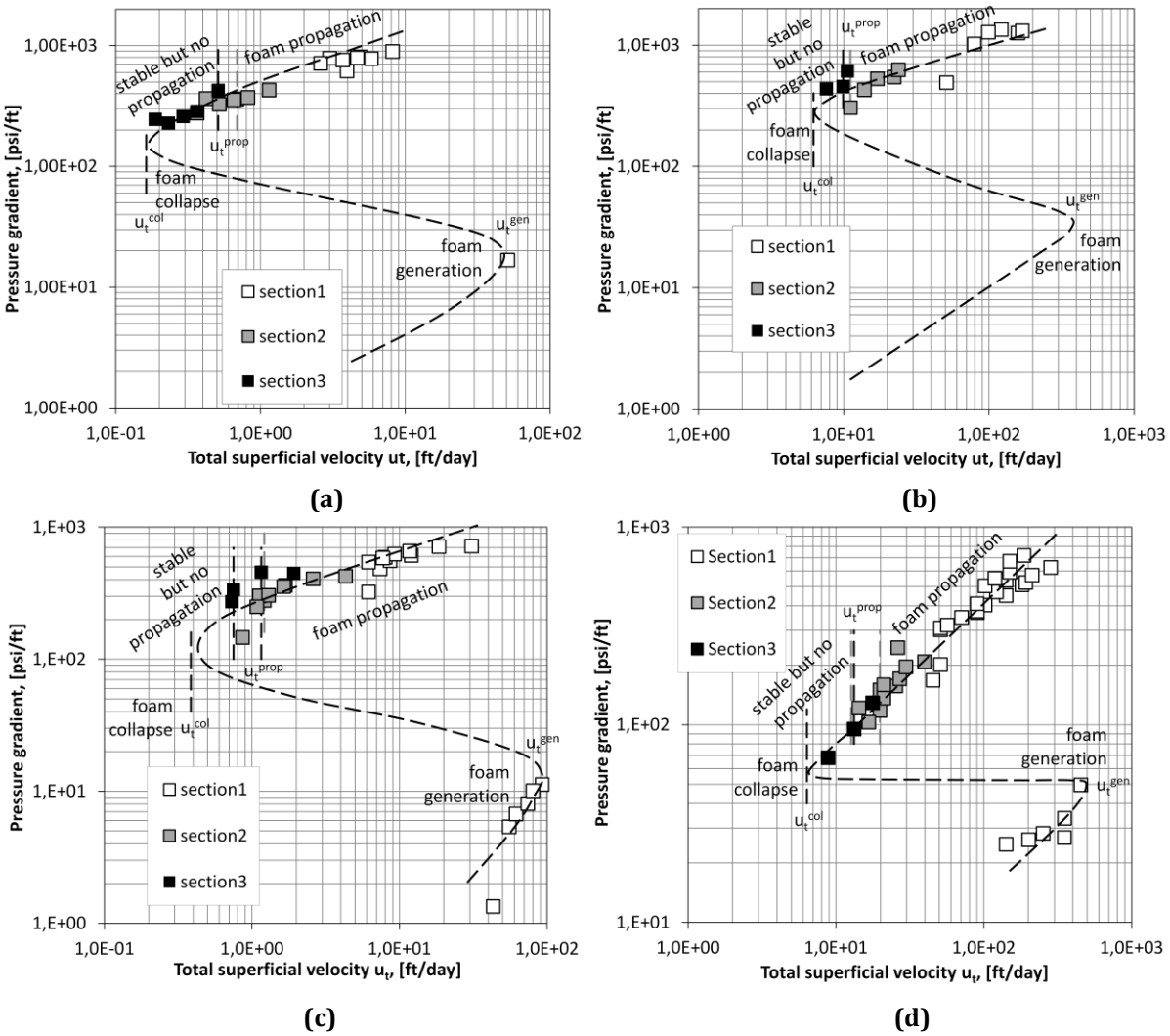

Figure 3.9. Plots of superficial velocity and steady-state pressure gradient in experiments. (a) Steady-state data from experiment with f_g = 88% and C_s = 0.3 wt%. (b) Steady-state data from experiment with f_g = 98% and C_s = 0.3 wt%. (c) Steady-state data from experiment with f_g = 82% and C_s = 0.05 wt%. (d) Steady-state data from experiment with f_g = 98% and C_s = 0.05 wt%. A summary of experimental results is available in Tables 3.B1 and 3.B2 in Appendix 3.B. The schematic curve is drawn to guide the eye, not based on a particular model. The pressure gradient for foam generation is based on data from the first core section; pressure gradient for the steady-state of strong foam are estimated from all three sections of the core. In Fig. 3.9b, for experiment of C_s = 0.3 wt% and f_g = 98%, the pressure gradient for triggering foam generation in Section 1 is not recorded. The shape of the dashed curve in the weak-foam state represents a qualitative estimation. The vertical dashed lines represent the critical superficial velocities for foam generation, propagation and collapse. The values are taken from Figure 3.8. The dashed line in grey represent the critical velocity taken from Section 2 of the core, and black lines represent the critical velocity taken from Section 3. Foam collapse is indicated by an abrupt decline in pressure gradient. Therefore the value of u_t^{col} is determined from the data but we have no direct data on the pressure gradient triggering foam collapse.

◊ The population-balance model of Kam and Rossen (2003), Kam et al. (2007) and Kam (2008), as applied by Ashoori et al. (2012), predicts the existence of minimum velocities and pressure gradients for foam generation, propagation, and stability in place. In this model, foam generation, propagation and stability are the result of competing effects of lamella creation and destruction. Increasing velocity and decreasing foam quality help lamella creation, and increasing surfactant concentration (through its effect on the limiting capillary pressure (Khatib *et al*., 1988; Apaydin and Kovscek, 2001)) and decreasing foam quality help lamella stability. The trends with velocity, foam quality and surfactant concentration seen in Fig. 3.8 agree with trends predicted by that model and with theories of foam stability.

◊ In field application, if superficial velocity is insufficient at the well, there are ways to improve foam generation. Slugs of surfactant solution and gas are often injected alternatively (SAG). In the near-well region, alternative drainage and imbibition of liquid then creates favourable conditions for foam generation. At distances far away from injection well, however, the effects of alternating slug injection are greatly damped, where the flow of surfactant solution and gas comingles as if they are being co-injected. In our experiments, surfactant and N_2 are co-injected at a fixed liquid volume fraction, a condition that closely resembles the flow condition far from injection well.

◊ Determining the implications of the trends shown here for a given field would require experiments conducted under conditions of, and with fluids from, that field. In our experiments, N_2 foam is generated and flows at low temperature (averagely 22˚C) and low pressure (10~60 bar back-pressure). The salinity of solutions we use is relatively low (3.0 wt% NaCl). The porous media used in the core-floods is homogeneous, free of oil, and highly permeable (which also implies low capillary pressure). Under reservoir conditions (much higher temperature and salinity, lower permeability, presence of oil, etc.), the difficulty of foam propagation observed in our experiments is likely to be magnified. Placing foam far from a well in a heterogeneous reservoir may not depend on direct propagation of foam from the well, however (Falls et al., 1988; Tanzil et al., 2002; Shah et al., 2019). Moreover, a process that depends on altering the injection profile in a layered reservoir may not depend on deep foam propagation.

Nomenclature

Symbol	Definition	Unit
CMC	critical micelle concentration	wt%
Cs	surfactant concentration	wt%
fw	injected liquid volume fraction	-
fg	foam quality	-
k	permeability	Darcy
PV	pore Volume	ml
ut^{gen}	critical superficial velocity for foam generation	ft/day
ut^{prop}	critical superficial velocity for foam propagation	ft/day
ut^{col}	critical superficial velocity for foam collapse	ft/day
ϕ	porosity	-
∇P^{min}	minimum pressure gradient for foam generation	Pa/m
ΔP	pressure difference	bar

Table 3.1. Symbols and nomenclature.

References

Ashoori, E.; Marchesin, D.; and Rossen, W.R. (2012). Multiple Foam States and Long-Distance Foam Propagation in Porous Media, *SPE J.* 17(04): 1231-1245, Dec 2012. https://doi.org/10.2118/154024-PA.

Apaydin, O.G. and Kovscek, A.R. (2001). Surfactant Concentration and End Effects on Foam Flow in Porous Media, *Transport in Porous Media* 43(03): 511-536, Jun 2001, https://doi.org/10.1023/A:1010740811277.

Baghdikian, S. and Handy, L.L. (1991). Transient Behavior of Simultaneous Flow of Gas and Surfactant Solution in Consolidated Porous Media, Topical Report performed under U.S. DOE contract FG22-90BC14600, July 1991, https://doi.org/10.2172/5434448, https://www.osti.gov/servlets/purl/5434448-JphSnd/.

Burman, J.W. and Hall, B.E. (1986). Foam as a Diverting Technique for Matrix Sandstone Stimulation. SPE Annual Technical Conference and Exhibition, 5-8 Oct 1986, New Orleans, Louisiana. https://doi.org/10.2118/15575-MS.

Falls, A. H., Hirasaki, G. J., Patzek, T. W., Gauglitz, D. A., Miller, D. D., & Ratulowski, T. (1988). Development of a Mechanistic Foam Simulator: The Population Balance and Generation by Snap-Off. Society of Petroleum Engineers. https://doi.org/10.2118/14961-PA.

Friedmann, F.; Chen, W.H.; Gauglitz, P.A. (1991). Experimental and simulation study of high-temperature foam displacement in porous media, *SPE J.* 6(01): 37–45. https://doi.org/10.2118/17357-PA.

Friedmann, F.; Smith, M.E.; Guice, W.R.; Gump, J.M.; Nelson, D.G. (1994): "Steam-foam mechanistic field trial in the midway-sunset field, *SPE J.* 9(04): 297–304. https://doi.org/10.2118/21780-PA.

Gauglitz, P.A.; Friedmann, F.; Kam, S.I. and Rossen, W.R. (2002). Foam Generation in Homogeneous Porous Media, *J Chem. Eng. Sci*. 57(19): 4037-4052. https://doi.org/10.1016/S0009-2509(02)00340-8.

Hirasaki, G.; Miller, C.; Szafranski, R.; Tanzil, D.; Lawson, J.B.; Meinardus, H.; Jin, M.; Londergan, J.T.; Jackson, R.; Pope, G.A.; Wade, W.H. (1997). Field Demonstration of the Surfactant/Foam Process for Aquifer Remediation, SPE Annual Technical Conference and Exhibition, 5-8 Oct 1997, San Antonio, Texas. https://doi.org/10.2118/39292-MS.

Izadi, M., & Kam, S. I. (2019). Bubble-Population-Balance Modeling for Supercritical Carbon Dioxide Foam Enhanced-Oil-Recovery Processes: From Pore-Scale to Core-Scale and Field-Scale Events. *SPE J*. https://doi.org/10.2118/191202-PA

Jones, S. A.; Laskaris, G.; Vincent-Bonnieu, S.; Farajzadeh, R. and Rossen, W. R. (2016). Effect of Surfactant Concentration on Foam: From Coreflood Experiments to Implicit-Texture Foam-Model Parameters, *J. Ind. & Eng. Chem.* 37: 268-276. https://doi.org/10.1016/j.jiec.2016.03.041.

Kam, S.I. (2008). Improved Mechanistic Foam Simulation with Foam Catastrophe Theory, *J Coll & Surf A* 318(1-3): 62-77. https://doi.org/10.1016/j.colsurfa.2007.12.0417.

Kam, S.I.; Nguyen, Q.P.; Li, Q. and Rossen, W.R. (2007). Dynamic Simulations With an Improved Model for Foam Generation, *SPE J.* 12(01): 35-28. https://doi.org/10.2118/90938-PA.

Kam, S.I. and Rossen, W.R. (2003). A Model for Foam Generation in Homogeneous Media, *SPE J.* 8(04): 417-42. https://doi.org/10.2118/87334-PA.

Kennedy, J.W.; Kitziger, F.W.; and Hall, B.E. (1992). Case Study on the Effectiveness of Nitrogen Foams and Water-Zone Diverting Agents in Multistage Matrix Acid Treatments, *SPE J.* 7(02): 203-211. https://doi.org/10.2118/20621-PA.

Khatib, Z.R.; Hirasaki, G.J. and Falls, A.H. (1988). Effects of Capillary Pressure on Coalescence and Phase Mobilities in Foams Flowing Through Porous Media, *SPE J.* 3(3): 919-926. https://doi.org/10.2118/15442-PA.

Lee, W., Lee, S., Izadi, M., & Kam, S. I. (2016). Dimensionality-Dependent Foam Rheological Properties: How To Go From Linear to Radial Geometry for Foam Modeling and Simulation. *SPE J*. https://doi.org/10.2118/175015-PA

Lotfollahi, M., Kim, I., Beygi, M. R., Worthen, A. J., Huh, C., Johnston, K. P., … DiCarlo, D. A. (2016). Experimental Studies and Modeling of Foam Hysteresis in Porous Media. *SPE J*. https://doi.org/10.2118/179664-MS

Nguyen, Q. P.; Currie, P. K. and Zitha, P. L. J. (2003). Determination of Foam Induced Fluid Partitioning in Porous Media Using X-Ray Computed Tomography, International Symposium on Oilfield Chemistry, 5-7 Feb 2003. https://doi.org/10.2118/80245-MS.

Patzek, T. W. (1996). Field Applications of Steam Foam for Mobility Improvement and Profile Control, *SPE J.* 11(02): 79-85. https://doi.org/10.2118/29612-PA.

Ransohoff, T.C. and Radke, C.J. (1988). Mechanics of Foam Generation in Glass Bead Packs, *SPE J.* 3(02): 573-585.https://doi.org/10.2118/15441-PA.

Rossen, W.R. (1996). Foams in Enhanced Oil Recovery, In: Prud'homme, R.K., Khan, S., "Foams: Theory, Measurements, and Applications", Surfactant science series Vol. 57, Chap 11, Marcel Dekker, Inc. 270 Madison Avenue, New York 10016.

Rossen, W.R. and Gauglitz, P.A. (1990). Percolation Theory of Creation and Mobilization of Foams in Porous Media, *J AIChE.* 36(8): 1176-1188. https://doi.org/10.1002/aic.690360807.

Shah, S. Y., As Syukri, H., Wolf, K.-H., Pilus, R. M., & Rossen, W. R. (2019). Foam Generation in Flow Across a Sharp Permeability Transition: Effect of Velocity and Fractional Flow. *SPE J.* https://doi.org/10.2118/195517-PA

Simjoo, M. and Zitha, P. L. J. (2013). Effects of Oil on Foam Generation and Propagation in Porous Media, SPE Enhanced Oil Recovery Conference, 2-4 July 2013, Kuala Lumpur. https://doi.org/10.2118/80245-MS.

Tanzil, D., Hirasaki, G. J., & Miller, C. A. (2002). Mobility of Foam in Heterogeneous Media: Flow Parallel and Perpendicular to Stratification. *SPE J.* https://doi.org/10.2118/78601-PA

Yu, G., Rossen, W. R., and Vincent-Bonnieu, S. (2019). Coreflood Study of Effect of Surfactant Concentration on Foam Generation in Porous Media, *J I&EC* 58(01): 420-427. https://doi.org/10.1021/acs.iecr.8b03141.

Appendix 3.A–Flowcharts

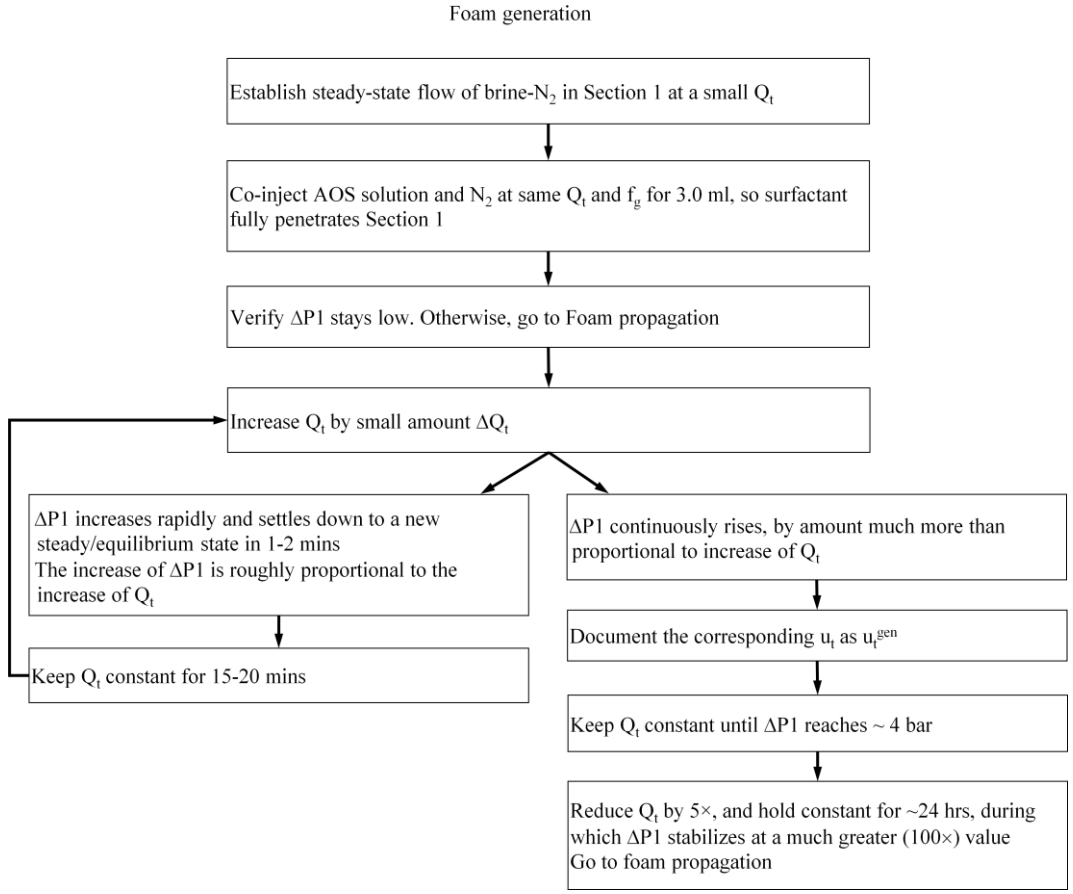

Figure 3.A1. Procedures for verifying foam generation.

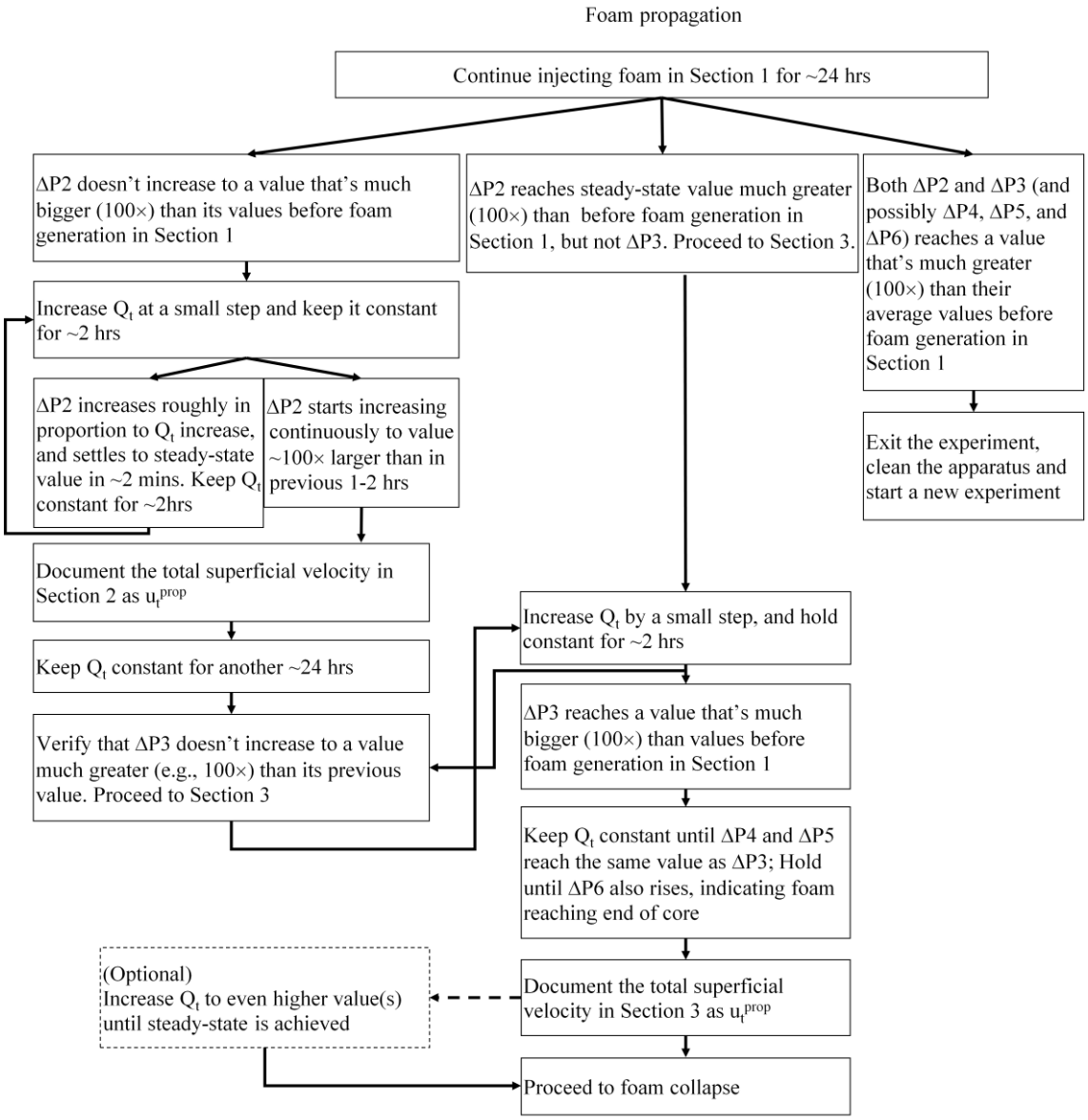

Figure 3.A2. Procedures for verifying foam propagation.

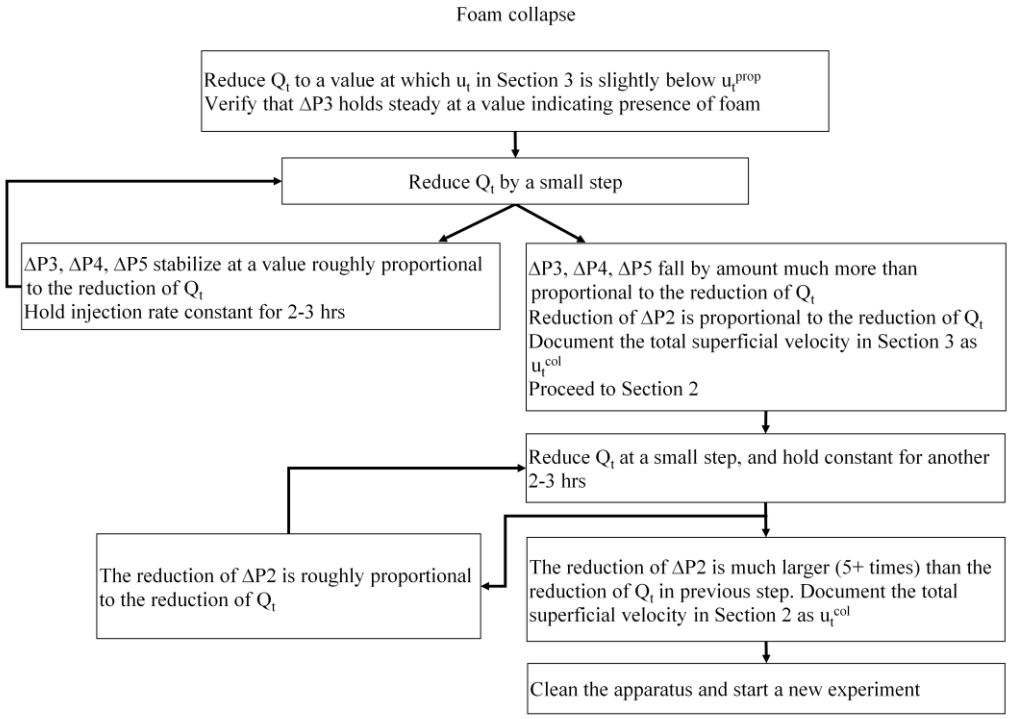

Figure 3.A3. Procedures for verifying foam collapse.

Appendix 3.B–Critical superficial velocity and uncertainty

Cs 0.05 wt%			ut [ft/day]	Uncertainty [ft/day]	ut [ft/day]	Uncertainty [ft/day]
fg 82%	ut^{gen}	Section1	92.44	-12.32	–	–
	ut^{prop}	Section2	1.21	-0.09	1.74	-0.01
		Section3	0.75	-0.21	1.15	-0.27
	ut^{col}	Section2	–	–	–	–
		Section3	0.39	0.19	0.5	0.25
fg 88%	ut^{gen}	Section1	153.2	-13.3	–	–
	ut^{prop}	Section2	3.11	-0.56	–	–
		Section3	2.51	-1.12	–	–
	ut^{col}	Section2	0.43	0.36	–	–
		Section3	0.63	0.32	–	–
fg 95%	ut^{gen}	Section1	–	–	–	–
	ut^{prop}	Section2	6.42	-1.6	–	–
		Section3	3.58	-0.72	–	–
	ut^{col}	Section2	–	–	–	–
		Section3	1.43	0.72	–	–
fg 98%	ut^{gen}	Section1	450	-25.5	–	–
	ut^{prop}	Section2	12.71	-1.59	19.86	-2.78
		Section3	–	–	13.27	-1.24
	ut^{col}	Section2	–	–	–	–
		Section3	6.38	3.0	–	–

Table 3.B1. Critical superficial velocities and uncertainties for experiments with C_s = 0.05 wt%. Fig. 8a is created based on the values in this table. The uncertainties represent the step size of total superficial velocity. The sum of critical superficial velocity and the corresponding uncertainty gives the total superficial velocity of previous step. Negative uncertainty values relate to the sequence of stepwise increase of superficial velocity, and positive values relate to the sequence of stepwise decrease of superficial velocity.

Cs = 0.3 wt%			ut [ft/day]	Uncertainty [ft/day]	ut [ft/day]	Uncertainty [ft/day]
fg 82%	ut^{gen}	Section1	43	×	–	–
	ut^{prop}	Section2	–	–	–	–
		Section3	–	–	–	–
	ut^{col}	Section2	–	–	–	–
		Section3	–	–	–	–
fg 88%	ut^{gen}	Section1	50.13	×	–	–
	ut^{prop}	Section2	0.69	-0.13	–	–
		Section3	0.51	-0.20	–	–
	ut^{col}	Section2	–	–	–	–
		Section3	0.16	0.03	–	–
fg 95%	ut^{gen}	Section1	221	-19.9	251	-23.38
	ut^{prop}	Section2	2.96	-1.09	–	–
		Section3	1.94	-0.63	–	–
	ut^{col}	Section2	–	–	–	–
		Section3	0.69	0.15	–	–
fg 98%	ut^{gen}	Section1	300	-158	–	–
	ut^{prop}	Section2	11.12	-1.19	–	–
		Section3	9.91	-4.93	–	–
	ut^{col}	Section2	3.97	1.41	–	–
		Section3	6.19	2.78	–	–

Table 3.B2. Critical superficial velocities and uncertainties for experiments with C_s = 0.3 wt%. Fig. 8b is created based on the values in this table. The uncertainties represent the step size of total superficial velocity. The sum of critical superficial velocity and the corresponding uncertainty gives the total superficial velocity of the previous step. Negative uncertainty values relate to the sequence of stepwise increase of superficial velocity, and positive values relate to the sequence of stepwise decrease of superficial velocity. The experiments with f_g = 82% and f_g = 88% are exceptional because foam generation was not triggered through a sequence of stepwise increases of total superficial velocity. Instead, we began injection of AOS solution immediately at the values of u_t^{gen} estimated from previous experiments on foam generation (Yu et al., 2019). The uncertainty of u_t^{gen} in these two experiments (marked with ×) is therefore not documented.

Chapter 4

Simulation Models for the Minimum Velocity for Foam Generation and Propagation

Abstract

Foam in porous media is the agglomeration of gas bubbles separated by thin liquid films. Foam injection is promising means of reducing the relative mobility of gas, and hence greatly improving the sweep efficiency of gas. Foam injection method can be applied for CO_2 and H_2 storage, soil-contaminant removal in aquifer remediation, enhanced oil recovery, and matrix-acid well stimulation etc. Theory (Rossen and Gauglitz, 1990; Ashoori et al., 2012) and experiments (Gauglitz et al., 2002; Yu et al., 2019; 2020) indicate that both foam generation and propagation in steady flow in porous media require the attainment of a sufficiently large superficial velocity or pressure gradient. Here we examine several of foam-simulation models for their ability to represent a minimum velocity, or trigger, for foam generation. We define criteria for representation of such a trigger. For simplicity, we assume a homogeneous porous medium and absence of an oleic phase. We examine the Population-Balance (PB) models of Kam and Rossen (2003) and one of its variants (Kam, 2008), and the model of Chen et al. (2010); the implicit-texture (IT) models in CMG-STARS (Martinsen and Vassenden, 1999; Cheng et al., 2000) and of Lotfollahi et al. (2016).

Our result show that the PB models of Kam and Rossen (2003) and its variant (Kam, 2008), the IT models of CMG-STARS (Martinsen and Vassenden, 1999; Cheng et al., 2000) and of Lotfollahi et al. (2016), do represent a minimum velocity for foam generation. The model of Chen et al. (2010) is based on the model of Kovscek and Radke (1994; 1995), which was not intended to represent a trigger for foam generation (Kovscek and Radke, 1994). We cannot say categorically whether it could predict a trigger for any set of model parameter values. Instead, we derive criteria that must be satisfied by the choice of parameters to represent a trigger for foam generation.

In simulations of radial foam propagation the STARS foam model predicts that foam propagation fails at the radius at which local ∇p cannot maintain stable foam, not at a greater ∇p as seen in experiments (Yu et al., 2020). In addition, we identify a fundamental challenge in representing foam generation at the large ∇p at the wellbore in a numerical simulation: conventional simulators do not represent ∇p at the wellbore. Foam generation at the very high superficial velocity at the well radius is not represented in the absence of truly exceptional grid refinement.

4.1 Introduction

Injecting foam into geological formations can lead to enhanced oil recovery by reducing the relative mobility of the gas, which helps mitigate the unfavourable mobility ratio at the leading edge of gas bank as well as the effects of the unfavourable density ratio between gas and water (Schramm, 1994; Rossen, 1996). The impact of foam on controlling gas mobility ultimately leads to a greater sweep efficiency of gas.

Foam in porous media is composed of gas bubbles dispersed in the aqueous phase. The degree to which gas mobility is reduced by foam largely depends on the average bubble size (Falls et al., 1988; Friedman et al., 1991; Kovscek and Radke, 1995; Rossen and Gauglitz, 1990; Rossen, 1996; Kam and Rossen, 2003), or inversely, on the bubble/lamella density (number per unit volume, also referred to as foam texture), n_f. A lamella is a very thin liquid film stabilized by surfactant molecules that occupy the gas/water interface. Previous theory and experimental studies (Rossen and Gauglitz, 1990; Gauglitz et al., 2002; Yu et al., 2019) identify a minimum total superficial velocity (related to a minimum pressure gradient) for foam generation in homogeneous porous media. Such experiments begin with steady flow of gas and aqueous phase, which then switch to co-injection of surfactant solution and gas at the same injected gas fraction f_g (also called foam quality). This experimental approach is directly relevant to the field application of steam foam (Friedmann et al., 1994; Patzek, 1996), where steam is usually injected for a long period of time prior to the introduction of surfactant solution at the same gas fraction. It is also relevant to the issue of foam propagation in surfactant-alternating-gas foam processes far from an injection well, where gas fractional flow is roughly constant (Yu et al., 2020).

In this and related studies (Rossen and Gauglitz, 1990; Gauglitz et al., 2002; Kam and Rossen, 2003; Ashoori et al., 2012; Yu et al., 2019), *foam generation* means an abrupt jump from a state of high gas mobility (no/weak foam) to a state of much lower (e.g., 100× or more) gas mobility (strong foam) upon attaining a sufficiently large total superficial velocity or pressure gradient. In the following text, we express the minimum superficial velocity for foam generation as u_t^{gen}, and the minimum pressure gradient as ∇P^{gen}.

In the experiments of Gauglitz et al. (2002), foam is generated in-situ either by fixing total superficial velocity (fixed-rate experiment), or by fixing the pressure drop along the flow direction (fixed-ΔP experiment) (Fig. 4.1). Both types of experiments begin with a steady state of no/weak foam at relatively low superficial velocity (and pressure gradient). In a fixed-rate experiment (Fig. 4.1a), superficial velocity is then increased in steps until the minimum superficial velocity u_t^{gen} for foam generation is reached. At u_t^{gen}, pressure drop across the core increases sharply while flow rate remains constant. After a steady state of strong foam is established, foam remains stable at superficial velocities much lower than u_t^{gen}. In fixed-ΔP experiments (Fig. 4.1b) pressure drop across the core is increased in steps instead of superficial velocity. At u_t^{gen}, superficial velocity decreases with increases in velocity. These experiments reveal a third steady state between the two identified in the fixed-rate experiments.

The dependence of foam generation on pressure gradient is explained by Rossen and Gauglitz (1990) in their network model of foam generation in homogenous porous media. A percolation model relates the minimum superficial velocity to the pressure difference required to mobilize a lamella in a pore throat. In their study, the underlying mechanism that triggers foam generation is the mobilization and subsequent division of lamellae; the fundamental driving force is pressure gradient instead of velocity. However, since velocity is usually fixed and much easier to control in a foam-generation experiment, one usually reports experimental results in terms of u_t^{gen}. In the model of Rossen and Gauglitz (1990), the critical condition to trigger lamella division and foam generation depends also on aqueous surface tension and the permeability of the porous medium, as well as injected liquid fraction. The model fits trends in u_t^{gen} with permeability in sand- and beadpacks and with f_g in sandstone cores, and also predicts

much-lower values of u_t^{gen} for supercritical CO_2 foam (with lower surface tension). Their model predicts the trigger for foam generation in steady flow, but doesn't account for the dynamics of foam such as convection, generation and destruction of lamellae after foam generation begins.

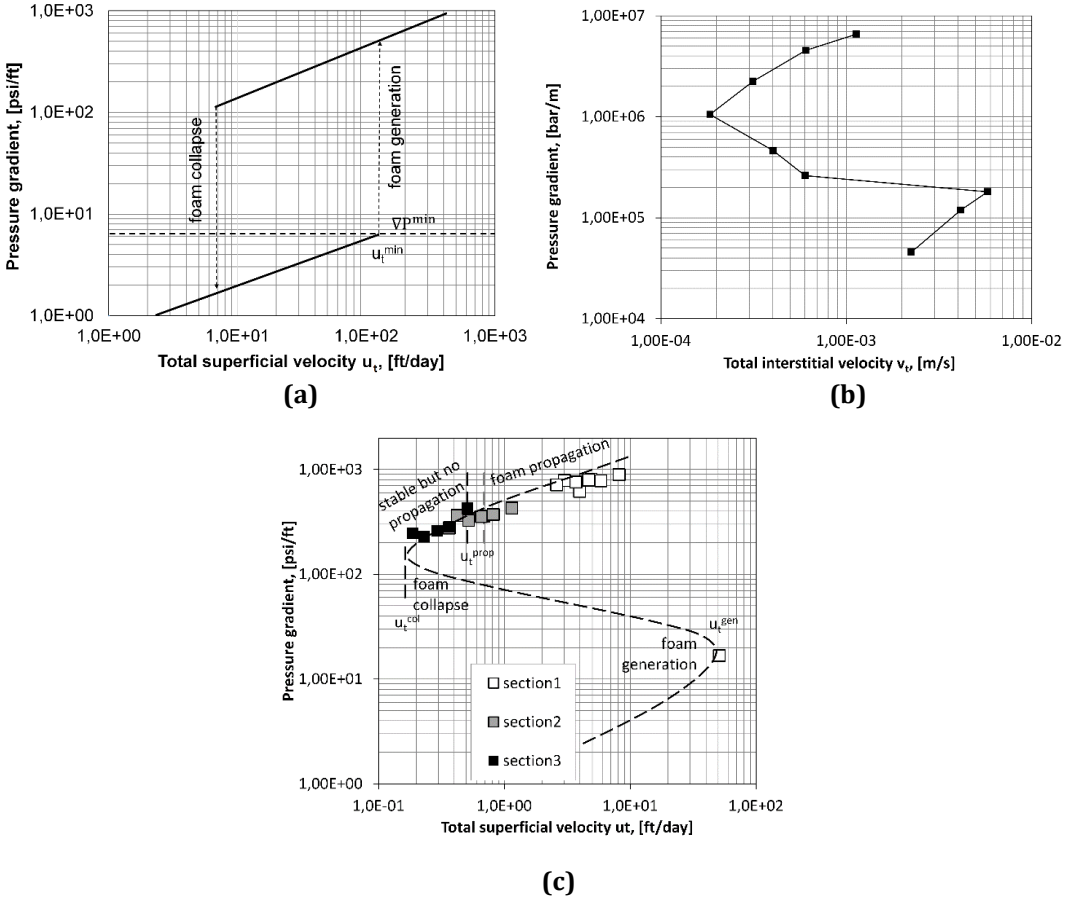

Figure 4.1. (a) Qualitative illustration of a fixed-rate foam-generation experiment (Gauglitz et al., 2002). The steady-state of foam is obtained by fixing total superficial velocity u_t at constant foam quality f_g. These experiments did not specifically verify a minimum velocity for foam collapse. (b) Data from fixed-ΔP experiment of Gauglitz et al. (2002). In this experiment, pressure difference across the core is raised in a series of steps at a fixed foam quality. (c) Experimentally measured multiple steady-states of foam translated from the data from a dynamic foam-propagation test (Yu et al., 2020). In this experiment, foam is generated with a surfactant concentration of C_s = 0.3wt% and a foam quality of f_g = 0.88. The experiment is conducted in a Bentheimer sandstone core of stepwise increasing radius, i.e. stepwise decreasing total superficial velocity. The plotted data points are taken after steady-state of either strong foam or weak foam/no foam is achieved in the various core sections (see legend). The vertical dashed lines draw the approximate boundaries for the values of superficial velocities that are crucial to foam.

Previous experimental studies also suggest a minimum superficial velocity for foam propagation. This minimum velocity, if present, could limit foam propagation out to large distances from an injection well in radial flow. Friedmann et al.'s (1994) foam-propagation experiment in a cone-shaped sandpack suggests that foam created near the well at large superficial velocity may not be able to propagate far from the well at much-lower superficial velocity. In the same study, they also report a failure of foam propagation 42 ft from the injection well after 18 months of steam-foam injection, though this conclusion is contested by Patzek (1996). The traveling-wave analysis of Ashoori et al. (2012) shows a connection between the minimum superficial velocity for foam generation and a minimum velocity for foam propagation u_t^{prop}. This u_t^{prop} is greater than the velocity at which foam becomes unstable

and collapses u_t^{col}, i.e. where the slope of the upper portion of the plot of ∇p v. u_t in Fig. 4.1b reverses sign to negative values. In their model, the failure of foam propagation is due to insufficient lamella creation at the leading edge of foam front. Yu et al. (2020) provide experimental evidence for this prediction of Ashoori et al. (2012), illustrated in Fig. 4.1c. They report values for the three critical superficial velocities u_t^{gen}, u_t^{prop}, and u_t^{col}. If a foam model is able to represent a minimum velocity or trigger for foam generation, this raises the question whether it also predicts minimum velocities for foam propagation and collapse.

This paper reviews current simulation models for foam in porous media, and whether these models can represent a minimum superficial velocity, or minimum pressure gradient, for foam generation. In this study, we do not address the usefulness of these foam models for all applications. Instead, we focus on one facet: the ability of the models to predict an abrupt change of steady state from no/weak foam to strong foam upon a modest increase in total superficial velocity at constant foam quality. If a model can describe a minimum superficial velocity for foam generation, the local-equilibrium solution of the model must be able to represent a sharp jump of state from no-foam to strong-foam upon reaching a critical value of velocity (Fig. 4.1a), and the multiple steady-states of foam (Fig. 4.1b), both implied by foam-generation experiments of Gauglitz et al. (2002). In this study, we first specify the criteria and mathematical constraints required to describe a minimum superficial velocity for foam generation. We then examine the structures and formulations of the various foam models alongside the criteria we define.

Our analysis considers both Population-Balance (PB) foam models (or Explicit-Texture/ET foam models), where foam texture n_f is represented explicitly, and Implicit-Texture (IT) foam models (or local steady-state/equilibrium foam models), where the effects of foam texture are represented implicitly by a factor reducing gas mobility as a function of local conditions. We first examine the PB model of Kam and Rossen (2003) and one of its variants (Kam, 2008). These models have already demonstrated minimum superficial velocities for foam generation and for foam propagation (Ashoori et al., 2012). We also examine the PB model of Chen et al. (2010), a variant of the model first proposed by Kovscek and Radke (1995). Among IT foam models, we examine the STARS foam model (Computer Modeling Group) and a modified version of this model proposed by Lotfollahi et al. (2016). In addition, we consider the prediction of the STARS foam model regarding long-distance foam propagation in radial flow, using numerical simulation, and challenges to any model representing foam generation as a function of pressure gradient in numerical simulation.

4.2 Criteria for a minimum superficial velocity for foam generation

Our definition of a trigger for foam generation focuses on pressure gradient ∇p as a function of total superficial velocity u_t at fixed quality f_g, illustrated in Fig. 4.1. At low ∇p there is a steady state where ∇p increases with u_t. In this state gas mobility is large and foam texture n_f is too small to significantly affect gas mobility. At some point, upon a small increase in u_t, there is an abrupt change of steady state to one with large ∇p and low gas mobility, with significant increases in both gas saturation and capillary pressure. Foam texture in this state is large enough to have a dominant effect on gas mobility. In this regime, again, ∇p is an increasing function of u_t.

The models described below all predict ∇p as a smooth, continuous function of u_t at fixed f_g. This implies the existence of an intermediate regime where

$$\left(\frac{du_t}{d\nabla P}\right)_{f_g} < 0 \qquad \text{Eq. 4.1}$$

with

$$u_t = k\,\lambda_{rt}(S_w, \nabla P)\nabla P \qquad \text{Eq. 4.2}$$

This behaviour is, of course, the result of changes in gas mobility. Therefore it is useful to examine the predicted behaviour of total relative mobility λ_{rt} as a function of ∇p. Eq. 4.1 implies

$$\left(\frac{d\log_{10}(\lambda_t(S_w,\nabla P))}{d\log_{10}(\nabla P)}\right)_{f_g} < -1 \qquad \text{Eq. 4.3}$$

We employ these criteria to examine whether a model can predict a minimum velocity or pressure gradient for foam generation.

4.3 Population-balance model of Kam and Rossen (2003)

In the Population-Balance model of Kam and Rossen (2003) and variants of this model (i.e., Kam, 2008), as in other PB models, gas-phase mobility is an explicit function of lamella density (or foam texture) n_f. Steady-state foam texture is in turn the result of processes of creation and destruction of lamellae (Eqs. 4 to 6 below). In the equations listed below, version (a) of an equation is that of Kam and Rossen (2003) and version (b) that of Kam (2008). In these models, the relative permeability of gas k_{rg} is unaffected by the presence of foam and remains a unique function of water saturation S_w. The impact of foam on the reduction of gas-phase mobility is represented as an increase in the viscosity of gas, μ_g^f (Eq. 4.7).

Lamella density is determined by the simultaneous processes of lamella generation and destruction. Upon achieving Local Equilibrium (LE), the rate of lamella generation r_g (Eq. 4.4) and destruction r_c (Eq. 4.5) are equal (Eq. 4.6), and bubble density arrives at its equilibrium value $n_{f,LE}$. The rate of lamella generation r_g is function of pressure gradient ∇P (Eq. 4.4), with the specific function differing in the two models. Lamella coalescence depends on foam texture and a water saturation (Eq. 4.5). The impact of capillary pressure is not explicitly defined in the model. Instead, its impact on foam stability is linked to the concept of limiting water saturation S_w^*, and implicitly to the limiting capillary pressure P_c^* (Khatib et al., 1988), through the relation between water saturation and capillary pressure embodied in the Leverett J-function (Eq. 4.8) (Leverett, 1941).

$$r_g = C_g \nabla P^m \qquad \text{Eq. 4.4a}$$

$$r_g = C_g \int_{-\nabla P_0}^{-\nabla P_0+\nabla P} \frac{1}{\sqrt{2\pi}} e^{\left(-\frac{1}{2}t^2\right)} dt = \frac{C_g}{2}\left[\mathrm{erf}\left(\frac{\nabla P-\nabla P_0}{\sqrt{2}}\right) - \mathrm{erf}\left(\frac{-\nabla P_0}{\sqrt{2}}\right)\right] \qquad \text{Eq. 4.4b}$$

$$r_c = C_c n_f \left(\frac{1}{S_w - S_w^*}\right)^n \qquad \text{Eq. 4.5a}$$

$$r_c = C_c n_f \left(\frac{S_w}{S_w - S_w^*}\right)^n \qquad \text{Eq. 4.5b}$$

$$n_{f,LE} = \frac{C_g}{C_c}\nabla P^m (S_w - S_w^*)^n \qquad \text{Eq. 4.6a}$$

$$n_{f,LE} = \frac{C_g}{2C_c}\left[\mathrm{erf}\left(\frac{\nabla P-\nabla P_0}{\sqrt{2}}\right) - \mathrm{erf}\left(\frac{-\nabla P_0}{\sqrt{2}}\right)\right]\left(\frac{S_w - S_w^*}{S_w}\right)^n \qquad \text{Eq. 4.6b}$$

$$\lambda_{rg} = \frac{k_{rg}(S_w)}{\mu_g^f} = \frac{k_{rg}(S_w)}{\mu_g^0 + \left(\frac{C_f n_f}{v_g^{\frac{1}{3}}}\right)} \qquad \text{Eq. 4.7}$$

$$P_c(S_w) = \sigma_{gw}\sqrt{\frac{\phi}{k}}\,J(S_w) \qquad \text{Eq. 4.8}$$

The local-equilibrium version of the model is determined by two governing equations. The first (Eq. 4.9) is obtained by combining Darcy's law for water and gas at a constant gas fractional flow f_g:

$$\frac{u_w}{u_g} = \text{constant} = \frac{u_t(1-f_g)}{u_t f_g} = \frac{k\,\lambda_{rw}\,\nabla P}{k\,\lambda_{rg}\,\nabla P} = \frac{\frac{k_{rw}(S_w)}{\mu_w}\nabla P}{\frac{k_{rg}(S_w)}{\mu_g^0+\frac{C_f n_{f,LE}}{v_g^{\frac{1}{3}}}}\nabla P} \qquad \text{Eq. 4.9}$$

where v_g is gas interstitial velocity. In these equations, C_g, m, ∇p_0, C_c, n, and S_w* are model parameters. Details on the symbol definitions in the various models discussed here can be found in the cited references.

The local-equilibrium bubble density (Eq. 4.6) is a function of pressure gradient and water saturation. In these models, pressure gradient is a model input, and the LE solution is analogous to the experimental procedure of a fixed-ΔP experiment. Substituting the definition of bubble density (Eq. 4.4) into effective gas viscosity in Eq. 4.9 and rearranging yields,

$$\frac{(1-f_g)}{f_g} = \frac{\frac{k_{rw}(S_w)}{\mu_w}}{\frac{k_{rg}(S_w)}{\mu_g^0+\left[\frac{C_f}{v_g^{\frac{1}{3}}}\frac{C_g}{C_c}(S_w-S_w^*)^n\right]\nabla P^m}} \qquad \text{Eq. 4.10a}$$

$$\frac{(1-f_g)}{f_g} = \frac{\frac{k_{rw}(S_w)}{\mu_w}}{\frac{k_{rg}(S_w)}{\mu_g^0+\left[\frac{C_f}{v_g^{\frac{1}{3}}}\frac{C_g}{2C_c}\left(\frac{S_w-S_w^*}{S_w}\right)^n\right]\left[\text{erf}\left(\frac{\nabla P-\nabla P_0}{\sqrt{2}}\right)-\text{erf}\left(\frac{-\nabla P_0}{\sqrt{2}}\right)\right]}} \qquad \text{Eq. 4.10b}$$

Eq. 4.10 in either form relates ∇P to $v_g = [(u_t\,f_g)/\phi]$, which means it relates ∇P to u_t for given f_g.

We first examine the model of Kam and Rossen (2003). For a given pressure gradient, Eq. 4.10a determines a unique combination of equilibrium water saturation and bubble density that satisfies fixed injected gas fraction f_g. Once water saturation and LE bubble density is determined, the relative mobilities of gas and water as well as the total superficial velocity can be determined. Figs. 4.2 and 4.3 illustrate the model's prediction of foam properties as a function of ∇P. The model parameter values employed in this example (Figs. 4.2, 4.3 and 4.4) are from Kam and Rossen (2003) (Table A1).

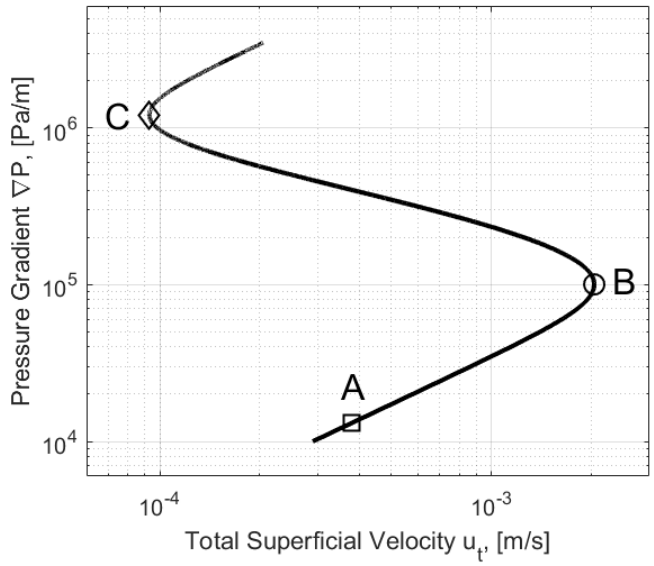

Figure 4.2. Local-Equilibrium solution for the Population-Balance model of Kam and Rossen (2003) at foam quality f_g = 91%. B marks the trigger for foam generation. The curve between A and B represents the steady-state of weak/no foam; the curve between B and C represents the unstable steady-state of intermediate foam; and the curve above C represents the steady-state of strong foam. Parameter values used in this plot are listed in Table A1.

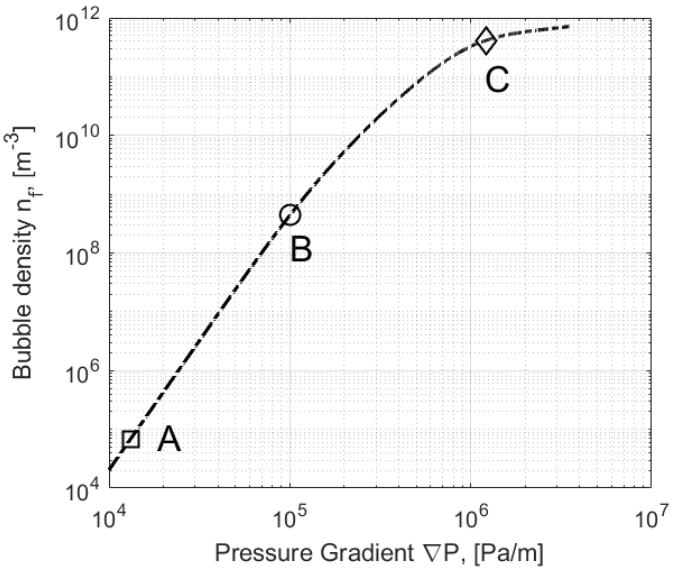

Figure 4.3. Local-Equilibrium bubble density of foam $n_{f,LE}$ as a function of pressure gradient in the model of Kam and Rossen (2003). Parameter values are in Table A1.

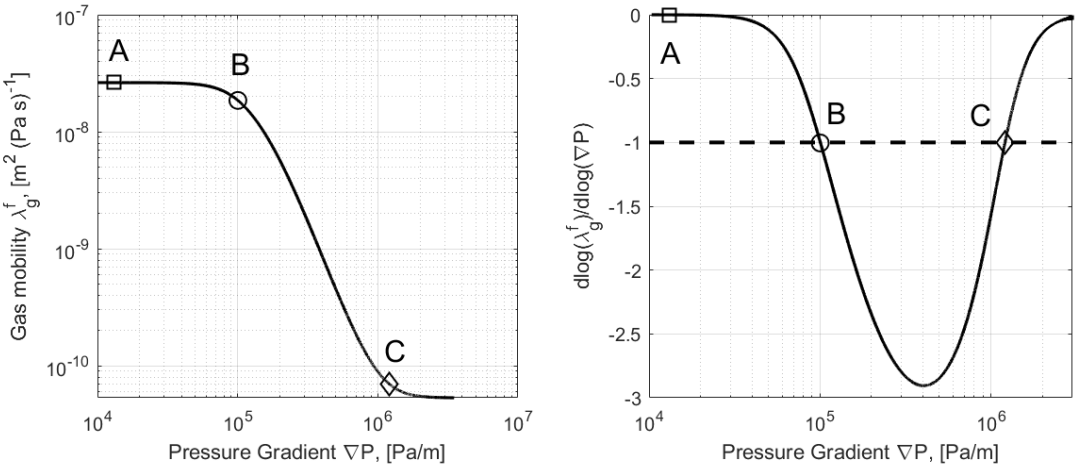

(a) **(b)**

Figure 4.4. (a) Mobility of gas (with foam) ($k \times \lambda_{rg}^f$) as a function of pressure gradient, and (b) dlog(λ_g^f)/dlog(∇P) as a function of pressure gradient for the Population-Balance model of Kam and Rossen (2003). dlog(λ_g^f)/dlog(∇P) < -1 between B and C. This enables the model to represent a trigger for foam generation defined in Eqs. 2 and 3. Parameter values are in Table A1.

Bubble density n_f doesn't increase enough with increasing pressure gradient to reduce gas mobility significantly until pressure gradient reaches a value of about 1×10^5 Pa/m (Figs. 4.3 and 4.4a). Upon further increase of pressure gradient, increasing bubble density reduces gas mobility λ_g^f greatly (Figs. 4.3 and 4.4a). As gas mobility decreases, water saturation falls to maintain water mobility at its fixed ratio to gas mobility. As a result, total mobility λ_t decreases faster than the increase in pressure gradient (Fig. 4.4b). The pressure gradient at point B in these figures represents the minimum pressure gradient or velocity that triggers foam generation, ∇P^{gen} or u_t^{gen} . As dlog(λ_g^f)/dlog(∇P) falls below -1, u_t decreases with increasing ∇p (Eq. 4.2; Fig. 4.2). In the highly non-linear equations of this model, the key factor for triggering foam generation is the power-law dependency of lamella generation upon pressure gradient (Eq. 4.5a).

4.4 Population-balance model of Kam (2008)

The variant of this model (Kam and Rossen, 2003) introduced by Kam (2008) employs a modified version of the lamella-creation function r_g: an error function of pressure gradient (Eq. 4.4b). In addition, the lamella-coalescence function r_c includes a small modification, from Kam et al. (2007) (Eq. 4.5b), in comparison with the original version (Eq. 4.5a) defined by Kam and Rossen (2003). The lamella-creation rate is thus normalized between 0 and an upper limiting value. The reference pressure gradient ∇P_0 (Eq. 4.4b) indicates the pressure gradient near which the rate of lamella generation starts increasing sharply. Fig. 4.5 illustrates the LE solution of this model obtained using Eq. 4.10b. The model parameters employed in this example are from Kam (2008) (Table 4.A2). Fig. 4.6b plots bubble density as a function of ∇p. Figs. 4.7a and 4.7b show the relation between the reduction of gas mobility and the increase of pressure gradient, which explains the model's representation of a trigger for foam generation specified in Eq. 4.2.

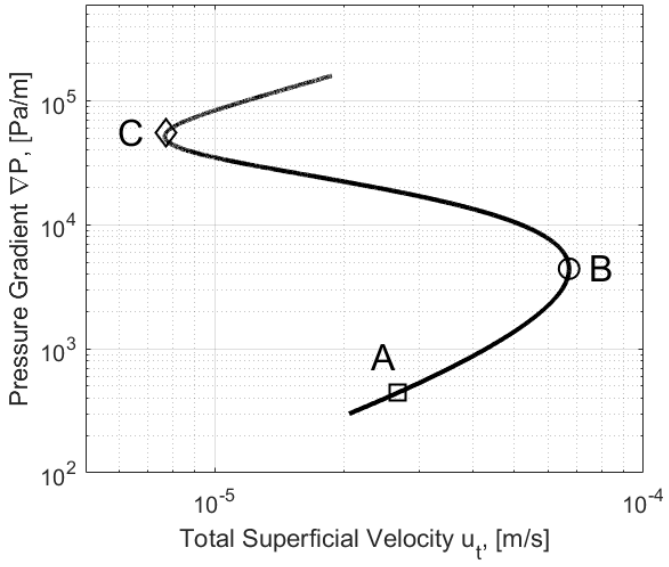

Figure 4.5. Local-Equilibrium solution for the Population-Balance model of Kam (2008) at foam quality f_g = 91%. As in Figs. 4.2-4.4, B marks the trigger for foam generation. The curve between A and B represents the steady-state of weak/no foam; the curve between B and C represents the unstable steady-state of intermediate foam; and the curve above C represents the steady-state of strong foam. Parameter values are in Table A2.

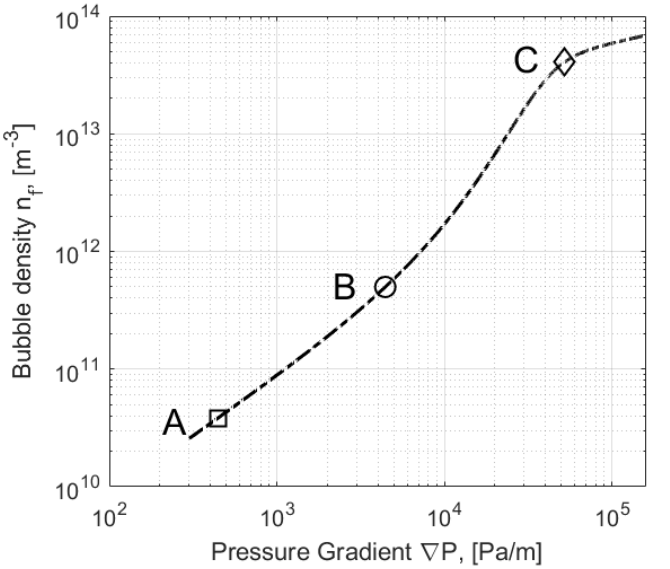

Figure 4.6. Local-Equilibrium bubble density of foam $n_{f,LE}$ as a function of pressure gradient for the LE solution of the model of Kam (2008) illustrated in Figure 4.5. Parameter values are in Table A2.

4.5 Population-balance model of Chen et al. (2010)

The population-balance model of Kovscek and Radke (1993, 1994, and 1995) and its variants (Kovscek and Bertin, 2003; Tang and Kovscek, 2006; Chen et al, 2010) account for an explicit definition of bubble density n_f as well as gas trapping and flowing fraction of gas X_f. In this model, repeated Roof snap-off (Roof, 1970) is taken to be the prevailing mechanism of lamella generation in steady flow. This mechanism is assumed to operate repeatedly in a fraction of pore throats in steady-state foam flow.

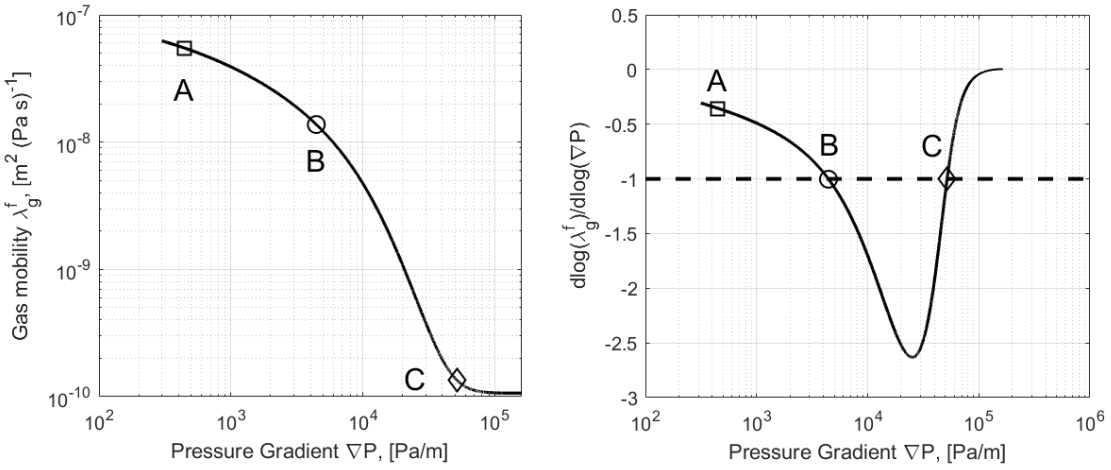

(a) **(b)**

Figure 4.7. (a) Mobility of gas μ_g^f as a function of pressure gradient for the Population-Balance model of Kam (2008). (b) dlog(λ_g^f)/dlog(∇P) as a function of pressure gradient. Parameter values are in Table A2.

Here we analyse the Population-Balance model of Chen et al. (2010), a version of the model first introduced by Kovscek and Radke (1993). Kovscek and Radke (1993) report that representing a minimum velocity and pressure gradient for foam generation is not a goal of their foam model. They argue that foam generation occurs readily as gas invades a porous medium initially fully saturated with surfactant solution; hence it's unnecessary to include an onset velocity or pressure gradient in the lamella-creation function.

Like other Population-Balance models (Friedmann et al., 1991; Kam and Rossen, 2003; Kam, 2008), the equations in this family of models are nonlinear and complex. We have not been able to reproduce such a trigger with the model parameters we tested. Here we do not attempt to provide a rigorous proof that this family of models cannot reproduce a minimum velocity for foam generation. Instead, we describe conditions under which it could produce a minimum velocity for foam generation.

As in other population-balance models (Friedmann et al., 1991; Kam and Rossen, 2003; Kam, 2008), in the model of Chen et al. (2010), foam texture n_f is the result of the simultaneous processes of lamella creation and destruction. The lamella-generation rate r_g in this model depends on the interstitial velocities of gas and water through generation sites in the pore network

$$r_g = k_1 v_w v_f^{1/3} \qquad \text{Eq. 4.11}$$

with

$$k_1 = k_1^0 \left[1 - \left(\frac{n_f}{n^*}\right)^{\omega}\right] \qquad \text{Eq. 4.12}$$

where v_w and v_f are the interstitial velocities of water and of flowing gas, respectively, and n^* is the maximum possible foam texture. The term in brackets shuts off foam generation as foam approaches a limiting texture n^*. In these and the following equations, k_1^0, ω, n^*, $X_{t,max}$,, β, k_1^0, and P_c^* are model parameters.

The water interstitial velocity v_w is a function of water saturation S_w, porosity ϕ and water superficial velocity u_w.

$$v_w = \frac{u_w}{\phi S_w} \qquad \text{Eq. 4.13}$$

The gas interstitial velocity is a function of gas saturation S_g, gas superficial velocity u_f, porosity, and the flowing gas fraction X_f.

$$v_f = \frac{u_f}{\emptyset S_g X_f} \qquad \text{Eq. 4.14}$$

The flowing gas fraction in turn depends on foam texture n_f:

$$X_f = 1 - X_{t,max}\left(\frac{\beta n_f}{1+\beta n_f}\right) = \frac{X_{t,max}}{1+\beta n_f} + \left(1 - X_{t,max}\right) \qquad \text{Eq. 4.15}$$

where $X_{t,max}$ is the maximum trapped-gas fraction.

In another version of the model (Tang and Kovscek, 2006), the flowing fraction depends on pressure gradient as well as foam texture. In the rest of this derivation we assume the dependency is on foam texture alone.

The lamella-destruction rate depends on foam texture, the interstitial velocity of gas through lamella-destruction sites and capillary pressure

$$r_c = k_{-1} n_f v_f \qquad \text{Eq. 4.16}$$

with

$$k_{-1} = k_{-1}^0 \left(\frac{P_c}{P_c^* - P_c}\right)^2 \equiv k_{-1}^0 f(P_c) \qquad \text{Eq. 4.17}$$

where k_{-1}^0 is a constant, P_c^* is the limiting capillary pressure for foam stability, and we define $f(P_c)$ for convenience in notation below. Note that $f(P_c)$ increases as P_c increases toward P_c^*, where $f(P_c)$ approaches infinity.

Equating the lamella-creation and -destruction rates gives an expression for local-equilibrium (LE) foam texture n_f

$$n_f = \left(\left[\frac{k_1^0}{k_{-1}^0}\right]\left[\frac{u_w}{u_f}\right]\phi^{\frac{1}{3}}\right)\left[\frac{1-\left(\frac{n_f}{n^*}\right)^{\omega}}{f(P_c(S_w))}\right]\left[\frac{(1-S_w)^{\frac{2}{3}}}{S_w}\right]\left[X_f^{\frac{2}{3}}\right]\left[u_f^{\frac{1}{3}}\right] \qquad \text{Eq. 4.18}$$

At a given injected gas fraction, the term in the first bracket is constant. Removing the constant terms for steady flow at fixed quality, one can write,

$$n_f \sim \left[\frac{1-\left(\frac{n_f}{n^*}\right)^{\omega}}{f(P_c(S_w))}\right]\left[\frac{(1-S_w)^{\frac{2}{3}}}{S_w}\right]\left[X_f^{\frac{2}{3}}\right]\left[u_f^{\frac{1}{3}}\right] \qquad \text{Eq. 4.19}$$

At a trigger for foam generation at fixed foam quality, as ∇p increases, total superficial velocity decreases (Fig. 4.1b), n_f increases, S_w decreases, and P_c increases. This trend continues as ∇p increases through the intermediate unstable state of foam, while foam texture rises from nearly zero to near its maximum value, flowing fraction falls from a value close to 1 toward its minimum value, water saturation falls from a value near $(1-S_{gr})$ to a value near S_{wc} (cf. Figs. 4.2 to 4.4 or 4.5 to 4.7). The initial triggering of foam generation occurs at a relatively large value of S_w, given the high mobility of gas in the absence of foam.

How could Eq. 4.19 represent increasing n_f as total superficial velocity decreases? The individual terms in Eq. 4.19 affect n_f as follows:

1) The first term in brackets decreases as $f(P_c)$ increases with increasing P_c.
2) The third term in brackets decreases as foam texture increases (Eq. 4.15). In the model of Tang and Kovscek (2006), where flowing fraction depends also on foam pressure gradient, flowing fraction is an increasing function of pressure gradient. Thus in that version of the model, the superficial velocity of flowing foam would likewise fall as flowing fraction increases.
3) The fourth term in brackets decreases, as overall total superficial velocity decreases at fixed gas fraction.

4) The second term in brackets is the only term that increases as foam is generated and water saturation falls. This term derives from the dependence of gas and water interstitial velocities through generation sites (Eq. 4.11) and the relations between interstitial and superficial velocities of water and gas (Eqs. 4.13 and 14).

Therefore, an increase in foam texture upon a reduction in superficial velocity is in principle possible if the increase in the second term is larger than the decreases in the first, third and fourth terms.

The extent to which water saturation falls as foam is created depends on the mobility functions for gas and water. The mobility of water depends on the water-relative-permeability function. The mobility of gas depends on the foam-free gas relative-permeability function and foam texture

$$\lambda_{rg} = \frac{k_{rg}^{f}}{\mu^{f}} = k_{rg}(S_w)\left(\mu_g^0\left[1 + \frac{\alpha}{\mu_g^0} * \frac{n_f}{v_g^{\frac{1}{3}}}\right]\right)^{-1} \qquad \text{Eq. 4.20}$$

where k_{rg}^{f} and k_{rg} are the gas relative permeabilities as a function of S_w with and without foam, μ^f and μ_g^0 are gas viscosity with and without foam, and α is a parameter in the gas-viscosity model. The decrease in gas mobility, which causes the fall in water saturation, is tempered by the shear-thinning rheology of foam and the effect of decreasing water saturation on foam-free gas relative permeability. At the trigger itself, X_f is close to 1, and hence that term is unlikely to reduce gas mobility greatly (via reducing the gas phase relative permeability).

4.6 STARS foam interpolation model

The foam interpolation model in the STARS simulator (Martinsen and Vassenden, 1999; Cheng et al., 2000; Computer Modeling Group, 2017) is a widely used Implicit-Texture foam model. Lotfollahi et al. (2016) state that the STARS model cannot represent an abrupt transition from weak/no foam to strong foam. In the model, the effect of foam on gas mobility is represented as a reduction in gas relative permeability in the presence of foam. The relative permeability of gas is the product of gas relative permeability without foam, k_{rg}, and a mobility-reduction factor FM (Eq. 4.21). FM is in turn a function of seven factors representing the effects of pressure gradient, water and oil saturations, surfactant concentration, etc. (Ma et al., 2013). Parameter fmmob (Eqs. 4.21, 22, and 28) is the reference gas-mobility-reduction factor, which represents the maximum achievable reduction in gas mobility. In the following equations, fmmob, fmgcp, epgcp, epdry, fmdry, fmcap and epcap are model parameters.

$$\lambda_{rg} = \frac{k_{rg(S_w)}}{\mu_g} FM \quad ; \quad FM = \frac{1}{1 + fmmob \times \prod_{i=1}^{7} F_i} \qquad \text{Eq. 4.21}$$

Here we examine three F_i functions from Eq. 4.21 to represent the model's ability to represent a trigger for foam generation in an oil-free homogeneous porous medium:

1) The foam-generation function (Eq. 4.24), called F_{gen} by Lotfollahi et al. (2016) and F_4 by Ma et al. (2015), is a function of capillary number N_{ca}, which is defined in terms of pressure gradient ∇P (Eq. 4.23).
2) The dry-out function (Eq. 4.25) F_{dry} (also called F_7) is a function that relates water saturation to the reduction of gas-phase mobility by foam. As in the coalescence function in the models of Kam and Rossen (2003), it implicitly reflects the limiting capillary pressure.
3) The shear-thinning function (Eq. 4.26) F_{shear} (Lotfollahi et al., 2016) (aka F_3) is also a function of capillary number N_{ca} (Eq. 4.13). It accounts for the shear-thinning rheology of

strong foam. F_3 equals unity when capillary number (Eq. 4.23) is smaller than a reference capillary number fmcap (Eq. 4.26) (Jamshidnezhad et al., 2009; Boeije and Rossen, 2013).

$$FM = \frac{1}{1+\text{fmmob}\, F_{gen} F_{dry} F_{shear}} \quad \text{Eq. 4.22}$$

$$N_{ca} \equiv \frac{k|\nabla P|}{\sigma} \quad \text{Eq. 4.23}$$

$$F_{gen} = \begin{cases} 0, & N_{ca} \le \text{fmgcp} \\ \left(\frac{N_{ca}-\text{fmgcp}}{\text{fmgcp}}\right)^{\text{epgcp}}, & N_{ca} > \text{fmgcp} \\ 1, & \text{Nca} > 2\ \text{fmgcp} \end{cases} \quad \text{Eq. 4.24}$$

$$F_{dry} = 0.5 + \frac{1}{\pi}\arctan\big(\text{sfbet}(S_w - \text{sfdry})\big) \quad \text{Eq. 4.25}$$

$$F_{shear} = \begin{cases} 1, & N_{ca} \le \text{fmcap} \\ \left(\frac{\text{fmcap}}{N_{ca}}\right)^{\text{epcap}}, & N_{ca} > \text{fmcap} \end{cases} \quad \text{Eq. 4.26}$$

$$\lambda_{rg} = \frac{k_{rg}(S_w)}{\mu_g} \frac{1}{1+\text{fmmob}\, F_{gen} F_{dry} F_{shear}} \quad \text{Eq. 4.27}$$

$$\frac{u_w}{u_g} = \text{constant} = \frac{(1-f_g)}{f_g} = \frac{\frac{k_{rw}(S_w)}{\mu_w}}{\frac{k_{rg}(S_w)}{\mu_g} \frac{1}{1+\text{fmmob}\, F_{gen(\nabla P)} F_{dry} F_{shear}}} \quad \text{Eq. 4.28}$$

The function F_{gen} plays the key role in the model's representation of a trigger for foam generation. This function employs a critical capillary number fmgcp. In Eq. 4.23, permeability k and surface tension between gas and water (with surfactant) σ are constants in an isothermal and homogeneous system. Therefore foam generation is a function of pressure gradient. If $\nabla p < (\text{fmgcp} \times \sigma/k)$, $F_{gen} = 0.0$ and FM = 1.0: no foam can exist. As pressure gradient exceeds this value, F_{gen} increases with increasing ∇P until it reaches unity at 2(fmgcp). Parameter epgcp (Eq. 4.24) is an exponent that dictates how F_{gen} increases with increasing pressure gradient.

The definition of F_{gen} (Eq. 4.24) makes gas mobility a function of pressure gradient in a similar way to the effect of the lamella-creation function r_g (Eqs. 4.4a and 4.4b) of the population-balance model of Kam and Rossen (2003). However, in contrast to the model of Kam and Rossen (2003) and other Population-Balance models (Friedmann et al., 1991; Kam, 2008; Kovscek and Radke, 1995; Chen et al., 2010), the STARS foam model doesn't account explicitly for the dynamics of lamella transport, creation and destruction.

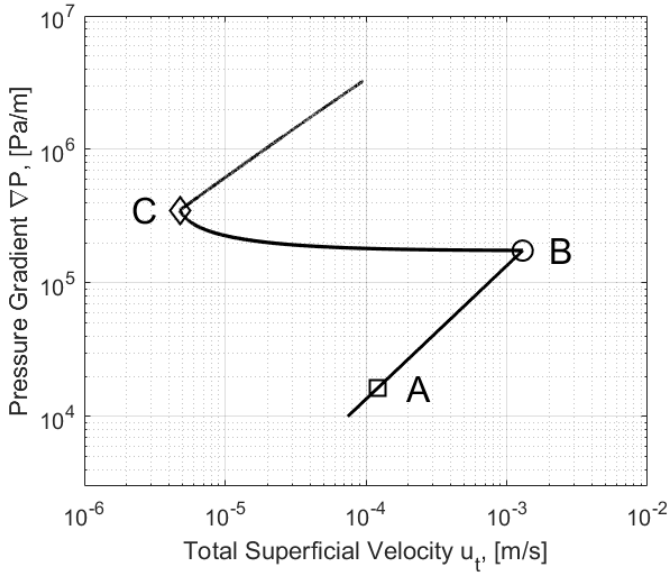

Figure 4.8. Local-Equilibrium solution for the Foam Interpolation model in STARS simulator at foam quality of f_g = 90%. Points A, B and C have the same meanings as in Figs. 4.2 to 4.7. Parameter values are in Table A3.

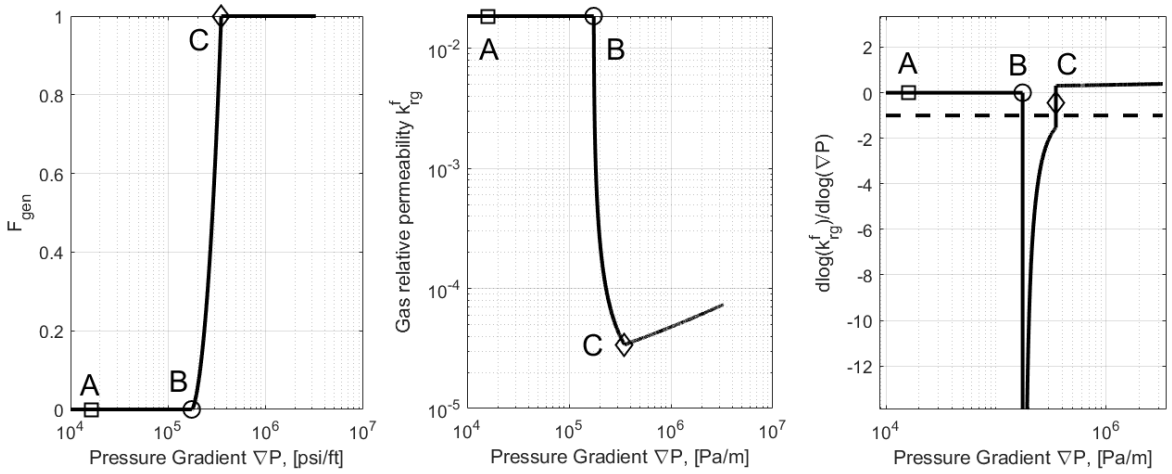

(a) **(b)** **(c)**

Figure 4.9. (a) Foam-generation factor F_{gen} as a function of pressure gradient for the Foam Interpolation model in STARS simulator at foam quality of f_g = 90%. (b) Gas relative permeability as a function of pressure gradient. (c) dlog(λ_g^f)/dlog(∇P) as function of pressure gradient. Parameter values are in Table A3.

As in the model of Kam and Rossen (2003) and its variants (Kam et al., 2007; Kam, 2008), foam generation is triggered by increasing pressure gradient. Weak foam (between points A and B in Figs. 4.2-4.7) in those models refers to a state where some lamellae exist but have relatively little effect on gas mobility. In the Foam Interpolation model of STARS, however, there is no foam (no mobility reduction) for $\nabla P < (\text{fmgcp} \times \sigma/k)$ (Eq. 4.23).

Figs. 4.8 and 4.9 illustrate the predictions of the model for parameter values in Table A3. The system shifts abruptly from no foam to full-strength foam upon a twofold increase in ∇p. As long as fmmob is large enough, total mobility decreases by more than twofold in this range of ∇p, and there is a discontinuous change of state at fixed superficial velocity. Thus the STARS model can represent a trigger for foam generation.

4.7 Lotfollahi et al. (2016) model

Lotfollahi et al. (2016) focus not on an abrupt change from weak/no foam to strong foam but on hysteresis in foam strength in strong foam: specifically, in the strong-foam state, ∇p decreasing but a small amount upon a reduction in superficial velocity. They propose a new formulation for the foam-generation function F_{gen} in STARS (Eq. 4.14), which we denote F_{gen}^{L} (Eq. 4.29)

$$F_{gen}^{L} = \begin{cases} 0 \\ fgenc + \left[\frac{(1-fgenc)N^{epgcp}}{1+N^{epgcp}}\right], \\ 1 \end{cases} \qquad \text{Eq. 4.29}$$

with N_{ca} defined by Eq. 4.23 and

$$N \equiv (N_{ca} - fmgcp)/(N_{ca}^{max} - N_{ca}). \qquad \text{Eq. 4.30}$$

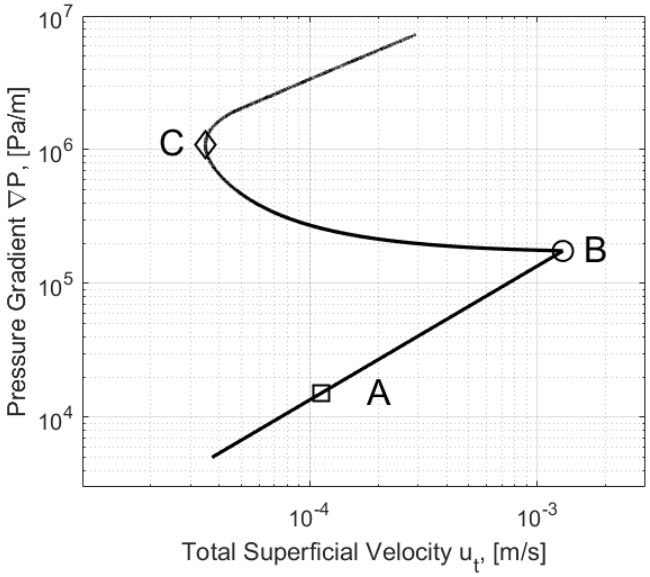

Figure 4.10. Local-Equilibrium solution for the foam model of Lotfollahi et. al. (2016), a modification of the STARS model, at foam quality f_g = 90%. Parameter values are in Table A4.

Apart from examining hysteresis in the strong-foam state, Lotfollahi et al. (2016) show that the new function can be used to predict a minimum velocity (and minimum pressure gradient) for foam generation. In the revised function, a maximum capillary number N_{ca}^{max} (related to a maximum pressure gradient ∇P^{max}) is introduced in addition to the minimum capillary number for foam generation fmgcp. The foam-generation function F_{gen}^{L} is a power-law function of a normalized capillary number N (Eq. 4.30). For N_{ca} < fmgcp, $F_{gen}^{L} = 0.0$: gas and water flow in the absence of foam. For $N_{ca}^{min} \leq N_{ca} < N_{ca}^{max}$, foam generation is triggered and F_{gen}^{L} increases with increasing pressure gradient. For $N_{ca} \geq N_{ca}^{max}$, F_{gen}^{L} = 1.0, indicating the steady-state of strong foam is achieved. The difference between N_{ca}^{min} and N_{ca}^{max} governs the range of the steady-state of intermediate foam (points B-C in Figs. 4.10 and 4.11).

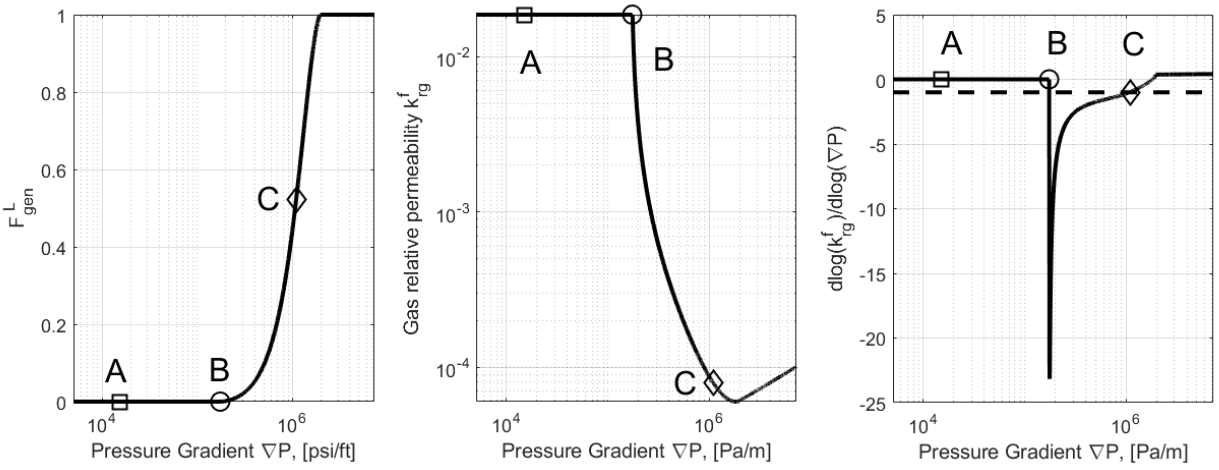

(a) **(b)** **(c)**

Figure 4.11. (a) Foam-generation function F_{gen}^{L} (Eq. 4.19) as function of pressure gradient ∇P or the foam model of Lotfollahi et. al. (2016). (b) Gas relative permeability (with foam) as a function of pressure gradient ∇P. (c) $d\log(k_{rg}^f)/d\log(\nabla P)$ as a function of pressure gradient. Dashed line indicates value of $d\log(\lambda_g^f)/d\log(\nabla P) = -1$ (Eq. 4.3). Parameter values are in Table A4.

In analysing the Lotfollahi et al. (2016) foam model, we employ the same combination of FM functions shown in Eq. 4.12 and the updated foam-generation function (Eq. 4.29), the dry-out function F_{dry} (Eq. 4.25), and the shear-thinning function F_{shear} (Eq. 4.26). Fig. 4.10a shows one realization of this model, where Lotfollahi et al. (2016) fitted their parameters to an experiment of Gauglitz et al. (2002). Fig. 4.13b shows the impact of increasing pressure gradient on the velocity as well as the magnitude of reduction of gas mobility. As pressure gradient exceeds the minimum pressure gradient for foam generation, FM (Eq. 4.22) decreases sharply, which brings about a significant reduction of gas mobility λ_g^f (Eq. 4.27). Figs. 4.11b and 4.11c illustrate the range of pressure gradient where $d\log(\lambda_g^f)/d\log(\nabla P) < -1$, within which total superficial velocity decreases with increasing pressure gradient. The foam model of Lotfollahi et al. (2016) can represent a trigger for foam generation.

4.8 Simulation of long-distance foam propagation

4.8.1 Introduction

Since the STARS foam model includes the effect of a minimum superficial velocity for foam generation (Fig. 4.8), we investigate how this model represents foam propagation in radial flow. Ashoori et al. (2012) and Yu et al. (2020) find that the velocity of the foam front decreases and approaches zero at a finite total superficial velocity u_t^{prop}. This critical velocity for foam propagation is greater than that at which foam cannot be maintained in place, u_t^{col}. We examine whether or not the simulation result from the IT foam model STARS can match this result.

We assume a one-dimensional horizontal cylindrical reservoir with homogeneous permeability (10 Darcy, i.e. 1×10^{-11} m^2) and porosity (0.199), and an outer radius of 80 m. The simulation uses a 36° radial arc, but the superficial velocities cited below are scaled to injection in the full radial direction. The model has 8000 grid blocks of length 0.01 m in the radial direction. Both gas and surfactant solution are co-injected from an injection well of radius 0.1 m.

The reservoir is initially fully saturated with brine without surfactant. We start the simulation by co-injecting gas and brine solution for around 9 days, until a quasi-steady-state

between gas and water is achieved in the first half of the reservoir (between the injector and the producer). We then switch to the co-injection of gas and surfactant solution.

The initial reservoir pressure is 6000 kPa, and the production well is controlled by a minimum bottom-hole pressure of 5990 kPa. The initial and injection temperatures (27°C) are far below the bubble point of water (275K) at this pressure. The relative-permeability tables for gas and water phases are based on Brooks-Corey expressions (Table A3), with parameters taken from Lotfollahi et al. (2016). Rock and fluid properties used in our simulation are also given in Table A3.

4.8.2 Simulation result

Co-injection of N_2 gas and surfactant solution starts on Jan 1, 2020 and stops on Dec 31, 2020. The total volumetric injection rates of gas and liquid are fixed at surface conditions corresponding to a foam quality of 90% at the initial reservoir pressure. This indicates an initial total superficial velocity of about 1.67×10^{-3} m/s in at the injection well. This injection rate guarantees that the initial total superficial velocity u_t at the boundary of the well-block is greater than the minimum superficial velocity for foam generation u_t^{gen} based on the LE equations (Fig. 4.8). As a result, the pressure gradient and capillary number (Eq. 4.23) inside the well-block (as well as the blocks nearby) is high enough to satisfy the criterion (Eq. 4.24) for foam generation. Later, pressure rises greatly near the well (Fig. 4.12a) and results in gas compression and a reduction of gas injection rate. However, since foam propagation is determined at the leading edge of the foam bank, which remains near the initial reservoir pressure, this does not affect foam propagation.

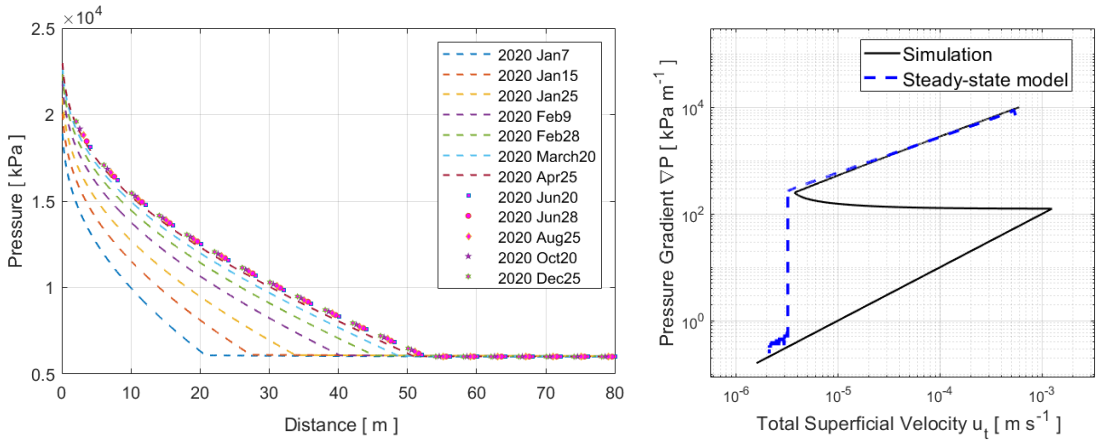

(a) **(b)**

Figure 4.12. (a) Reservoir pressure distribution between injection wells and production well as a function of time. (b) Grid-block values of pressure gradient and superficial velocity (blue dotted line) at the end of the simulation. The black curve is the local-equilibrium behaviour predicted by STARS.

Fig. 4.12a illustrates the evolution of reservoir pressure during foam injection. The separation of pressure profiles from Jan 7 to Jun 20 indicates the propagation of foam to greater distances. Foam propagation stops on Jun 20 at a distance of about 52 m from the well. The leading edge of foam bank remains at a radius of about 52 m for another 6 months of foam injection.

In the STARS simulation, the failure of foam propagation is directly related to the inability to maintain foam, not to a separate condition for foam propagation. Fig. 4.12b compares the result of numerical simulation (blue dashed-curve) of foam generation and subsequent propagation to the solution of the local-steady-state model (black solid curve). The numerical simulation result represents grid-block superficial velocities and pressure gradients on Dec 25,

2020, one year since the start of foam injection. At steady-state, the increase in pressure in the first grid block, combined with gas compressibility, has reduced total superficial velocity there significantly from that when foam was triggered (Fig. 4.12b). The numerical simulation is still in good agreement with the local-equilibrium model for the nominal gas fractional flow (Fig. 4.12b).

In this simulation, we avoid another, more-fundamental problem in representing foam generation near an injection well in reservoir-scale simulation. The Peaceman (1978) equation represents injection-well pressure based on averaged fluid properties in the grid block containing the injection well. If fluid properties depend on pressure gradient, in the simulation they are based on an estimate of pressure difference between the well-block and its neighbouring grid blocks instead of at the wellbore. Injection/production wells are modelled as a source/sink term in governing equations. As a result, the pressure gradient at the wellbore is not calculated explicitly anywhere in a conventional reservoir simulation. In Fig. 4.12b foam generation reflects the pressure difference between the first and second grid blocks (V. Chandrasekar, Computer Modeling Group, personal communication): in our simulation, at a position 1 cm from the wellbore (or equivalently 11 cm from the centre of injection well).

In a simulation of the same radial reservoir using grid blocks that are 0.1 m long, foam generation fails. There is no foam generation in this case, because superficial velocity (about 9.2×10^{-4} m/s) and pressure gradient at the outer surface of the first grid block around the well is not sufficient for the triggering of foam generation. In a conventional reservoir simulation the distance from the well to a grid-block boundary would usually be much greater. Pressure gradient as calculated between grid blocks in the simulation would not reflect wellbore pressure gradient and therefore foam generation at the wellbore.

This issue would affect not only the STARS model, but that of Lotfollahi at al. (2016) and the Population-Balance model of Kam and Rossen (2003) and its variants (Kam et al., 2007; Kam, 2008). Unless grid resolution gives a superficial velocity at the grid-block scale sufficient for foam generation, the models would not indicate that foam generation occurs. The Population-Balance model of Kam and Rossen has the option of injecting gas with a non-zero value of n_f reflecting the presence of foam; this foam would presumably be maintained in propagation to other grid blocks. But this then reflects a choice of the properties of injected gas made manually by the user, not a triggering of foam generation in situ at the injection face. If the user makes this choice, there would be foam entering the grid block whether or not the velocity at the injection face were sufficient to trigger foam generation.

Simulations of foam in linear flow (Kam et al., 2007; Kam et al., 2008; Lotfollahi et al., 2016) with these models provide valuable insights into foam mechanisms. They avoid the issue described in the previous paragraph, because total superficial velocity is uniform in the linear model (apart from possible effects of the compressibility of gas). This issue would arise, however, in reservoir application of the model with injection wells located inside a relatively large grid block.

IT foam models do not track foam propagation directly. Foam is created in the next grid block at the foam front when the estimated pressure gradient in that grid block exceeds ∇p^{min} (Eqs. 23 and 24). Pressure gradient in that grid block is inferred from the pressures in grid blocks upstream and downstream of it. Therefore, with no foam in the given grid block or that ahead of it, the creation of foam in the grid block at the foam front requires a large-enough pressure in the upstream grid block that the pressure gradient calculated for the grid block at the front exceeds ∇p^{min}. For PB models gas enters the grid block with the foam texture of the upstream grid block and this is not an issue.

Thus if foam generation is achieved, foam propagation depends on the pressure gradient assigned to the grid block at the foam front. The STARS simulator uses the Euclidian average of the pressure differences upstream and downstream of that grid block (V. Chandrasekar,

Computer Modeling Group, personal communication). This heavily weights the large upstream pressure difference, giving successful foam propagation in our simulations. If an arithmetic average were used, foam propagation would be expected to fail when the pressure gradient, based on the difference in pressure between the grid block at the front and that upstream, is roughly twice that required for foam propagation.

4.9 Conclusions and Discussion

- ◊ Among the various models examined, the LE version of Kam's Population-Balance model (Kam and Rossen, 2003) and its variant (Kam, 2008), the IT STARS foam model (Martinsen and Vassenden, 1999; Cheng et al., 2000; Computer Modeling Group, 2017), and that of Lotfollahi et al. (2016) can represent a minimum superficial velocity or pressure gradient for foam generation. All of these models are designed in a way that the mobility reduction of gas by foam is a strongly increasing function of pressure gradient over some range of pressure gradient. In steady flow at constant foam quality f_g, if the reduction in gas mobility is greater than the increase in pressure gradient, total superficial decreases with increasing pressure gradient (Eq. 4.3). In such cases, a foam model can represent a trigger for foam generation.
- ◊ In the Population-Balance model of Chen et al. (2010), foam generation and destruction depend on interstitial velocities of gas and liquid. Due to the nonlinearity of the model's equations, we cannot say conclusively whether or not the model can represent a trigger for foam generation for all parameter values. Instead, we define criteria that must be satisfied if a trigger for foam generation is to be represented in this model. This family of models (Kovscek and Radke, 1994,1995,1996; Kovscek and Bertin, 2003; Tang and Kovscek, 2006 Chen et al., 2010) wasn't originally intended to include a critical velocity/pressure gradient for foam generation, according to a report by the creators of the original model (Kovscek and Radke, 1993).
- ◊ The STARS simulator can represent a minimum velocity for foam propagation at the condition for foam collapse u_t^{col}, but not a criterion for propagation distinct for that for foam stability. Our simulation results suggest that foam propagation stops at the distance with a local pressure gradient where strong foam cannot be maintained.
- ◊ Successful representation of a trigger for foam generation is a necessary but insufficient condition for a foam model to predict a criterion for propagation distinct from that for foam stability. The Population-Balance model of Kam (2008) can represent a critical superficial velocity for both foam generation and propagation at steady flow, because it includes the dynamics of convection, creation and destruction of foam in relation to local pressure gradient and water saturation. In implicit-texture foam models, such as the foam model in STARS, foam itself is not transported, in the absence of an explicit definition of foam texture as a component in the model. In implicit-texture models, creation and propagation of foam can happen upon achieving sufficient local pressure gradient. The mechanism for failure to propagate identified by Ashoori et al. (2012) is not represented.
- ◊ The propagation of foam in IT models is not tracked directly. If foam generation depends on pressure gradient ∇p exceeding ∇p^{min}, the propagation of foam to the next grid block requires a pressure in the upstream grid block large enough that the pressure gradient calculated for the grid block at the front exceeds $\nabla p^{min.}$
- ◊ Our results suggest a serious problem for all foam models where foam generation is based on pressure gradient in conventional simulation with relatively large grid blocks: superficial velocity and pressure gradient at the well are not represented explicitly, which means that foam generation near the injection face would not be represented without truly extraordinary grid resolution near the well. Simulations of linear displacements or of radial flow with

extraordinarily fine grid refinement can still provide valuable insights into foam mechanisms that affect behavior on a larger scale.

References

Ashoori, E.; Marchesin, D.; and Rossen, W.R. (2012). Multiple Foam States and Long-Distance Foam Propagation in Porous Media, *SPE J.* 17(04): 1231-1245. https://doi.org/10.2118/154024-PA

Cheng, L., Reme, A. B., Shan, D., Coombe, D. A., and Rossen, W. R. (2000). Simulating Foam Processes at High and Low Foam Qualities. Paper presented at the SPE/DOE Improved Oil Recovery Symposium, Tulsa, Oklahoma, April 2000. https://doi.org/10.2118/59287-MS

Chen, Q., Gerritsen, M. G., & Kovscek, A. R. (2010). Modeling Foam Displacement with the Local-Equilibrium Approximation: Theory and Experimental Verification. *SPE J.* 15 (01): 171–183. https://doi.org/10.2118/116735-PA.

Computer Modeling Group, STARS User's Guide, Version 2017.10, Calgary, Alberta, Canada.

Falls, A. H., Hirasaki, G. J., Patzek, T. W., Gauglitz, D. A., Miller, D. D., & Ratulowski, T. (1988). Development of a Mechanistic Foam Simulator: The Population Balance and Generation by Snap-Off. *SPE J*. https://doi.org/10.2118/14961-PA

Friedmann, F.; Chen, W.H.; Gauglitz, P.A. (1991). Experimental and simulation study of high-temperature foam displacement in porous media, *SPE J.* 6(01): 37–45. https://doi.org/10.2118/17357-PA

Friedmann, F.; Smith, M.E.; Guice, W.R.; Gump, J.M.; Nelson, D.G. (1994). Steam-foam mechanistic field trial in the midway-sunset field, *SPE J.* 9(04): 297–304. https://doi.org/10.2118/21780-PA

Gauglitz, P.A.; Friedmann, F.; Kam, S.I. and Rossen, W.R. (2002). Foam Generation in Homogeneous Porous Media, *J Chem. Eng. Sci*. 57(19): 4037-4052. https://doi.org/10.1016/S0009-2509(02)00340-8

Jamshidnezhad, M., Shen, C., Kool, P., Mojaddam Zadeh, A., & Rossen, W.R. (2009). Improving Injectivity To Fight Gravity Segregation in Gas Enhanced Oil Recovery. *SPE J.* 15(01): 91-104. https://doi.org/10.2118/112375-PA

Khatib, Z.R.; Hirasaki, G.J. and Falls, A.H. (1988). Effects of Capillary Pressure on Coalescence and Phase Mobilities in Foams Flowing Through Porous Media, *SPE J.* 3(3): 919-926. https://doi.org/10.2118/15442-PA

Kovscek, A. R., & Radke, C. J. (1993). Fundamentals of Foam Transport in Porous Media. United States: N. P., https://doi.org/10.2172/10192736

Kovscek, A. R., & Radke, C. J. (1994). Fundamentals of foam transport in porous media. In: L. L. Schramm (Ed.), Foams: Fundamentals and applications in the petroleum industry. Washington DC: ACS Advances in Chemistry Series No. 242 (Am. Chem. Soc.).

Kovscek, A.R., Patzek, T.W., & Radke, C.J. (1995). A mechanistic population balance model for transient and steady-state foam flow in Boise sandstone, *Chemical Engineering Science*, 50(23): 3783-3799. https://doi.org/10.1016/0009-2509(95)00199-F

Kovscek, A. R., & Radke, C. J. (1996). Gas bubble snap-off under pressure-driven flow in constricted noncircular capillaries, *Coll. Surf. A: Physicochem. Engng Aspects* 117: 55-76.

Kovscek, A.R., Bertin, H.J. Foam Mobility in Heterogeneous Porous Media. *Transport in Porous Media* 52**:** 37–49 (2003). https://doi.org/10.1023/A:1022368228594

Kam, S.I. and Rossen, W.R. (2003). A Model for Foam Generation in Homogeneous Media, *SPE J.* 8(04):417-42. https://doi.org/10.2118/87334-PA

Kam, S.I.; Nguyen, Q.P.; Li, Q. and Rossen, W.R. (2007). Dynamic Simulations With an Improved Model for Foam Generation, *SPE J.* 12(01): 35-28. https://doi.org/10.2118/90938-PA

Kam, S.I. (2008) Improved Mechanistic Foam Simulation with Foam Catastrophe Theory, *J Coll & Surf A* 318(1-3): 62-77. https://doi.org/10.1016/j.colsurfa.2007.12.0417

Leverett, M C. (1941). Capillary behavior in porous solids. *Trans. AIME*, 142(01), 152-169. https://doi.org/10.2118/941152-G

Lotfollahi, M., Kim, I., Beygi, M. R., Worthen, A. J., Huh, C., Johnston, K. P., … DiCarlo, D. A. (2016). Experimental Studies and Modeling of Foam Hysteresis in Porous Media. Paper SPE-179664-MS presented at the SPE Improved Oil Recovery Conference, Tulsa, Oklahoma, USA, April 2016. https://doi.org/10.2118/179664-MS

Martinsen, H. and Vassenden, F. (1999). Foam Assisted Water Alternating Gas (FAWAG) Process on Snorre, 10th European Symposium on Improved Oil Recovery.

Ma, K., Lopez-Salinas, J.L., Puerto, M.C., Miller, C.A., Biswal, S.L., and Hirasaki, G.J. (2013). Estimation of Parameters for the Simulation of Foam Flow Through Porous Media. Part 1: The Dry-out Effect. *Energy & Fuels.* 27(5): 2363-2375.

Peaceman, D. W.(1978). Interpretation of Well-Block Pressures in Numerical Reservoir Simulation, *SPE J.* 18(03): 183-194. https://doi.org/10.2118/6893-PA

Patzek, T. W. (1996). Field Applications of Steam Foam for Mobility Improvement and Profile Control. Society of Petroleum Engineers. https://doi.org/10.2118/29612-PA

Ransohoff, B, T. C., & Radke, C. J. (1988). Mechanisms of foam generation in glass-bead packs. *SPERE*. 3(02): 573–585. https://doi.org/10.2118/15441-PA

Roof, J.G. (1970). Snap-Off of Oil Droplets in Water-Wet Pores. Journal of Society of Petroleum Engineers. *SPE J*. 10(01): 85-90. Mar 1970. http://dx.doi.org/10.2118/2504-PA

Rossen, W.R. (1996). Foams in Enhanced Oil Recovery", In: Prud'homme, R.K., Khan, S., "Foams: Theory, Measurements, and Applications, Surfactant science series Vol. 57, Chap 11, Marcel Dekker, Inc. 270 Madison Avenue, New York 10016.

Rossen, W.R. and Gauglitz, P.A. (1990). Percolation Theory of Creation and Mobilization of Foams in Porous Media, *J AIChE.* 36(8): 1176-1188. https://doi.org/10.1002/aic.690360807

Rossen, W. R., and Boeije, C. S. (2013). Fitting Foam Simulation Model Parameters for SAG Foam Applications. Paper SPE-165303-MS presented at the SPE Enhanced Oil Recovery Conference, Kuala Lumpur, Malaysia, July 2013. https://doi.org/10.2118/165282-MS

Schramm, L. L. (1994). Foams: Fundamentals and applications in the petroleum industry. Washington DC: ACS Advances in Chemistry Series No. 242 (*Am. Chem. Soc.*).

Tang, G., and Kovscek, A. R. (2006). Trapped Gas Fraction During Steady-State Foam Flow. *Transport in Porous Media* 65(2): 287-307. https://doi.org/10.1007/s11242-005-6093-4

Yu, G., Rossen, W. R., and Vincent-Bonnieu, S. (2019). Coreflood Study of Effect of Surfactant Concentration on Foam Generation in Porous Media, *J I&EC.* 58(01): 420-427. https://doi.org/10.1021/acs.iecr.8b03141

Yu, G., Vincent-Bonnieu, S., and Rossen, W. R. (2020). Foam Propagation at Low Superficial Velocity: Implications for Long-Distance Foam Propagation. *SPE J.* 25(06): 3457–3471. https://doi.org/10.2118/201251-PA

Appendix 4.A-Parameter values for foam models

Foam parameters (Kam and Rossen, 2003)		Other parameters (Kam and Rossen, 2003)	
C_g/C_c	1×10^{-13}	k [m^2]	7.1×10^{-12}
C_f	1×10^{-14}	ϕ	0.199
m	4.4	μ_w [Pa s]	0.001
n	0.85	μ_g [Pa s]	0.00002
S_w^*	0.22	S_{wc}	0.2
		S_{gr}	0.1
		k_{rw}^0	0.7888
		k_{rg}^0	1.0
		nw	1.9575
		ng	2.2868

Table 4.A1. Population-Balance model of Kam and Rossen (2003).

Foam parameters (Kam, 2008)		Other parameters (Kam, 2008)	
C_g/C_c	3.6×10^{-16}	k [m^2]	30.4×10^{-12}
C_c	0.01	ϕ	0.31
C_f	1.535×10^{-16}	μ_w [Pa s]	0.001
∇P_0 [Pa/m]	9.5×10^4	μ_g [Pa s]	0.00002
n	1.0	S_{wc}	0.04
S_w^*	0.0585	S_{gr}	0.0
n_f^* [m^{-3}]	8×10^{13}	k_{rw}^0	0.7888
		k_{rg}+	1.0
		nw	1.9575
		ng	2.2868

Table 4.A2. Population-Balance model of Kam (2008).

Foam parameters	Value (Lotfollahi et al., 2016)	Other parameters	Steady-state model (Figs. 4.8 and 4.9) (Lotfollahi et al., 2016)	Simulation (Fig. 4.12)
fmmob	85700	k [m^2]	7.2×10^{-12}	10×10^{-12}
fmgcp	4.2×10^{-5}	Φ	0.199	0.199
epgcp	1.5	k_{rw}^0	0.15	0.15
fmcap	2.46×10^{-5}	k_{rg}^0	1.0	0.8
epcap	0.5	nw	1.95	1.9575
sfdry	0.22	ng	2.28	2.2868
sfbet	100	S_{wc}	0.2	0.2
		S_{gr}	0.1	0.0
		σ [N/m]	0.03	0.03 (independent of reservoir temperature)

Table 4.A3. STARS implicit-texture foam model (Martinsen and Vassenden, 1999; Cheng et al., 2000; Computer Modeling Group, 2017). Parameter values are from Lotfollahi et al. (2016).

Foam parameters	Value (Lotfollahi et al., 2016)	Other parameters	Steady-state model (Figs. 4.10 and 4.11) (Lotfollahi et al., 2016)
fmmob	85700	k [m^2]	7.2×10^{-12}
fmgcp	4.2×10^{-5}	Φ	0.199
epgcp	1.5	k_{rw}^0	0.15
fmcap	2.46×10^{-5}	k_{rg}^0	1.0
epcap	0.5	nw	1.95
sfdry	0.22	ng	2.28
sfbet	100	S_{wc}	0.2
Ncamax	4.7×10^{-4}	S_{gr}	0.1
fgenc	0.0	σ [N/m]	0.03

Table 4.A4. Implicit-texture foam model Lotfollahi et al. (2016).

Chapter 5

Conclusion and Suggestions for Further Research

5.1 Conclusions and discussion

5.1.1 Experiments on foam generation

In **Chapter 2**, our data (Fig. 2.5) show that the minimum velocity for foam generation in steady flow decreases with increasing surfactant concentration and increasing injected liquid fraction f_w. Despite the scatter in the data, our results suggest a clear relation between the trigger velocity u_t^{gen} and the injected water fraction f_w (Figs. 2.7 and 2.8). Such a trend agrees well with the theoretical predictions of Rossen and Gauglitz (1990) as well as the model of Kam and Rossen (2003) (Figs. 2.7 and 2.8). The percolation model of Rossen and Gauglitz (1990) implies a trend of decreasing trigger velocity (and pressure gradient) for foam generation with increasing liquid fraction injected. Their model suggests that the percolation fraction of gas decreases with increasing injected liquid volume fraction. The population-balance model of Kam and Rossen (Kam and Rossen, 2003) predicts that the critical velocity (and pressure gradient) for foam generation is also related to the stability of lamellae after the onset of lamella mobilization. In a porous medium with strong capillary forces, surfactant concentration affects lamella stability through its impact on the limiting capillary pressure P_c^* of foam (Khatib et al., 1988). At higher surfactant concentration, limiting capillary pressure becomes greater, i.e. lamellae remain stable at a higher capillary pressure (and lower water saturation). Last but not least, the trend in Figs. 2.5 and 2.6 suggests that the impact of surfactant concentration is more pronounced at higher foam qualities. Such a trend also stresses the significant role played by the fractional flow of water on the stability of lamellae.

The dynamic model of foam propagation at low superficial velocity (Ashoori et al., 2012) suggests a strong correlation between foam generation and foam propagation: the same pressure gradient-driven mechanisms that dominate lamella creation and coalescence at steady-state also dominate the evolution of foam texture at the advancing foam front. It's therefore a reasonable assumption that foam propagation has a similar dependency on water fractional flow and surfactant concentration. A wetter foam of larger surfactant concentration should promote the propagation and the stability of foam, even at surfactant concentrations far above the CMC (Critical Micelle Concentration) (Laskaris & Jones et al., 2016). This is tested in Chapter 3.

5.1.2 Experiments on foam propagation

In **Chapter 3**, our experimental results demonstrate the existence of three critical superficial velocities for the generation, propagation and collapse of foam in steady gas-liquid flow in homogeneous porous media (specifically, Bentheimer sandstone). In agreement with the theoretical predictions of Ashoori et al. (2012), and the implications of previous experiments on foam propagation (Friedmann et al., 1991, 1994), we find that mobilizing the leading edge of foam bank into a region of no foam requires exceeding a minimum superficial velocity u_t^{prop} (Fig. 3.8). At superficial velocities smaller than u_t^{prop}, the steady-state of strong foam cannot move forward, but is still stable until a yet-lower superficial velocity u_t^{col} is reached (Figs. 3.8 and 3.9).

The critical superficial velocities for foam in homogeneous porous media were tested and documented at various combinations of surfactant concentration and injected water fraction. As in the experiments of Chapter 2, foam generation becomes easier with increasing surfactant

concentration C_s, even far above the CMC, and injected liquid volume fraction f_w. The same trend applies to foam propagation and maintenance (Figs. 3.8a and 3.8b). The impact of f_w and C_s on foam propagation is less significant compared to their impact on foam generation; however, the increase of propagation velocity u_t^{prop} as f_w increases is still substantial. The difficulty of generating and maintaining foam in porous media reflects the decrease in lamella stability.

The critical velocities for foam propagation u_t^{prop} documented in our experiments represent the velocity below which foam either doesn't propagate at all, or advances at such a small pace that significant progress is hardly detectible. Both the minimum superficial velocities for foam propagation u_t^{prop} and foam stability u_t^{col} are considerably less than the superficial velocity required for triggering foam generation in steady flow of gas and aqueous solution (Figs. 3.8a and 3.8b). There is a substantial range of velocities at which there are two stable steady states, strong foam and weak or no-foam. Below the critical superficial velocity for foam stability u_t^{col}, however, pressure gradient falls to very low values, representing the collapse of strong foam. This may reflect a state of continuous-gas foam (Falls et al., 1988; Rossen and Gauglitz, 1990), at which one or more tortuous continuous flow channels of gas is formed around regions of trapped gas. Comparing Fig. 3.5 and Fig.3.7 suggests that the total mobility of fluid after foam collapse is somewhat lower than that before the triggering of foam generation. This comparison shows that, even after foam collapses, there may still be a significant amount of trapped gas in the medium rather than a complete destruction of foam bubbles. Such a result is an indicator that foam mobility depends on injection history, a different type of foam hysteresis than that for strong foams studied and modeled by Lotfollahi et al. (2016).

Theory (Rossen and Gauglitz, 1990; Kam and Rossen, 2003) and experiment (Gauglitz et al., 2002) reveal the significant role of pressure gradient on lamella creation and hence the generation as well as the stability of foam. When it comes to foam propagation, however, the superficial velocity at the traveling foam front is of parallel importance. Ashoori et al.'s (2012) model reveals that there are three fundamental factors that dominate the velocity of traveling foam front: the rate of bubble advection, $u_g n_f$; the rate of lamella creation at foam front (a function of pressure gradient, and is influenced by the rate of lamella advection); as well as the rate of lamella destruction at foam front (as function of capillary pressure and water saturation). When the sum of the first two factors dominates over the rate of bubble destruction, foam can propagate efficiently. A higher rate of lamella advection greatly enhances the rate of on-site lamella creation, which overcomes bubble destruction and leads to successful foam propagation. The failure (or the slow rate) of foam propagation is a direct result of dissipation of both superficial velocity and pressure gradient with increasing drainage area (of radial flow).

In Figs. 3.9a-3.9d, the minimum superficial velocity for foam propagation is roughly 2 to 3 times greater than the minimum superficial velocity for foam stability in place. This relatively small difference in velocities makes a substantial difference to radial distance and area. Swept volume is proportional to radius squared, suggesting a difference of 4 to 9 times in swept volume/area (in a formation layer of relatively constant thickness). Therefore, if foam can somehow be placed further from the well than direct propagation in steady flow could place it, it could be maintained stably over a substantially larger volume. If fracturing of the injection well can be avoided, it may be advisable to first inject foam at high velocity to reach a large target distance, and then slowly reduce the injection rate to smaller values while maintaining the foam in place. Implementing this strategy would require more research on foam stability at low superficial velocities.

In field application, alternating slugs of surfactant solution and gas are often injected (SAG) instead of co-injecting gas and surfactant solution. In the near-well region, alternating drainage and imbibition of liquid then creates favourable conditions for foam generation. At distances far away from the injection well, however, the effects of alternating slug injection are greatly

damped. The fractional flows of surfactant solution and gas can be expected to be relatively constant, as if they are being co-injected. The fixed f_w in our propagation experiments thus resembles the flow conditions for foam propagation far from an injection well even in a SAG process.

5.1.3 Modeling of foam generation and propagation

Among the various models examined, the LE version of Kam's population-balance model (Kam and Rossen, 2003) and its variants (Kam, 2008), the IT STARS foam model (Martinsen and Vassenden, 1999; Cheng et al., 2000; Computer Modeling Group, 2017), and that of Lotfollahi et al. (2016) can represent a minimum superficial velocity or pressure gradient for foam generation. All of these models are designed in a way that the local-equilibrium gas-mobility reduction by foam is a strongly increasing function of pressure gradient over some range of pressure gradient. In steady flow at constant foam quality f_g, if the reduction in gas mobility is greater than the increase in pressure gradient, total superficial decreases with increasing pressure gradient (Eq. 4.2). In such cases, a foam model can represent a trigger for foam generation.

In the population-balance model of Chen et al. (2010), lamella creation and coalescence strongly depend on the interstitial velocities of gas v_f and water v_w. Due to the nonlinearity of the model's equations, we cannot say conclusively whether or not the model can represent a trigger for foam generation for all parameter values. Instead, we pose several criteria that must be satisfied if a trigger for foam generation were to be represented by the model. This family of models (Kovscek and Radke, 1993, 1994, 1995; Kovscek and Bertin, 2003; Tang and Kovscek, 2006; Chen et al., 2010) was not originally intended to include a critical velocity/pressure gradient for foam generation, based on a report by the creators of the original model (Kovscek and Radke, 1993).

The STARS simulator (Martinsen and Vassenden, 1999; Cheng et al., 2000; Computer Modeling Group, 2017) can represent a minimum velocity for foam propagation at the condition for foam collapse u_t^{col}, but not a separate criterion for propagation distinct from that for foam stability. Our simulation result suggests that foam propagation stops at the distance with a local pressure gradient corresponding to the minimum pressure gradient for a steady-state of strong foam.

Successful representation of a trigger for foam generation is a necessary but insufficient condition for a foam model to predict a criterion for propagation distinct from that for foam stability. The population-balance model of Kam (2008) can represent a critical superficial velocity for both foam generation and propagation at steady flow, because it includes the dynamics of convection, creation and destruction of foam in relation to local pressure gradient and water saturation. In implicit-texture foam models, such as the foam model in STARS, transport of foam itself is explicitly represented, in the absence of an definition of foam texture as a component in the model. In implicit-texture models, creation and propagation of foam can happen upon achieving sufficient local pressure gradient. The mechanism for failure to propagate identified by Ashoori et al. (2012) is not represented.

Our results also indicate a major limitation in representing processes where foam is created at high pressure gradient near an injection well and propagates outward at lower pressure gradient. The pressure gradient at an injection well is not represented in the grid-block pressure gradient in conventional simulators. Rather, pressure gradient for all grid blocks is evaluated based on the fluxes at the boundaries of the grid blocks. We illustrate this issue with the IT STARS model, but it would affect any model, such as the population-balance model of Kam et al. (2007), which depends on pressure gradient to determine foam properties. More broadly, foam generation and propagation depends on the accuracy of evaluating pressure gradient from the properties of upstream and downstream grid blocks along with the grid block itself.

A failure of foam propagation directly from the well grid block does not mean foam cannot be placed far from a well. For instance, foam can be created at a sharp increase in permeability without a requirement of a minimum velocity or pressure gradient (Falls et al., 1988; Tanzil et al., 2002a; Shah et al., 2020).

Our study of foam propagation assumes that surfactant and gas are both transported together to distances far from the injection well. Gravity segregation (Stone, 1982; Jenkins, 1984; Rossen and van Duijn, 2004; Rossen et al., 2010; Jamshidnezhad et al., 2009) and surfactant adsorption may place limits on this assumption separate from the considerations of this study.

5.2 Recommendations for future research

5.2.1 Experiments and modeling of foam generation and propagation

An extension of our results is needed for a more complete view of the correlation between foam generation and propagation. To begin with, experiments at fixed pressure difference ought to be done. With completion of these experiments, the model of Kam and Rossen (2003) or the variants (Kam, 2008) could be fit to results, Then the traveling-wave solution of Ashoori et al. (2012) can be applied to obtain the critical superficial velocity for foam propagation. Such a procedure can be repeated for experimental results for foam propagation at various foam qualities f_g, surfactant concentrations C_s, types of porous media (permeability, porosity, pore structure, clay concentration, or microchip model), and other conditions (temperature salinity, etc.), as described in more detail in Section 5.2.5. The validity of the population-balance model (Kam and Rossen; 2003) and/or its variants (Kam, 2008) requires comparison with experimental results. Modifications (if necessary) to the model could be implemented for a more accurate physical description of foam.

In our study, we have assumed that co-injection of gas and aqueous phase solution(s) is an apt experimental method to study foam propagation at large distances. In field applications of foam, the most common practice of foam creation is Surfactant-Alternating-Gas (SAG) injection. Experiments could be extended to consider mild variations in water fraction or injection rate to represent SAG processes far from the well more accurately.

5.2.2 Prediction of critical velocity for foam propagation

As mentioned in 5.1.2, Ashoori et al. (2012) presented a mathematical approach that serves a theoretical explanation for the complicated mechanisms of dynamic foam propagation. Their study implies the significance of both superficial velocity and pressure gradient for foam propagation at a large distance.

Both traveling-wave analysis and population-balance numerical simulation of foam propagation requires construction of sophisticated mathematical tools. They are accurate and rigorous approaches of estimating the efficiency of foam propagation at various injection condition and propagation distances. However, this doesn't rule out the possibility of an empirical approach. Measuring the advancing rate of foam front (i.e., the shock velocity v_{shock}) at various total superficial velocities can be applied in a core of varying diameters. Such a measurement helps obtain an empirical, but easier and straightforward correlation between the shock velocity v_{shock} of foam front and the total superficial velocity u_t (at a constant f_g). This empirical relationship could be useful for prediction of foam propagation in steady-state modeling (such as CMG-STARS foam model) of foam propagation. Based on the dependence between u_t and drainage radius r, a correlation between v_{shock} and u_t also could lead to an analytical solution for radial distance of propagation as function of the time/pore volume of foam injection.

5.2.3 Optimization of foam-injection strategy

At a chosen foam quality f_g, injecting foam at a higher surfactant concentration works in favour of foam generation (by lowering u_t^{gen}) and propagation (by lowering u_t^{prop}). However, the total cost of surfactant is proportional to its concentration and hence the total mass of surfactant. An alternative is to inject foam at a lower foam quality and lower surfactant concentration. There is a trade-off between the impact of surfactant concentration and the injected water fraction on foam propagation. The optimal injection strategy that's efficient economically and in speed of propagation is non-trivial and requires quantitative assessment of various scenarios. These considerations also must include surfactant adsorption, of course, which can slow the propagation of surfactant injected at a lower concentration (Lake et al., 2014).

5.2.4 Pressure limits on deep penetration of foam

Wellbore pressure increases with increasing foam propagation distance. Our experimental results (Fig. 3.9) suggest enormous pressure gradients required for propagation of strong foam. A possible solution is to reduce surfactant concentration, or create foam at very high foam quality. Both scenarios reduce pressure gradient, but also make creation of foam (in terms of velocity) much more difficult (Yu et al., 2019). SAG injection improves injectivity of foam near the well (Xu and Rossen, 2004; Salazar-Castillo and Rossen, 2020; Gong et al., 2020a and 2020b), but the issue of a large pressure gradient away from the well remains.

Supercritical CO_2 has lower surface tension with surfactant solutions, which reduces the threshold pressure gradient for foam generation (Rossen and Gauglitz, 1990; Gauglitz et al., 2002). Supercritical-CO_2 foams also exhibits lower pressure gradient than N_2 foams in the strong-foam regime (Laskaris & Jones et al., 2016; Shah et al., 2019). Thus supercritical CO_2 foam in a miscible-flood EOR process may avoid the large pressure gradient for foam propagation without increasing the critical velocities for generation, propagation and stability. In addition, as mentioned in the Introduction, CO_2 foam combines the advantageous EOR and carbon sequestration. The potential of this technique deserves further study.

5.2.5 Foam generation and propagation at reservoir conditions

In this dissertation, we experimentally tested some of the factors controlling foam generation and propagation in one homogeneous porous medium. In a water-wet porous medium of relatively high permeability and low clay content, like the Bentheimer sandstone used in these experiments, at modest temperatures (20~35°C) and back-pressure (mostly 15~40 bar), and low salinity (3.0 wt% NaCl), we conclude that surfactant concentration and the injected water fraction play predominant roles in the generation and propagation of foam. Foam application in an oil reservoir or contaminated soil, however, faces a harsher physical-chemical environment. For a petroleum reservoir, the temperature in the reservoir varies typically in the range of 90~150°C (Muffler and Cataldi, 1978; Hochstein, 1990; Benderitter and Cormy, 1990; Alimonti et al., 2014). Higher salinity and hardness of formation water may also affect foam stability. In addition, more realistic conditions include lower permeability (in petroleum reservoirs), presence of oleic phase, adverse or mixed wettability, etc. Future research on foam generation and propagation ought to be extended to these more-realistic conditions for field application.

Type of gas. For steam foam, propagation distance is also influenced by the balance of heat exchange. For CO_2 foam, the interfacial tension between CO_2 and aqueous phase is lower than for insoluble gases such as N_2. As mentioned above, CO_2 may have the advantage of lowering the mobility reduction of gas by foam and hence the risk of over-pressurizing the formation while also making propagation easier.

Higher salinity. 'Salting out' (Beunen and Ruckenstein, 1982; Zhao, 2012) is a process during which inorganic salt is added to an aqueous solution of weakly polar substance (i.e.,

surfactant) and the substance precipitates. Surfactant may become less effective (or ineffective in a worse case) in sea water. The impact of a higher salinity in reservoirs on the ability of foam generation and propagation ought to be tested quantitatively in future experiments. Salinity may affect the stability of surfactant and its impact must be tested before a foam flooding experiment is conducted. Depending on the goal of experiment, it's an imperative task either to test the range of salt concentration that renders the optimal stability of foam, or to test the formula and concentration of surfactant that works best at a given salinity of a reservoir.

Temperature. Bulk-foam tests show faster foam coalescence with increasing temperature. This can be explained by accelerated bubble coarsening (Saint-Jalmes & Langevin, 2002; Kapetas et al., 2015) and faster liquid drainage at higher temperatures (Saint-Jalmes & Langevin, 2002; Farajzadeh et al., 2009; Kapetas et al., 2015). The faster liquid drainage may reflect in part lower water viscosity at higher temperature. In one study in porous media (Kapetas et al., 2015), the apparent viscosity of foam became two times lower as temperature increases from 20℃ to 80℃. However, the significant reduction of foam apparent viscosity couldn't be explained by the joint effect of decreasing surface tension and aqueous phase viscosity with increasing temperature.

Presence of oil. Foam-oil interactions are dominated by a group of complex surface phenomena (Harkins and Feldman, 1922; Schramm and Novosad, 1990, 1992; Bergeron et al., 1993; Aveyard et al., 1993; Farajzadeh et al., 2012; Almajid and Kovscek, 2016; Hussain et al., 2019). The presence of most oil in porous media reduces foam stability (Mannhardt et al., 1997; Andrianov et al., 2011; Namdar et al., 2011; Namdar and Rossen, 2013; Tang et al., 2018), or kills foam completely when oil saturation is high (Mannhardt et al., 1997), by affecting the limiting capillary pressure and the limiting water saturation of foam. Tang et al. (2019) tested two different types of model oil on the stability of foam. Their study showed that at the same fractional flows of gas, oleic phase and aqueous phase, there could be multiple steady-states of foam. This mechanism arises from the effect of oil on foam stability rather than foam generation as a function of pressure gradient. A steady-state of weak/no foam may be present even at $u_t > u_t^{gen}$ as a result of a high oil saturation. In their study, they also find that oil phase reduces the strength of both high- and low-quality foams, as well as the transition water fraction f_w^*. Different research approaches, including core-flooding experiments of foam, microfluidic experiments, population-balance modeling of foam etc, are required in the future to investigate the impact of oil on foam generation, propagation and stability.

Heterogeneity and gravity. Better understanding on foam generation and propagation at a sharp transition of permeability (Falls et al., 1988; Shah 2019) is needed. Their results suggest the opportunity of foam placement at a greater distance, even at regions of low superficial velocity and pressure gradient. This may help resolve the issue of the high pressure gradient around injection wells and the risk of fracking the formation. It would be worthwhile to combine the implications of this study (Yu et al., 2019; 2020) on foam propagation and research (Shah et al., 2019) on foam placement without direct propagation, to optimize the efficiency of both foam generation and propagation.

Rossen et al. (2010) reviews several foam-injection strategies to prevent gravity segregation. Their equation relate the radial distance of segregation to the injection pressure. For foam propagation in a homogeneous formation, such a method indicates a limit on the radius of the foam region. Our results suggest a possible separate limitation on foam propagation.

References

Alimonti, Claudio , Falcone, Gioia , and Liu, X. L. (2014). Potential for Harnessing the Heat from a Mature High-Pressure-High-Temperature Oil Field in Italy. Paper presented at the SPE Annual Technical Conference and Exhibition, Amsterdam, The Netherlands, October 2014. https://doi.org/10.2118/170857-MS.

Almajid, M.M., Kovscek, A.R. (2016). Pore-level mechanics of foam generation and coalescence in the presence of oil. *Advances in Colloid and Interface Science*, 233: 65-82, ISSN 0001-8686, https://doi.org/10.1016/j.cis.2015.10.008

Andrianov, A.I., Liu, M.K., Rossen, W.R. (2011). Sweep Efficiency in CO2 Foam Simulations With Oil, SPE 142999, Proc. of the SPE EUROPEC/EAGE Annual Conference and Exhibition, Vienna, Austria, 23–26 May 2011.

Ashoori, E.; Marchesin, D.; and Rossen, W.R. (2012). Multiple Foam States and Long-Distance Foam Propagation in Porous Media. *SPE J.* 17(04): 1231-1245. https://doi.org/10.2118/154024-PA.

Aveyard, R., Binks, B. P., Fletcher, P. D. I., Peck, T. G. and Garrett, P. R. (1993). Entry and spreading of alkane drops at the air-surfactant solution interface in relation to foam and soap film stability, *J. Chem. Soc. Faraday Trans*. 89: 4313-4321. https://doi.org/10.1039/FT9938904313

Benderitter, Y. and Cormy, G. (1990). Possible approach to geothermal research and relative cost estimate. In: Dickson MH and Fanelli M (eds) Small geothermal resources, UNITARRJNDP Centre for Small Energy Resources, Rome, Italy, 61-71.

Bergeron, V., Fagan, M. E., Radke, C. J. (1993). Generalized entering coefficients: a criterion for foam stability against oil in porous media, Langmuir. 9(07): 1704-1713. https://doi.org/10.1021/la00031a017.

Beunen, J. A., Ruckenstein, E. (1982). The effect of salting out and micellization on interfacial tension. *Advances in Colloid and Interface Science*, 16(01): 201-231, ISSN 0001-8686. https://doi.org/10.1016/0001-8686(82)85017-3.

Chen, Q., Gerritsen, M. G., & Kovscek, A. R. (2010). Modeling Foam Displacement with the Local-Equilibrium Approximation: Theory and Experimental Verification. *SPE J.* 15(01): 171–183. https://doi.org/10.2118/116735-PA.

Cheng, L., Reme, A. B., Shan, D., Coombe, D. A., and Rossen, W. R. (2000). Simulating Foam Processes at High and Low Foam Qualities. Paper presented at the SPE/DOE Improved Oil Recovery Symposium, Tulsa, Oklahoma, April 2000. https://doi.org/10.2118/59287-MS

Computer Modeling Group, STARS User's Guide, Version 2017.10, Calgary, Alberta, Canada.

Falls, A. H., Hirasaki, G. J., Patzek, T. W., Gauglitz, P. A., Miller, D. D., & Ratulowski, J. (1988). Development of a mechanistic foam simulator: The population balance and generation by snap-off. *SPERE*. 3(03): 884–892. https://doi.org/10.2118/14961-PA.

Farajzadeh, R., Andrianov, A., Bruining, H., and Zitha. P. L. J. (2009). Comparative Study of CO2 and N2 Foams in Porous Media at Low and High Pressure−Temperatures. *Industrial & Engineering Chemistry Research 48* (9),: 4542-4552. https://doi.org/10.1021/ie801760u.

Farajzadeh, R.. , Andrianov, A.. , Krastev, R.. , Hirasaki, G. J., and W. R. Rossen. "Foam-Oil Interaction in Porous Media: Implications for Foam Assisted Enhanced Oil Recovery." Paper presented at the SPE EOR Conference at Oil and Gas West Asia, Muscat, Oman, April 2012. https://doi.org/10.2118/154197-MS.

Friedmann, F., Chen, W.H., Gauglitz, P.A. (1991). Experimental and simulation study of high-temperature foam displacement in porous media. SPERE 6(01): 37–45. https://doi.org/10.2118/17357-PA

Friedmann, F., Smith, M.E., Guice, W.R., Gump, J.M., Nelson, D.G. (1994). Steam-foam mechanistic field trial in the midway-sunset field. SPERE 9(04): 297–304. https://doi.org/10.2118/21780-PA

Gauglitz, P.A.; Friedmann, F.; Kam, S.I. and Rossen, W.R. (2002). Foam Generation in Homogeneous Porous Media, J Chem. Eng. Sci. 57(19): 4037-4052. https://doi.org/10.1016/S0009-2509(02)00340-8

Gong, J., Flores Martinez, W., Vincent-Bonnieu, S., Kamarul Bahrim, R. Z., Che Mamat, C. A. N. B., Tewari, R. D., Mahamad Amir, M. I., Farajzadeh, R., and Rossen, W. R. (2020a). Effect of Superficial Velocity on Liquid Injectivity in SAG Foam EOR. Part 1: Experimental Study, *Fuel*, 278, 118299. https://doi.org/10.1016/j.fuel.2020.118299

Gong, J., Flores Martinez, W., Vincent-Bonnieu, S., Kamarul Bahrim, R. Z., Che Mamat, C. A. N. B., Tewari, R. D., Mahamad Amir, M. I., Farajzadeh, R., and Rossen, W. R. (2020b). Effect of Superficial Velocity on Liquid Injectivity in SAG Foam EOR. Part 2: Modeling, *Fuel*, 278, 118302. https://doi.org/10.1016/j.fuel.2020.118302

Harkins, W. D. and Feldman, A. 1922. Films: The Spreading of Liquids and the Spreading Coefficient. *J. Am. Chem. Soc.* 44(12): 2665–2685. https://doi.org/10.1021/ja01433a001.

Hochstein, M.P. (1990). Classification and assessment of geothermal resources. In: Dickson MH and Fanelli M (eds) Small geothermal resources, UNITAEWNDP Centre for Small Energy Resources, Rome, Italy, 31-59.

Hussain, A. A. A., Vincent-Bonnieu, S., Kamarul Bahrim, R. Z., Pilus, R. M., & Rossen, W. R. (2019). The impacts of solubilized and dispersed crude oil on foam in a porous medium. *Colloids and Surfaces A: Physicochemical and Engineering Aspects*, *579*, [123671]. https://doi.org/10.1016/j.colsurfa.2019.123671.

Jamshidnezhad, M., Shen, C., Kool, P., Mojaddam Zadeh, A., & Rossen, W.R. (2009). Improving Injectivity To Fight Gravity Segregation in Gas Enhanced Oil Recovery. *SPE J.* 15(01): 91–104. https://doi.org/10.2118/112375-PA.

Jenkins, M. K. (1984). An Analytical Model for Water/Gas Miscible Displacements. SPE-12632-MS, presented at the 1984 SPE/DOE Symposium on Enhanced Oil Recovery, Tulsa, OK, 15-18 April.

Jones, S. A.; Laskaris, G.; Vincent-Bonnieu, S.; Farajzadeh, R. and Rossen, W. R. (2016) Effect of Surfactant Concentration on Foam: From Coreflood Experiments to Implicit-Texture Foam-Model Parameters, *J. Ind. & Eng. Chem.* 37: 268-276. https://doi.org/10.1016/j.jiec.2016.03.041.

Kam, S.I. and Rossen, W.R. (2003). A Model for Foam Generation in Homogeneous Media, *SPE J.* 8(04): 417-42. https://doi.org/10.2118/87334-PA.

Kam, S.I. (2008). Improved Mechanistic Foam Simulation with Foam Catastrophe Theory, *J Coll & Surf A* 318(1-3): 62-77. https://doi.org/10.1016/j.colsurfa.2007.12.0417.

Kapetas, L., Bonnieu, S. Vincent, Danelis, S.. , Rossen, W.R.. R., Farajzadeh, R.. , Eftekhari, A.A.. A., Shafian, S. R., and R. Z. Bahrim. (2015) Effect of Temperature on Foam Flow in Porous Media. Paper presented at the SPE Middle East Oil & Gas Show and Conference, Manama, Bahrain, March 2015. https://doi.org/SPE-172781-MS

Khatib, Z.I., Hirasaki, G.J., and Falls, A.H. (1988). Effects of Capillary Pressure on Coalescence and Phase Mobilities in Foams Flowing Through Porous Media. *SPERE*. 3(03): 919–926. https://doi.org/10.2118/15442-PA.

Kovscek, A. R., & Radke, C. J. (1993). Fundamentals of Foam Transport in Porous Media. Report to US Department of Energy. https://doi.org/10.2172/10192736.

Kovscek, A. R., & Radke, C. J. (1994). Fundamentals of foam transport in porous media. In: L. L. Schramm (Ed.), Foams: Fundamentals and applications in the petroleum industry. Washington DC: ACS Advances in Chemistry Series No. 242 (Am. Chem. Soc.).

Kovscek, A. R., Patzek, T. W., and Radke, C. J. (1995). A Mechanistic Population Balance Model for Transient and Steady-State Foam Flow in Boise Sandstone. *Chem. Eng. Sci.* 50: 3783–3799.

Kovscek, A.R., Bertin, H.J. (2003). Foam Mobility in Heterogeneous Porous Media. *Transport in Porous Media.* 52: 37–49. https://doi.org/10.1023/A:1022368228594.

Lake, L.W.; Johns, R.T.; Rossen, W.R. and Pope, G.A. (2014). Fundamentals of Enhanced Oil Recovery. *SPE, ISBN 978-1-61399-407-8*.

Lotfollahi, M., Kim, I., Beygi, M. R., Worthen, A. J., Huh, C., Johnston, K. P., … DiCarlo, D. A. (2016). Experimental Studies and Modeling of Foam Hysteresis in Porous Media. Paper SPE-179664-MS presented at the SPE Improved Oil Recovery Conference, Tulsa, Oklahoma, USA, April 2016. https://doi.org/10.2118/179664-MS.

Mannhardt, K., and Svorstol, I. (1997). Foam Propagation in Snorre Reservoir Core – Effects of Oil Saturation and Ageing. Paper 052, presented at the 1997 European Symposium on Improved Oil Recovery, The Hague, The Netherlands, 20-22 Oct.

Martinsen, H. and Vassenden, F. (1999). Foam Assisted Water Alternating Gas (FAWAG) Process on Snorre, 10th European Symposium on Improved Oil Recovery.

Muffler, P. and Cataldi, R. (1978). Methods for regional assessment of geothermal resources, Geothermics. 7: 53-89.

Namdar Zanganeh, M., Kam, S.I., LaForce, T.C., et al. 2011. The Method of Characteristics Applied to Oil Displacement by Foam. *SPE J.* 16(01): 8–23. http://dx.doi.org/10.2118/121580-PA.

Namdar Zanganeh, M., and Rossen, W. R. (2013). Optimization of Foam Enhanced Oil Recovery: Balancing Sweep and Injectivity." *SPE Res Eval & Eng.* 16(01): 51–59. https://doi.org/10.2118/163109-PA

Rossen, W. R. and Gauglitz, P. A. (1990). Percolation Theory of Creation and Mobilization of Foam in Porous Media. *AIChE J.* 36: 1176–1188.

Rossen, W. R., and van Duijn, C. J. (2004). Gravity Segregation in SteadyState Horizontal Flow in Homogeneous Reservoirs. *J. Petr. Sci. Eng.* 43: 99-111.

Rossen, W. R., van Duijn, C. J., Nguyen, Q. P., Shen, C., and Vikingstad, A.K. (2010). Injection Strategies To Overcome Gravity Segregation in Simultaneous Gas and Water Injection Into Homogeneous Reservoirs. *SPE J.* 15 (01): 76–90. https://doi.org/10.2118/99794-PA

Salazar-Castillo, Rodrigo O., and William R. Rossen. (2020). Scaleup of Laboratory Data for Surfactant-Alternating-Gas Foam Enhanced Oil Recovery. *SPE J.* 25(04): 1857–1870. https://doi.org/10.2118/201204-PA.

Schramm, L.L. and Novosad, J.J. (1990). Micro-visualization of foam interactions with a crude oil. *Colloids Surfaces.* 46: 21-43.

Schramm, L.L. and Novosad, J.J. (1992). The destabilization of foams for improved oil recovery by crude oils: Effect of the nature of the oil, *SPE J.*7(1-2): 77-90. https://doi.org/10.1016/0920-4105(92)90010-X.

Shah, S. Y., Wolf, K. H., Rashidah, M. P., and Rossen. W. R. (2019). Foam Generation by Capillary Snap-Off in Flow Across a Sharp Permeability Transition. *SPE J.* 24(01): 116–128. https://doi.org/10.2118/190210-PA.

Shah, S. Y., As Syukri, H., Wolf, K. H., Pilus, R. M., and Rossen., W. R. (2020). Foam Generation in Flow Across a Sharp Permeability Transition: Effect of Velocity and Fractional Flow. *SPE J.* 25(01): 451–464. https://doi.org/10.2118/195517-PA.

Stone, H. L. (1982). Vertical Conformance in an Alternating Water-Miscible Gas Flood, SPE-11130-MS, presented at the 1982 SPE Annual Tech. Conf. and Exhibition, New Orleans, LA, 26-29 Sept.

Tang, G., and Kovscek, A. R. (2006). Trapped Gas Fraction During Steady-State Foam Flow. *Transport in Porous Media*. 65(2): 287-307. https://doi.org/10.1007/s11242-005-6093-4.

Tang, J., Vincent-Bonnieu, S. V. B., and Rossen, W. R. (2019). Experimental Investigation of the Effect of Oil on Steady-State Foam Flow in Porous Media." *SPE J.* 24(01): 140–157. https://doi.org/10.2118/194015-PA.

Tanzil, D., Hirasaki, G. J., & Miller, C. A. (2002). Mobility of Foam in Heterogeneous Media: Flow Parallel and Perpendicular to Stratification. Society of Petroleum Engineers. https://doi.org/10.2118/78601-PA.

Xu, Q., and Rossen, W. R. (2004). Experimental Study of Gas Injection in Surfactant-Alternating-Gas Foam Process. *SPE Res Eval & Eng.* 7(06):438-448. https://doi.org/10.2118/84183-PA.

Yu, G., Rossen, W. R., and Vincent-Bonnieu, S. (2019) Coreflood Study of Effect of Surfactant Concentration on Foam Generation in Porous Media, *J I&EC.* 58(01): 420-427. https://doi.org/10.1021/acs.iecr.8b03141.

Yu, G. Y., Rossen, W. R., and Sebastien, V.B. (2020). Foam Propagation at Low Superficial Velocity: Implications for Long-Distance Foam Propagation. *SPE J.* 25(06): 3457–3471. https://doi.org/10.2118/201251-PA.

Zhao, L., Li, A., Chen, K., Tang, J. J., Fu, S. S. (2012). Development and evaluation of foaming agents for high salinity tolerance, *J. Petroleum Sci. Eng.* 81:18-23. https://doi.org/10.1016/j.petrol.2011.11.006

Scientific contributions

Journal articles

Yu, G., Rossen, W. R., and Vincent-Bonnieu, S. (2019). Coreflood Study of Effect of Surfactant Concentration on Foam Generation in Porous Media. *Journal of Industrial & Chemistry Engineering*.

Yu, G., Vincent-Bonnieu, S., and Rossen, W. R. (2020). Foam Propagation at Low Superficial Velocity: Implications for Long-Distance Foam Propagation. *Society of Petroleum Engineers Journal*.

Yu, G., Rossen, W. R., and Vincent-Bonnieu, S. Simulation Models for The Minimum Superficial Velocity for Foam Generation and Propagation. *To be submitted to journal*.

Thesis

Yu, G., and Rossen, W. R. (2015). Analytical and Simulation Study of Sweep Efficiency in Gas-Injection EOR (part I): Fractional-Flow Analysis of Miscible Hot WAG.

Yu, G., and Rossen, W. R. (2015). Analytical and Simulation Study of Sweep Efficiency in Gas-Injection EOR (part II): Simulation Study of Gravity Segregation in Non-Horizontal Reservoirs.

Conference proceedings and presentations

Yu, G., and Rossen, W. R. (2015). "Fractional-flow Analysis of Miscible Hot WAG". *Oral presentation at the 7th annual InterPore Conference (International Conference on Porous Media)*, Padova, Italy, 18-21 May.

Yu, G., Namani, M. N., Kleppe, J. K., and Rossen, W. R. (2017). "Gravity Override and Vertical Sweep Efficiency in Dipping Reservoirs". Conference paper published by EAGE (European Association of Geoscientists & Engineers), *poster presentation at the 19th European Symposium on Improved Oil Recovery*, Stavanger, Norway, Apr 2017.

Yu, G., Rossen, W. R., and Vincent-Bonnieu, S. (2018). "Foam Generation in Porous Media: Effect of Surfactant Concentration". Conference paper SPE-190398-MS, *poster presentation at SPE EOR Conference at OGWA (Oil and Gas West Asia)*, Muscat, Oman, March 2018.

Yu, G., Vincent-Bonnieu, S., and Rossen, W. R. (2019). "Foam Propagation at Low Superficial Velocity: Implications for Long-Distance Foam Propagation." Conference paper published by EAGE (European Association of Geoscientists & Engineers), *technical presentation at the 20th European Symposium on Improved Oil Recovery*, Pau, France, Apr 2019.

Yu, G., Vincent-Bonnieu, S., and Rossen, W. R. (2019). "Foam Propagation at Low Superficial Velocity: Implications for Long-Distance Foam Propagation." *Oral presentation at the 11th annual InterPore Conference (International Conference on Porous Media)*, Valencia, Spain, 6-10 May.

Acknowledgements

I first came to TU Delft for a pursue of a Master's degree in petroleum engineering. After attaining a Master's Degree of petroleum engineer, I started a PhD project on foam propagation promoted and supervised by Prof. Dr. W.R. Rossen, and co-supervised and advised by Dr. Sebastien Vincent-Bonnieu.

In the past 8 long years of my life in the Netherlands, I have the privilege to have met and known a great many of amazing people: tutors, colleagues, friends. This last chapter of dissertation, therefore, is an expression of my gratitude, along with my best expectations and wishes to all.

Prof. Dr. W.R. (William) Rossen. Thank you very much for granting me the great opportunity of doing research here at TU Delft. I really appreciate your trust in me by giving me the chance of leading this research on foam, when I didn't even have enough trust in myself. You have been an extraordinary supervisor and mentor to me in the past 7 years. When I first started doing research with you, I was stumbling with a lack of confidence. However, you have spared no effort in guiding me (and so many other students of yours) very patiently and thoughtfully. After years of learning in theory and practicing with experiment, I now find myself much more confident with respect to scientific and engineering substance. In addition, I also learned many valuable traits from you on (but not limited to) how to be a qualified researcher in science and engineering: coherence, integrity, patience, honesty to facts, critical thinking skills in face of uncertainty, and the invaluable skills in writing a high quality article of scientific & engineering substance.

Thank you a plenty for letting me in this big family full of intelligent, friendly and exceptionally talented people. I can learn valuable traits from every one of them, and also shared a great fun life all together. I never expected myself to have felt and learned so plenty in my life. I can happily claim that I have enjoyed and accomplished more than I ever thought I could. I shall forever treasure and cherish my memory of life and career at this University. Last but not the least, plenty of thanks for your unmeasurable amount of patience towards a variety of my shortcomings. For many times, I have had struggles both at work and in life. It is your patient guidance that gave me the chances to grow and gradually overcome my problems and troubles. I learned (and am still learning) very much about having integrity in myself, in addition to critical thinking ability in scientific research.

I sincerely wish you a good health, and a very pleasant, joyful, fulfilling and exciting life in the years to come! All the best.

Dr. Janice Rossen. Thank you very much for being such a lovely and caring friend for all of Bill's students, myself included. You have brought so much fun and pleasant experiences for our life outside of the office. I really admire your enthusiasm and devotion for music, art, and literature. Your comprehension and insights in these amazing subjects have been genuinely influential. Thank you so much for sharing your passion and your hard work with us. Now when I look back, I have gathered a full collection of the classical piano pieces composed and by you and your friends in the past four years, a collection of work you put your heart into. And of course, I surely remember loaning an electric piano for a very long time, during which I finally get to enjoy the pleasure of my favourite musical instrument. I don't think I could ever thank you enough for your tremendous amount of generosity and kindness. I wish you good health, good spirit, and above all, I wish you an exciting and adventurous journey for all the wonderful things you have passion for.

Dr. Sebastien Vincent-Bonnieu. Thank you sincerely for being a very kind, generous, knowledgeable and influential supervisor and colleague in our department. I remember vividly the diversity of invaluable advice you contributed to my PhD project. Your contribution to this big team is much appreciated. Many thanks for teaching me the significance of various aspects and traits that define a qualified Ph.D. candidate. I must admit the mistakes I made that I wasn't careful and serious enough with respect to some of your advice and recommendations at the beginning of my Ph.D.. In time, however, I begin to recognize the meaning of your advice and the reason why you insisted. I started focusing more on the fundamental knowledge that forms the theoretical background of the subject. And I also learned many skills from you on how to do experiments and write papers with more structure and efficiency.

Sponsors of JIP. My sincerest thanks to the Sponsors' financial support of the Joint-Industry-Project. Your years of consistent support facilitates the invaluable group of research on foam in porous media conducted at TU Delft.

My profound and sincerest gratitude to my dear parents **Xueying Han & Zhongxiang Yu**, grandma **Shuming Wong**, my aunt **Xiaoying Han** and uncle **Hongguang Zheng**, and my cousin **Wengfeng Zheng**. Mom and dad, you have done a fantastic job raising me, educating me and supporting me in various stages of my life, including all the past years when I stayed very far from home. Many thanks to your love and support throughout my entire life, in the past, present and future. I don't think I could have ever made it this far without you. And many thanks to my other families, you made up unforgettable fun memories throughout my entire life. I also thank you very much for reaching out and help me in time of difficulties. I wish you all the best in the future!

My great thanks to all the laboratory head and staffs: **Dr. Karl-Heinz Wolf, Prof. Dr. Pacelli Zitha, Wim Verwaal, Michiel Slob, Paul Vermeulen, Jens Berg, Karel Heller, Jolanda van Haagen, Ellen Meijvogel-de Koning.** Thank you all for building and maintaining such a clean and well established lab. And for your excellent level of technical support throughout the four years of my experiments. You all care very much about the PhD and Msc students working in the laboratory. **Michiel Slob,** thank you a plenty for your consistent support and invaluable advice for my experiments, and for being deeply involved in the projects of PhD and Msc students. You are very intelligent and hard working. I am impressed by your strong ability to tackle the various technical challenges in the laboratory, and your constructive advice in many of the ongoing research topics. Last but not the least, I also enjoy very much the nice conversations with you about the history and culture of different countries. I wish the best for you, in life and in career. **Jens Berg,** (thank you a great deal for your cores. This is the very essential part of my PhD project. At the beginning I was really concerned about having a high quality core. You beautifully conquered the technical challenge of making the core, which ensures the progresses of my experiment on foam propagation in the next two years. My sincere thanks again for the amazing cores you crafted! **Paul Vermeulen,** plenty of thanks to you for being very patient and available to help me (and many others) with the MP3 programme. You have been so positively responsive to the problems and struggles of students that work in the lab. Your frequent consultancy saves me from my troubles and helps me make quick progress in my experiments. It is a pleasure working with you, and I wish you the best. **Karel Heller,** due to various reasons, it is indeed pity that the work we did together wasn't published in the end. Nevertheless, it's undeniable that I learned a great deal from working with you. It has been a very nice and fun experience. Thank you for your passion, devotion and hard-work on the design and building of the Labview control system. The programme initialized and established by you is a textbook for me and helps me learn many things! You have my best wishes! **Jolanda van Haagen** and **Ellen Meijvogel-de Koning,** Many thanks to you for helping me with the NaCl supplement. And of course for the cheerful greetings from you from time to time, which really helps cheer me up from my daily struggles at work. You have my best wishes as well!

I'd also like to pass my thanks and good wishes to the international friends and colleagues. I have the great pleasure to have known many excellent people from the Petroleum Engineering Master's programme. **Fei Chen**, **Xiaofei Gan**, **Binyu Zhao**, **George Laskaris**, **Richard Tymotheous Purba**, **Khalid Saleh**, **Fix Capelle (aka. Fang Shu)**, **Shantnu Brajesh**, **Chaitanya Padalkar**, **Joris Roebroeks, Marjolein Nell**, **Cynthia Watanabe**, **Stefanos Danelis**, **Robert de Velde, Ahmed Al Ayesh**, **Juan Nobile**, **Rahul Ranjan**. My sincerest thanks to many of you for your kind support and welcome upon my first arrival in the Netherlands, and plenty of thanks to many others for your pleasant company and support both in studying and in life. Thank you for bringing a lot of joy and knowledge in my life, and for helping me and making my life much easier in time of difficulties. Last but not the least, many thanks to the loving couple **Qigui Chi** and **Lin** for taking care of my life during my two years' stay in Schiedam. You show me how to live a good life in the Netherlands, while letting me in as a member of this warm and interesting family of yours. My best wishes, for your wellbeing, good health and wealth.

During the four years of my PhD life, I have the privilege to have known a great number of talented and interesting people in this office.

Sian Jones, thank you for being a very lovely, caring and interesting friend and colleague. You have been very delightful and helpful, and having you in this big family is a good luck to us all. I admire your extensive experiences in teaching and scientific research. You have done very impressive experiments on foam in porous media, which is a great passion of yours. However, your passion is not limited to your research subjects. I am deeply impressed by your years' of teaching experience dedicated to the students in Africa. In addition, you are also actively involved in many other meaningful events, such as participating in the construction of a digital library, organizing graduation gifts for almost everyone you know. And of course, how could I forget about the delicious desserts? Your enthusiasm in research, in cooking and in helping others are great inspirations for people around you. I wish you a good health, and an exciting and happy life ahead.

Kevin Bisdom, Nikita Lenchenkov, Mark Khait, Chris Boejie, Jakolien van de Meer, Matteo Cusini, Siavash Kahrobaei, Rafael de Moraes, Durgesh Kawale, Eduardo de Barros, Mojtaba Hosseini-Nasab, Rodrigo Salazar, Dr. Chapiro, Siamak Abolhassani, it is my great privilege to have known so may intelligent, hard-working, and fun people. I may not have the good luck to become an intimate friend with all of you, nevertheless, it's a pleasure for me to be a part of this big team. The first 3 years of my PhD is really fun because of you, I will always remember all the academic event and parties we had. Cheers to you all!

Jiakun Gong, Jinyu Tang (aka. Alexander Tang), Longlong Li, Xiaocong Lyu, Kai Li, Yang Wang, Fanxiang Xu, Yuan Chen, thank you plenty for being very good Chinese friends and colleagues of mine. It is my privilege to have known all of your intelligent, caring and fun folks during the time of my Ph.D. career. Studying and making a living in a foreign country is not easy all the time. My deep gratitude for your care and help in the past years.

Jiakun, I really admire your leadership for all of us. You have organized so many amazing academic as well as social events. And of course, you are really good at your own research as well. It is really interesting and pleasant to have known you. I wish you a great success in career, great joy in life, in all the years to come.

Jinyu, your enthusiasm and coherent attitude towards science and engineering is an invaluable trait, a trait that encourages many people around you. You have achieved amazing accomplishments during your PhD and Post-doc life at TU Delft. I am certain that you will make even more astonishing accomplishments in the future. You have my best wishes.

Xiaocong, thank you a plenty for being such a nice friend to me (and everyone you know). You have made more friends than anyone ever could in life. Wherever you go, you always manage to bring a substantial amount of joy, company, and plenty of help to people around you. It is a wonderful gift you have. Well, my best wishes to you and your families. Wish you a successful, and (I am sure) a cheerful life in the years to come.

Longlong, Kai, Yang, Fanxiang and Yuan, you are all incredibly intelligent and hard working. It is a great privilege and pleasure to have met you all during my PhD. My best regards and sincere wishes to you all, for a brighter future and happy life in store for you.

My special thanks to **George Laskaris, Sian Jones, Matei Tene, Martijn Jessen, Swej Shah, Xiaocong Lyu, Mohsen Mirzaie Yegane, Ahmed Hussain, Kiarash Mansour,** for being such great friends of mine in the course of my Ph.D. life in the Netherlands. I owe you a big basket of gratitude for all the cherish memories I have, for now and for ever. The time that I have had with you, helps me survive, helps me live, makes me enjoy, makes me love, makes me think, learn, recover and grow. I am not entirely sure of my whereabouts in the future. I do hope, though, we shall meet again…

George, I have known you since when I was doing my Msc project at TU Delft. It is absolutely splendid times we had as we travel in the Netherlands, Greece and Spain. My impression is that you are a very smart, hard-working, patient, and responsible person. I have faith in you that you will find your dream job, dream place to live, dream partner to share your life with, in time, eventually. It's a real pleasure to have known you.

Matei, you are very talented in a variety of things in life. Aside from your excellent scores in study and in research, you are also passionate about and proficient in dancing, mastering foreign languages, cooking, socializing, and perhaps a dozen of other things I am not even aware of. Many thanks to your good wishes for me. It's not so easy for me to find "it", but I will never stop trying. I wish nothing but the same for you.

Swej, you have great gifts in life and in career, no doubt. Many thanks for bringing lots of optimistic and unexpectedly clever things to both work and life. Among your various great strength and abilities, your ability to think for and help others is definitely an invaluable quality to have. Nevertheless, don't try and save the whole world. My best wishes my friend. I will always remember the good times we had in Delft.

Martijn, you are a strong, fun, true and very dear friend for so many of us. We are very lucky to have you with us. You have managed to do very complex and impressive work during your PhD. You have created and shared so much great time with people you. The only regret is perhaps, I myself never get to have a nice vacation with you. I do hope it's going happen in the future.

There are some difficult moments in life indeed. But everything will be alright I believe, since you are not alone. I wish you have a good health and a joyful family life stored in the future.

Mohsen, I am very impressed by your tremendous amount of passion in movies (and in making them). It's definitely something great to celebrate, since there are many people out there who spent their lives looking for a passion and never get. I am also impressed by your diligence at work, and your carefulness for your friends and colleagues. Many thanks to your kind help in various occasions. I wish you find a new job of your passion and interest soon, and of course, a good health and good life.

Ahmed, it's a big pleasure to have you in this office for the past 5 years. Thank you very much for all the insightful thoughts and smart ideas during our group meetings, thank you a plenty for the tasty deserts/bakeries. Plenty of thanks also, for the positive atmosphere you bring along wherever you go. I wish you an exciting and fulfilling life in the future.

Kiarash, it's a pleasure to have you with us in this team. I hope you have also enjoyed your research and life with us. Many thanks for the cheerful, easy-going and friendly vibe. I believe you will get through the struggles and challenges, and produce a very cool and valuable work of your PhD. All the best wishes to you.

Many thanks to the secretaries, **Lydia Broekhuijsen**, **Marlijn Ammerlaan**, **Ralf Haak, Nancy van Veen**. I am not in particular good at managing my schedules and personal belongings. Many thanks for your kind help in various occasions, which save me big time from my own troubles. And also thank you a plenty for your consistent collaboration and support in helping me organise the weekly PE seminars. I couldn't have managed the events without your consistent collaborations.

Many thanks to **Graduate School**, for making such an abundant and diverse Doctorial Education curriculum. In the past 20 years, I spent most of my time doing independent work in school. The DE courses offered by GS bring me back to a group life. I get to meet a variety of fun and smart PhD students, enjoy plenty of interesting team-work projects, as well as learn a lot of valuable skills from these fun experiences.